THE ROLE OF INFLAMMATORY FACTORS AND DIFFERENTIALLY EXPRESSED MIRNAS IN CHORDOMA PATHOPHYSIOLOGY

by

Şükrü Güllüoğlu

Submitted to Graduate School of Natural and Applied Sciences
in Partial Fulfillment of the Requirements
for the Degree of Doctor of Philosophy in
Biotechnology

Yeditepe University

2017

THE ROLE OF INFLAMMATORY FACTORS AND DIFFERENTIALLY EXPRESSED MIRNAS IN CHORDOMA PATHOPHYSIOLOGY

APPROVED BY:

Assoc. Prof. Dr. Ömer Faruk Bayrak (Thesis Supervisor) .....

Prof. Dr. Ahmet Arman .....

Prof. Dr. Engin Ulukaya .....

Prof. Dr. Fikrettin Şahin .....

Assoc. Prof. Dr. Altay Burak Dalan .....

DATE OF APPROVAL: ..../..../2017

ACKNOWLEDGEMENTS

I would like to express my gratefulness for the immense and complete support of my Professor Ömer Faruk Bayrak, whose guidance and insight made this thesis real. Pursuing my thesis under his supervision has been an experience which broadens the mind and presents an unlimited source of learning. I present my special gratitude to Professor Fikrettin Şahin for his guidance and unabated support through my undergraduate years until getting my PhD degree. I would also like to thank Professor Ayşegül Kuşkucu for her generous mental support, by which I improved both as a scientist and person. These studies would not succeed without the presence of Professor Uğur Türe and Dr. Cumhur Kaan Yaltırık. I present my special thanks to Professor Altay Burak Dalan, whose assistance and support was vital throughout my PhD studies.

I thank my lab mates Mesut Şahin, Emre Can Tüysüz and Özlem Şilan Coşkun for being very hard workers and for their support. Further thanks go to Zeynel Demir, Sezin Gürkan and Dr. Öznur Suakar for their patience and assistance.

This thesis is dedicated to my late aunts Emine Gülseren and Refika Rezan.

ABSTRACT

THE ROLE OF INFLAMMATORY FACTORS AND DIFFERENTIALLY EXPRESSED MIRNAS IN CHORDOMA PATHOPHYSIOLOGY

Chordomas are rare tumors seen along the spine and skull base. Chordomas are locally destructive and chemoresistant, with poor prognosis and limited therapeutic options. Since there is no cure for the disease, molecular discoveries are needed to elucidate mechanisms behind chordoma initiation and progression. This study compared the expression profile of miRNAs in chordomas to that of healthy nucleus pulposus samples to gain insight into the molecular pathogenesis of chordomas. Selected miRNAs were transfected to chordoma cell lines, followed by viability assay, apoptosis assay, and cell-cycle analysis. miR-31 decreased cell viability in all chordoma cell lines after 72 hours. Although each miRNA had a similar pattern, miR-31 had the most effective S-phase arrest. Important genes for cancer progression were found to be targeted. The level of miR-222 in chordoma cell lines U-CH1 and MUG-Chor1 correlated positively with EMT markers.

Furthermore, pro-inflammatory cytokines leukemia inhibitory factor and tumor necrosis factor were found to increase the aggressive traits of chordoma cells and lead to a poor prognosis in patients. Treating chordoma cells with these cytokines resulted in increased migration, invasion, tumorosphere formation, colony formation, epithelial-mesenchymal transition, and chemoresistance accompanied by a dramatic activation in pro-inflammatory pathways. LIF was associated with tumor size and a poorer overall survival. Results indicate that tumor promoting inflammation plays a role in elevation of aggressiveness related functions and genes in chordomas in vitro. Overall, this thesis presents important molecular findings which contributes to molecular knowledge about chordoma.

ÖZET

İNFLAMATUVAR FAKTÖRLERİN VE FARKLI SEVİYELERDE İFADE EDİLEN MİRNALARIN KORDOMA PATOFİZYOLOJİSİNDEKİ ROLÜ

Kordomalar omurga ve kafatası tabanında görülen nadir tümörlerdir. Kordomalar yerel olarak yıkıcı ve kemoterapi dirençli olmakla birlikte kötü prognoz sergilerler ve tedavi seçenekleri kısıtlıdır. Bir tedavi yönteminin olmaması, kordoma tumorigenezi ve ilerlemesi ile ilgili moleküler yolakların çalışılması ihtiyacını doğurmaktadır.

Bu çalışmada miRNA ifade profili sağlıklı dokularla karşılaştırılıp kordoma moleküler patogenezi hakkında bilgiler ortaya konuldu. Seçilen miRNA'lar hücrelere transfekte edildi ve ardından canlılık, apoptoz ve hücre döngüsü analizleri yapıldı. miR-31 hücre canlılığını 72 saat sonunda düşürdü. Seçtiğimiz tüm miRNA'ların hücre döngüsü üzerinde benzer bir etki yapmasıyla birlikte en yüksek S-fazı tutuklanma etkisini miR-31'de gözlemledik. Kanser ilerlemisnde önemli genlerin bu miRNA'lar tarafından hedeflendiğini tespit ettik. miR-222 düzeyi U-CH1 ve MUG-Chor1 hücre hatlarında EMG işaretçileriyle uyumlu bulundu.

Yangı yapıcı sitokinler LIF ve TNF-α kordomanın agresif özelliklerini arttırdı ve hasta örneklerinde kötü prognozla ilişkili olduğu bulundu. Kordoma hücrelerine verilen bu sitokinler hücre göçü, invazyon, koloni oluşturma, kürecik oluşturma, EMG ve ilaç direncini arttırdı ve yangı yolaklarını harekete geçirdi. LIF seviyesi hastalarda tümör boyutu ve sağkalım ile ters orantılı bulundu. Bu sonuçlar tümör yangısının kordomaları daha gresif hale getirdiğini ortaya koymaktadır. Bu çalışma önemli moleküler bulgular ortaya koyarak kordoma moleküler biyolojisi hakkındaki bilgi havuzuna katkı sağlamıştır.

TABLE OF CONTENTS

LIST OF FIGURES

LIST OF TABLES

LIST OF SYMBOLS/ABBREVIATIONS

ABCG2	ATP-binding cassette sub-family G member 2
Akt	Protein Kinase B
bFGF	Basic fibroblast growth factor
BSA	Bovine serum albumin
CGH	Comparative genomic hybridization
CSC	Cancer stem cell
DAPI	4',6-diamidino-2-phenylindole
dH2O	Distilled water
DMEM	Dulbecco's Modified Eagle's Medium
DMSO	Dimethyl sulfoxide
DNA	Deoxyribonucleic acid
DMEM	Dulbecco's Modified Eagle's Medium
EDTA	Ethylenediaminetetraacetic acid
EGF	Epidermal growth factor
EGFR	Epidermal growth factor receptor
EMT	Epithelial to mesenchymal transition
EMA	epithelial membrane antigen
ERK	Extracellular signal-regulated kinase
EtBr	Ethidium Bromide
EtOH	Ethanol
FACS	Fluorescence-activated cell sorting
FBS	Fetal bovine serum
FGF2	Fibroblast Growth Factor 2
FISH	Fluorescent in-situ Hybridization
LOH	Loss of Heterozygousity
LT-TNF	Cells treated with TNF-a for 1 year
MRI	Magnetic Resonance Imaging
MTS	3-(4,5-di-methyl-thiazol-2-yl)-5-(3-carboxy-methoxy-phenyl)-2-(4 sulfo-phenyl)-2H-tetrazolium
NF-κB	Nuclear Factor kappa B

NGS	Next Generation Sequencing
PBS	Phosphate Buffered Saline
PCR	Polymerase chain reaction
PI	Propidium Iodide
PI3K	Phosphoinositide 3-kinase
PI3K-Akt-mTOR	Phosphatidylinositol 3-kinase (PI3K)/AKT/mammalian target of rapamycin
PSA	Penicillin/Streptomycin/Amphotericin
Ras	Rat sarcoma
STR	Short tandem repeat
TAMs	Tumor-associated macrophages
TILs	Tumor infiltrating lymphocytes
TNF-α	Tumor Necrosis Factor
VEGF	Vascular endothelial growth factor

1. INTRODUCTION

1.1. INTRODUCTION TO CHORDOMA

Chordoma is a rare tumor that is considered as a low-intermediate grade primary bone tumor. Chordoma is observed along the axial skeleton. There is a general consensus that the disease arises from notochord cells that remain in the spine after embryonic development [1] The annual incidence of chordoma is 0.08 per 100,000 people. Reports indicate that 29.1% of chordomas are sacral, 32.8% spinal, and 32% cranial, and the ratio of sex distribution is about 2:1 in males and females [2,3].

1.1.1. History

Chordoma was identified by Luschka in 1856 and Virchow first defined a chordoma as a tumor of the clivus in 1857 naming the tumor as ecchondrosisphysaliphoraspheno-occipitalis as a result of the belief that it originates from cartilage. The first microscopy data revealed that these tumor cells contain vacuoles. First claim that the tumor originates from the notochord was by Müller in 1858 after his observations that the skull base and sacrum contained notochordal remnants, locations where chordoma is most abundant. Thus, he named the disease as ecchordosis physaliphora. Ribbert first labeled the tumor as "chordoma" as his views matched those of Müller's. In 1895 Ribbert presented evidence in his experiments in which he used rabbits to observe that nucleus pulposus could mass transform into cells that histologically resemble chordoma.

The first report of a chordoma was by Klebs in 1864, which was in the skull base (spheno-occipital). Chordoma of sacrum was reported first in 1900 (Henning) and intervertebral chordoma was reported in 1924 (Raul and Hiss).

1.1.2. Tumor Character

Chordomas are predominantly mucin-secreting, lobulated, transparent, solid grey masses, similar to cartilage tumors, and can be classified structurally as ossified or calcified,

therefore, the tumor mass can be soft, firm or myxoid. Having pseudocapsules, chordomas are multilobulated in soft tissue and multifocal in the bone[4]. Microscopically, chordomas are a mixture of fusiform and physaliphorous cells, the latter being typical of chordoma. Keratin (CK19) and S-100 markers are used in histological staining for diagnosis. Growing evidence suggests that a chordoma might be the result of the malignant transformation of intraosseous notochord. Chordomas are strongly related to the incidence and location of notochordal vestiges, having histological and immunohistochemical similarities to embryonic notochord [5]. Chordomas are highly resistant to chemotherapy and radiotherapy, therefore radical surgery is the option of treatment for most cases [6]. The life expectancy of patients with a chordoma is 6 years on average; the 5-year survival rate is 70%, while the 10-year survival rate is 40% [7].

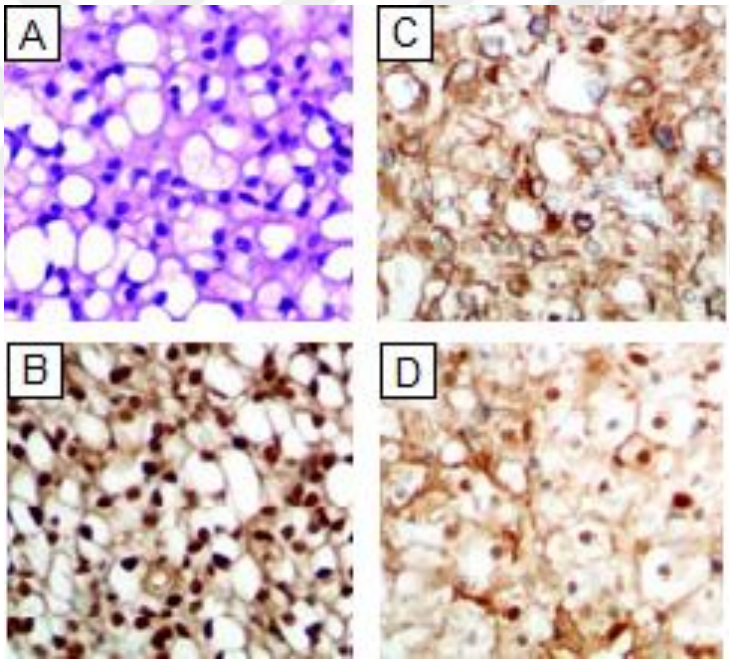

Figure 1.1 IHC staining of a chordoma tumor sample.

(A) H&E staining. A myxoid matrix and embedded tumor cells with eosinophilic cytoplasm and physaliphorous cells. (B) Nuclear brachyury expression. (C) cytokeratin and (D) S-100 protein [8].

1.1.3. Risk Factors

To date, no evidence of environmental factors that affect chordoma initiation has been reported. However, irradiation might play a role in formation of dedifferentiated subtype of the tumor [9,10].

Familial inheritance has been observed in some chordomas where eight families have been reported with at least 2 individuals diagnosed and familial chordoma has been linked to brachyury abnormalities [11-13].

Tuberous sclerosis complex syndrome might be associated with chordoma since they reportedly coincided in patients. Loss of TSC1 and TSC2 genes was associated with sacrococcygeal chordoma [14]. TSC1 and TSC2 associated chordoma is mostly pediatric and has distinct clinical features from chordoma in general [15].

1.1.4. Clinical Presentation

Chordomas grow slowly, however extensive local destruction and invasion of surrounding tissue is observed. Sacral chordomas are discovered relatively late with extensive tumor growth at diagnosis. Low back pain and anesthesia are distinguishable symptoms. Local pain and neurological symptoms such as loss of vision, headache and imbalance are presenting symptoms in skull-base chordoma [16].

Local recurrence of chordoma is mainly dependent on surgical margins. Recurrence occurred in 70% of the cases in which negative surgical margins could not be achieved with contrast to 10-20% in tumors with which negative margins could be applied during surgery [17,18]. Distant metastases was observed in 20-48% of spinal chordoma [19-21]. In skull-base chordoma the number decreases to less than 10% [22]. Metastasis is commonly observed in lungs, liver, skin, lymph nodes and bones [23]. Metastases can happen 3 months to 10 years after diagnosis [23,24].

1.1.5. Chordoma Treatment

1.1.5.1. Surgery

Surgery is the most preferred treatment approach in the disease. Radical surgery presents better survival rates and prevents local recurrence. A downside of this surgical approach is that patients can face multiple side effects since chordoma is usually located very close to sensitive organs and nerves. Radical surgery for chordoma is possible in 10-20% of the cases [25]. Emerging imaging techniques with MRI improved prognosis by locating intra-osseous tumors which can be removed by en-bloc resection [26]. Post-operative radiotherapy is a common approach [27].

1.1.5.2. Radiotherapy

Radiation therapy without surgery is the second choice of therapy in chordoma if it is obligatory to avoid surgery. Although chordoma is highly radio-resistant, it has been reported as beneficial. Photon radiotherapy is problematic since high doses of it are needed to treat the tumor, while the surrounding vital structures are poorly tolerant to it [28,29]. Proton beam radiotherapy is a better choice since the required high dosage of radiation can be focused on the tumor and less on the adjacent tissues. This method is used mainly for skull-base chordoma and beneficial effects have been reported [29,30]. Carbon-ion radiotherapy is also being used as a radiotherapy in chordoma [31].

1.1.5.3. Chemotherapy

Chordomas are strongly resistant to chemotherapy. In aggressive chordomas, a slightly positive effect of chemotherapeutic agents has been observed, but the number of studies and cases is very limited [32]. Tyrosine-kinase inhibitors may be used to inhibit many phosphorylated receptors and kinases that are altered in chordomas, including platelet-derived growth factor receptor B (PDGFRB) and kinases that participate in pathways, such as Akt, the mammalian target of rapamycin (mTOR). Other commonly phosphorylated target candidates in chordomas are TSC2 and the translational initiation factor binding protein

EIF4EBP1 [33]. Setuksimab, gefitinib, and talidomid have also been used, but the number of cases is too low for the results to be reliable [34,35].

In one study, chordoma tissue samples were found to contain a large amount of PDGFRB and less but active PDGFRA and KIT [36]. Therefore, imatinib, which is a tyrosine kinase inhibitor, is a good candidate for chordoma treatment. Although phase 2 studies are ongoing, it has already been proven to at least decrease the metastatic ability and improve prognosis [37,38].

In a phase 2 clinical study, lapatinib, which is a dual inhibitor of epidermal growth factor receptor (EGFR) and human epidermal growth factor receptor 2 (HER2) tyrosine kinases, has shown antitumor activity in patients with advanced EGFR-positive chordomas [39].

Yang and colleagues studied the role of Src/Stat3 pathways in chordomas in vitro. Chordomas were found to have high expression levels of Stat3, pSrc, Src, myeloid cell leukemia-1, and Bcl-xL as the key components of the Src/Stat3 signaling cascade. The growth of chordoma cells was inhibited after this pathway was inhibited with CDDO-Me, and apoptosis-associated cleavage was also detected [40]. Thus, c-MET oncoprotein inhibitors and signal transducers as well as blockage of the Src/Stat3 pathway can be considered potential drug targets for chordoma therapy.

Stacchiotti and associates combined the mTOR inhibitor sirolimus with imatinib mesylate and reported a partial tumor response in seven of nine advanced chordoma patients undergoing treatment. The PI3K/mTOR pathway inhibitor PI-103 also had antiproliferative and pro-apoptotic effects on U-CH1 in vitro [41,42]. A phase 2 study of an inhibitor of topoisomerase I, camptothecin (9-NC), showed a delay of progression in a small group of patients with advanced chordomas [43]. Because chordomas have abundant levels of EGFR and c-MET, erlotinib has been used in treatment [44,45]. Gefitinib, which is also an EGFR inhibitor, has been reported to inhibit the proliferation of U-CH1 cells in vitro and patient derived xenograft tumor growth in vivo [46]. A recent study presented promising data for the use of HDAC inhibitors as a therapeutic option for patients with chordomas [47,46].

1.1.6. Prognosis

Chordoma median survival is between 6-7 years with overall survival of 70% after 5 years and 40% after 10 years [48,2]. Skull-base chordoma patients generally have a worse survival rate than sacral chordoma. Complete surgical resection is the best method to treat chordoma in terms of long-term survival rates [22]. Post-surgical radiotherapy increases survival rates and decreases the chance of relapse by presenting a 77% and 69% disease free survival rates after 5 and 10 years respectively [49]. Local recurrence is the main obstacle in chordoma treatment since it is the most important factor in chordoma mortality [23]. Metastasis, which is a relatively rare event in the disease, decreases median survival to less than 12 months [23,24,20]

Skull-base chordoma has been associated with unfavorable prognosis. More clinical factors include older age, large tumor, and extensive local invasion of the primary tumor[50-52]. The position of the tumor and its surrounding tissue is also indicative of prognosis since surgical margins and resectability are significant prognostic factors for the disease [23,18,52].

1.1.7. Chordoma Cell Lines

Although several reported cell lines exist, the lack of full characterization with molecular techniques to evaluate their suitability as in vitro chordoma models means that there are only a few universally accepted chordoma cell lines available for study. Only five cell lines are available at ATCC cell line repository. U-CH1, U-CH2, and MUG-Chor, JHC7 originate from recurrent sacrococcygeal chordomas and UM-Chor1 which is of clivus origin. Four more cell lines are expected to be accepted by ATCC in the near future.

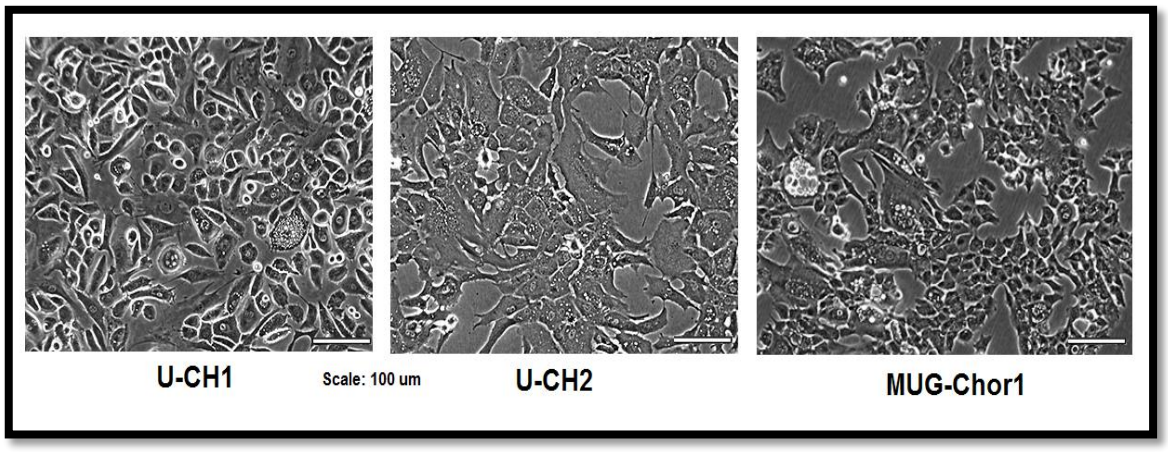

Figure 1.2 Image of three chordoma cell lines that have been used in the study.

1.2. MOLECULAR BIOLOGY OF CHORDOMA

Chordoma is an orphan disease without any specific cure. Although some progress has been seen in surgery and radiology, specific chemotherapy and targeted drugs do not exist for chordoma treatment. Pathways of chordoma initiation and progression should be elucidated for improved treatment options and life quality of chordoma patients. In recent years, molecular characterization has provided noteworthy improvements in the understanding of chordomas. Nonetheless, the tumor's rarity, the lack of sufficient in vitro and in vivo models, and the heterogeneity of this disease emphasize the difficulty in understanding it and developing effective therapies. Despite the concerted efforts to develop novel therapies, further molecular and integrated studies, including genomics, proteomics, animal models, and the precise study of clinical samples, are required to delineate a high-resolution view of chordoma biology. This view will then have an impact on classification, prognosis, treatment decisions, and the development of emerging therapies. We hope that our work here will guide and give fortitude to researchers who study the molecular biology and genetics of chordomas, as well as other types of cancer.

1.2.1. Chordoma cytogenetics

Tumorigenesis is directly related to alterations in the chromosomal structure in neoplasms. Almost half of all chordomas exhibit chromosomal anomalies occurring as late events in tumor progression [53]. Classical G-banding, comparative genomic hybridization (CGH)

and fluorescent in situ hybridization (FISH) techniques have been used to discover anomalies at the chromosomal level in chordomas [54-58].

Persons and colleagues were the first to discover a cytogenetic abnormality in chordomas [59]. Two sacral chordomas, one of which was cytogenetically normal was studied while the other had two different abnormal clones. Scheil and associates analyzed 16 chordomas using array CGH method and detected losses, most prevalently at 3p (five of seven primary tumors, 50%) and 1p (44%). Gains were present on chromosomes 20, 7q, 5q, and 12q (50%, 69%, 38%, and 38% of cases, respectively) [58]. A study of five sporadic and four inherited cases showed deletions on the 1p36 position [60]. In a study of six chordomas using CGH and interphase FISH techniques, duplications were observed in three of the tumors at 1q23~q24, 7p21~p22, 7q, and 19p13 [55].

21 sporadic chordoma samples were analyzed using a genome-wide high-resolution oligonucleotide microarray to detect copy number changes. Numerous stereotypical and recurrent chromosomal abnormalities and concluded that these tumors have significantly unstable genomes. 1p was partially or completely lost in all chordoma specimens. Other common losses were found in chromosomes 3, 4, 9p, 9q, 10, 13, 14, 18, and 22, and common gains were in chromosomes 7 and 19 [61].

1.2.2. Loss of heterozygosity (LOH) studies

Tumor suppressor genes are believed to be inactivated through high-frequency allelic losses at specific chromosomal regions. The first study of LOH in chordomas was done by Eisenberg and associates in 1997. They studied specimens from seven spheno-occipital or clival chordomas and detected LOH at 13q14 (Rb locus) in two, which were particularly aggressive tumors [62]. In a study of microsatellite instability, another group of authors found 12 patients with sacral chordomas with losses in 17p, 9p, and 18q, which are known to contain tumor suppressor genes [63].

In a segregation analysis, locus 1p36.31–1p36.13.3 was correlated with cancer susceptibility and LOH in one family with six sporadic tumors [60]. In a study of LOH in 27 sporadic chordomas, Riva and colleagues found 31 microsatellites localized to 1p36.13 in 25 of the samples, detecting an LOH region mapped to 1p36.13; this finding suggests the importance

of the 1p36 locus in chordomas. These investigators chose CASP9, PAX7, EPH2A, DVL1 and DAN for physical mapping of the LOH region, their possible role in notochord evolution, and their potential oncosuppressor function. The reverse transcription polymerase chain reaction results showed that CASP9, DVL1, and EPH2A transcripts were lacking in 5, 4, and 1 tumors, respectively, suggesting that the CASP9, DVL1 and EPH2A genes may act as a tumor suppressor in chordoma pathogenesis [64].

In a study of skull-base chordoma samples, polymerase chain reaction–based microsatellite LOH analysis of 1p, 9p, 10q, and 17p revealed 1p36 hemizygous deletion and/or 1p LOH frequency in 30%, and 9p LOH and/or 9p21 homozygous deletion frequency in 21%. In addition, 17p13 and 10q23 were shown to have LOH in 52% and 57% of cases, respectively. A correlation with clinical outcomes showed that 9p LOH was associated with a shorter overall survival while no relation to survival was found for LOH at 1p, 10q23, or 17p13 [3].

In one study using tissue microarray immunohistochemistry, 98% of sacral chordomas and 67% of skull-base chordomas were reported to have reduced or absent expression of the fragile histidine triad (FHIT) protein. These results suggest that the FHIT tumor suppressor in chordomas may be lost through epigenetic regulation of this gene and chromosome 3 aneuploidy [65].

1.2.3. Differential diagnosis of chordoma by molecular markers

Among various sarcomas, similar clinical presentations, anatomic locations, and radiologic findings often confuse skull-base chordomas and chondrosarcomas, but these tumors have different origins and prognoses. While chondrosarcomas originate from primitive mesenchymal cells or the embryonic rest of the cartilaginous matrix of the cranium, chordomas of the skull base arise from remnants of the primitive notochord at the spheno-occipital synchondrosis. Chordomas and chondrosarcomas have precise histologic and immunohistologic features, so they usually can be easily distinguished as chordoma is triple positive for EMA, S100 protein and wide spectrum keratins (Table 1.1) . The emergence of Brachyury has also been very helpful for more reliable diagnosis used in combination with the classical markers [66].

When compared to other connective tissue cancers, chordomas express higher levels of genes for collagen II, aggrecan, fibromodulin, cartilage-linking protein, and cartilage oligomeric matrix protein, as characteristic of the extracellular matrix and hyaline cartilage. They also have higher expression of the chondrogenic transcription factor SOX9, fibronectin, MMP9, and MMP19. This expression is like that of chondrosarcomas, chondroblastomas, and chondromyxoid fibromas [67,41,68].

Vujovic and colleagues analyzed the differences and similarities between chordomas and other chondroid neoplasms by examining their expression profiles, showing that brachyury, cytokeratins 8, 15, 18, and 19, CD24 antigen, periplakin, and discoidin domain receptor 1 were expressed in chordomas but not in the chondroid neoplasms. According to this study, the expression of brachyury is characteristic for chordomas. High levels of PDGFR-alpha, a mitogen for connective tissue cells, reticulocalbin 3, a putative endoplasmic reticulum protein, and collagen X, which is implicated in cartilage calcification, were not detected in chordomas [68]. K8 and, to a lesser degree, K19 have been infrequently observed in cases of extraskeletal myxoid chondrosarcomas with chordoid features but, when compared to chordomas, skeletal chondrosarcomas were not seen to express keratins [69].

Table 1.1 Chordoma markers for differential diagnosis.

The name of the marker, chromosomal location, the referring study and role in cancer has been listed.

Marker	**Chromosomal region**	**Study**	**Role in cancer**
EMA	1q21	Walker et al 1991	Promoting chemoresistance and cancer growth, invasion, inhibition of apoptosis
Galectin-3	14q22.3	Gotz et al 1997	Malignant transformation, cancer growth, angiogenesis, invasion and metastasis
E-cadherin	16q22.1	Naka et al 2001	Tumor cell adhesion

Vimentin	10p13	Niwa et al 1994	Metastasis, Tumor growth
CD24	6q21	Oakley et al 2008	Tumor growth, tumor cell invasion and metastasis
CD44	11p13	Saad and Collins 2005	Tumor growth, tumor cell adhesion,migration, invasion and metastasis
Cytokeratin-19	17q21.2	Walker et al 1991	Prevention of apoptosis, promotion of metastasis
Cytokeratin- 8	12q13	Vujovic et al 2006	Tumor progression, metastasis
Cytokeratin-13	17q12-q21.2	Schwab et al. 2009	Tumor growth
Cytokeratin-15	17q21.2	Vujovic et al 2006	Tumor progression
Cytokeratin-18	12q13	O'Hara et al. 1998	Tumor progression
c-met	7q31	Naka et al 1997	Tumor cell invasion and metastasis
Brachyury	6q27	Romeo and Hogendoorn 2006	Tumor progression
FOSB	19q13.32	Schwab et al. 2009	Tumor progression, tumor cell invasion
IL- 18	11q22.2-q22.3	Schwab et al. 2009	Tumor progression, angiogenesis, migration, metastasis, proliferation and immune escape.
FGF 1	5q31	Schwab et al. 2009	Tumor growth, invasion
Syndecan 4	20q12	Schwab et al. 2009	Tumor cell migration, invasion
Integrinbeta 4	17q25	Schwab et al. 2009	Tumor progression, tumor cell invasion
Stat3	17q21.31	Yang et al. 2010	Tumor progression, angiogenesis, invasion and metastasis, inhbition of apoptosis
SRC	20q12-q13	Yang et al. 2010	Tumor progression, metastasis

Bcl-xl	20q11.21	Yang et al. 2010	Chemoresistance
MCL1	1q21	Yang et al. 2010	Chemoresistance
Survivin	17q25	Chen et al. 2013	Inhibition of apoptosis
Periplakin	16p13.3	Vujovic et al 2006	Tumor progression,
PDGF receptor b	5q33.1	Negri et al 2007	Tumor progression, metastasis
KIT	4q11-q12	Negri et al. 2007	Tumor progression
EGFR	7p12	Weinberger et al. 2005	Tumor progression
TGF- alpha	2p13	Tamborini et al. 2010	Tumor progression

1.2.4. Hereditary chordoma

Inherited cases of chordomas have been reported, although they are generally sporadic, and few studies addressed their hereditary occurrence. In a linkage analysis, Kelley and associates revealed the importance of the 7q33 locus in a family with chordomas, while in a genetic study, Yang and coworkers discovered duplications of a region on 6q27 that contained only the brachyury gene in four multiplex families with more than three cases of chordoma. These findings suggest a major role for susceptibility to hereditary chordomas. Cytogenetic studies of familial chordomas focus on the loci 7q33 and 1p36, although, to date, no genes have been associated with the disease [70,54,71,11,72,13].

In another study on 40 chordoma patients and 358 ancestry-matched controls, over 95% of Caucasian chordoma patients were discovered to have an A substituted for a G in the DNA sequence at a specific site on the brachyury gene. These findings showed that this variation in the brachyury gene increased the risk of developing chordoma [73]. A study of genomic screening for linkage in a family showed that there may be a link between a region of chromosome 1, 17, or 19 and the disease [74].

1.2.5. Gene expression and cell signaling

Several studies have been done on the presence and effect of growth factors and structural proteins that are involved in tumor growth and aggressive behavior. Chordomas express

estrogen receptor alpha and progesterone receptor beta, which are associated with tumor progression [75]. In another study, high levels of transforming growth factor alpha and basic fibroblast growth factor expression was linked to higher rates of recurrence, and it was suggested that high fibronectin expression could be a marker of aggressive biological behavior [76]. The high-molecular weight melanoma-associated-antigen (HMW-MAA) is a human membrane-bound protein often overexpressed in melanoma and has a role in invasion and cell migration. The expression of HMW-MAA, also known as chondroitin sulphate proteoglycan 4 (CSPG4), was detected in 62% of 21 chordomas in one study [77].

Scheil-Bertram and colleagues recently carried out a molecular profiling study of chordomas to compare the transcriptional expression profile of one sacral chordoma recurrence, two chordoma cell lines (U-CH1 and U-CH2), and one chondrosarcoma cell line (U-CS2) with a vertebral disc using a high-density oligonucleotide array. These investigators found that 65 genes were expressed differentially. CD24, ECRG4, RARRES2, RAP1, HAI2, RAB38, IGFBP2, osteopontin, GalNAc-T3, and VAMP8 were found to be major potential candidate genes, and their differential expression may play a role in the development of a chordoma [78].

El-Heliebi and associates separated morphologically distinct cell phenotypes, from small to large physaliphorous cells, and analyzed their molecular genetics and transcriptomics. They reported that Mug-chor1 and U-CH1 showed an upregulated level of UCHL3 gene expression in the large physaliphorous cell phenotype. Furthermore, Mug-chor1 showed upregulated levels of ALG11 and PPP2CB expression and differentially regulated TMEM144 expression in the large physaliphorous cell phenotype. They determined that these are putative effector genes for chordoma cell development [79].

The only published proteomic study of chordomas was done by Zhou and colleagues. They conducted a differential proteomic analysis of chordomas and adjacent normal tissues, and identified 14 upregulated and 5 down-regulated proteins. PKM2, ENO1, and gp96 were upregulated in chordomas, and were higher in recurrent samples than in primary ones [80]. Further proteomic studies focusing on recurrence and metastasis would help our understanding of the disease and provide clinicians with novel predictive tools.

Defects in the progression of the cell cycle may cause persistent cell proliferation, and mutations and overexpression of the cell-cycle protein cyclin D1 may lead to cell-cycle

progression and contribute to tumorigenesis. This key regulator of cell proliferation was found to be highly available in 26 chordoma samples [81]. c-MET and epidermal growth factor receptors (EGFR), which are abundant in many types of cancer, are highly expressed in chordomas, whereas c-Erb-b2 (HER2/neu) has been found to be synthesized at various levels [82]. The discovery that chordomas contain high levels of phosphorylated platelet-derived growth factor receptors (PDGFR) has brought about the usage of new chemotherapeutic agents for its treatment [37].

1.2.6. Pathways of chordoma pathogenesis

Many of the signaling networks underlying the tumorigenesis of chordomas have been elucidated in recent years. Han and associates hypothesized that dysregulation in the TSC/mTORC1 pathway may be associated with sporadic chordomas. They examined mTORC1 signaling in the sacral chordoma-derived U-CH1 cell line, 10 sporadic sacral chordoma tumors, and one TSC-associated chordoma, and observed that aberrant hyperactivation of the Akt/mTORC1 pathway was commonly found in the sporadic sacrococcygeal samples [83]. Presneau and colleagues studied the PI3K/AKT/TSC1/TSC2/mTOR pathway in 50 chordoma samples, as there is a correlation between TSC and chordomas, and mTOR is downstream of the TSC1 and TSC2 molecules. In the study, p-mTOR or p-p70S6K was observed in 65% of the samples. In the same study, p-AKT and p-TSC2 were active in almost all of the samples (92% and 96%, respectively) [84]. PI3K/AKT and mTOR pathway activity has been detected in 13 chordoma samples and the inhibition of PI3K/mTOR by PI-103 decreased proliferation and increased apoptosis in U-CH1 cells [41]. FGFR/MEK/ERK/brachyury pathway was found to be important for chordoma cell survival and growth. Chordoma cells were found to express FGFR2, FGFR3 and extracellular signal-regulated kinase (ERK). However, the expression of FGFR1 and FGFR4 was absent. FGF2 was found to be produced by chordoma cells, and its elimination inhibited MEK/ERK phosphorylation [85]. In a recent study using a novel chordoma xenograft, Trucco and coworkers demonstrated the importance of NF-kB activity in dedifferentiated chordoma tumor growth. Bortezomib, an NF-kB inhibitor, slowed the growth of a fast-growing dedifferentiated chordoma tumor. The tumor was also sensitive to IκB inhibition, which is the direct activator of the NF-kB pathway [86].

Chordomas have abnormal activation of the IGF1R/IR signaling pathway, which is an important determinant of aggressive biological potential. In a study by Sommer and colleagues, 41% of chordoma tissue samples had active IGF1R/IR, which was significantly associated with shorter disease-free survival [87]. In a retrospective study on a series of 50 chordomas, 76% of the tumors expressed IGF-1R, 92% expressed IGF-1, and 50% expressed IGF-2; however, this study did not present any data about the activation of these molecules [88].

1.2.7. Cell adhesion and epithelial mesenchymal transition

Cell adhesion proteins participate in cell-cell or cell-ECM interactions during cancer stages. Chordoma tumors are positive for keratin. Several studies have shown that keratins CK8 and CK19, and keratin cocktail AE1/AE3, are expressed in a consistent manner. K5 is almost always expressed, while K7 and K20 are negative or showed sporadic reactivity [89,69,90]. Galectin-3 is available in chordoma tumors and is an immunohistochemical marker to distinguish these lesions from chondrosarcomas [91].

CAM cell adhesion proteins E-cadherin, alpha-catenin, beta-catenin, and gamma-catenin and neural cell adhesion protein NCAM have been found to be present in chordoma samples [92]. Horiguchi and associates showed that the nuclear expression of E-cadherin is a characteristic feature of chordoma. Immunoreactivity for E-cadherin in the nuclei of chordoma tumor cells was found in 68.8 % of cases whereas beta-catenin, a protein-binding E-cadherin, had normal localization [93].

A study of clival chordomas has shown that E-cadherin and N-cadherin expression was inversely correlated, and E-cadherin down-regulation and N-cadherin upregulation correlates with an increased probability of tumor recurrence and death [94]. This study suggests the possible role of epithelial-mesenchymal transition (EMT) in chordomas. Epithelial cells gain their migratory and invasive capability by losing their cell-cell adhesion and turn into mesenchymal cells during the EMT process. EMT is involved in embryogenesis, wound healing, organ fibrosis, invasion, and metastasis in cancer. The loss or reduction of the expression of E-cadherin has been known to have a crucial role in EMT, which accelerates the invasive and metastatic phenotype. N-cadherin is upregulated in many invasive carcinomas and is inversely correlated with E-cadherin.

1.2.8. Significance of Brachyury in Chordoma

A study on the gene expression analysis of mesenchymal tumors showed that a protein specific for the notochord is synthesized in chordoma cells [67]. After this study, microarray and immunohistochemistry experiments disclosed that the brachyury gene is overexpressed in chordoma cells. These findings not only made it possible to distinguish cartilage tumors and chordomas, but also proved that chordomas are of notochordal origin [95,68]. Brachyury, meaning "short tail" in Greek, is a member of the T-box transcription family, which plays an important role in mesodermal development in the embryonic stage [96-98]. It was first cloned in 1991 [99]. Many studies have shown the important role of brachyury in the tail formation of mice [98-100]. In recent years, the focus has been on the presence and effects of brachyury on embryonic stem cells [101-103]. Brachyury expression has also been found in teratomas [104-106], and is highly expressed in several other tumor types including breast, colon, lung, and prostate.

Recently, familial chordomas have been discovered to have a major susceptibility mutation, brachyury gene duplication [13]. Brachyury has been silenced in the JHC7 primary sacral chordoma cell line by shRNA in vitro, which arrested growth [107]. Nelson and associates searched for brachyury target genes with an integrated functional genomics approach, and brachyury was determined to activate transcription. These investigators revealed that brachyury binds directly to 99 targets and controls the expression of 64 other genes indirectly [108].

Pillay and colleagues conducted a genotyping study of 40 individuals with chordomas by sequencing T exons of germline DNA using Sanger and whole-exome sequencing methodologies. The findings showed a strong association between single nucleotide polymorphism (SNP) and rs2305089 in the brachyury gene with the occurrence of chordoma. The variant genotype at this SNP changes the function of brachyury and may cause the misregulation of some genes controlled by this transcription factor. This action can be the leading mechanism underlying the initiation or progression of chordomas [73].

While brachyury is widely accepted as a marker to distinguish chordomas from other tumors of the spine, some data contradicts its functional prognostic role in the disease. Zhang and associates used a tissue microarray to evaluate the effects of the brachyury expression level

on the overall survival rate. Their study found no correlation between the brachyury expression level and clinical situations that indicate a poor prognosis [109].

In studies of adenocystic carcinoma cell lines, the knockdown of brachyury reversed cancer stem-cell and epithelial- mesenchymal properties [110]. Another study showed the immunogenic properties of brachyury, in which specific CD8+ cytotoxic T-cells damaging brachyury-expressing tumor cells were developed from several cell lines. These findings suggest that brachyury is a possible therapeutic target for treating chordomas that express brachyury [111].

1.2.9. miRNA expression

Short RNA sequences 20-30 nucleotides in length are known to regulate the expression of eukaryotic genes. After their discovery in 1993, microRNAs (miRNAs) have been found to be critical in silencing genes and causing transcriptional and translational inhibition. Currently, about 1000 human specific miRNAs have been discovered and there is growing evidence that they contribute to initiation and progression of cancer. miRNAs are known to take part in several biological events including differentiation, proliferation, apoptosis, cancer and metastasis via a variety of mechanisms. Differential regulation of gene expression by miRNAs has been shown in several cancers including non-small-cell lung cancers, prostate cancer, and breast cancer. Using the miRNA profile as a tool in cancer research has provided researchers with very valuable data on cancer molecular biology as well as developmental biology research.

In the miRNA study by Duan and associates two chordoma tissues and the U-CH1 cell line was used. It has been found that miR-1 and miRNA-206 are down-regulated in chordomas when compared to muscle cells [112]. In a follow-up study, miR-1 was found to be down-regulated in 93.7% of the 35 confirmed sporadic chordomas. Furthermore, miR-1 expression was inversely correlated with its putative target, Met expression. The miR-1 level was also correlated with patient survival. In addition, the ectopic expression of miR-1 in chordoma cells resulted in decreased cell growth and proliferation [113].

In a study by Bayrak and colleagues, the miRNA expression profile of eight fresh skull-base chordoma samples and U-CH1 was determined through microarray. In this study, eight

nucleus pulposus samples were used as a healthy control. Nucleus pulposus is a good candidate for a healthy control because increasing data shows that it originates from the notochord. A total of 53 miRNAs were found to be dysregulated. Most notable was that miRNA genes were involved in the initiation and progression of many cancer types, such as miR-31, miR-140-3p, miR-148a, and the miR-221/222 cluster. Functional analyses showed that hsa-miR-31 has an apoptotic effect on chordoma cells and down-regulates the expression of c-MET and radixin [114].

To define the mechanism of the pathogenesis of chordomas, another study compared the miRNA and mRNA profiles of three paraffin-embedded chordomas with three embryonic paraffin-embedded notochord tissues through microarray. The results showed that 33 miRNAs and 2,791 mRNAs were dysregulated between the two groups. Furthermore, 911 of the mRNAs matched up with putative miRNA targets. The MAPK pathway was shown to increase in chordomas in a constant manner through KEGG pathway analysis and down-regulation of miR-663a, miR-149-3p, miR-1908, miR-2861, and miR-3185, which might explain the increase in the activity of their corresponding mRNAs in the pathway [115].

1.2.10. DNA methylation

DNA methylation is an epigenetic modification and a crucial mechanism in mammalian development. Alterations in the pattern of DNA methylation of specific gene regions have roles in the development of diseases and tumorigenesis.

Rinner and associates used 10 chordoma samples for array CGH analysis. In a comparison of blood from chordoma patients with that of healthy individuals, 20 genes were found to be differentially methylated in a significant manner, including tumor suppressor genes such as XIST, FMR1, C3, HIC1, RARB, DLEC1, TACSTD2, RASSF1 and KL in chordomas [116]. An analysis of PTEN and CDKN2A methylation done by Le and colleagues showed that the CDKN2A mechanism was limited to only a small fraction of samples. Data on the availability of methylation in the silencing of PTEN was inconclusive [61].

A clonality study employing methylation-specific PCR has been done on eight sacral chordomas by using an X chromosome inactivation protocol and a polymorphic human androgen receptor gene located on the X chromosome as a marker. The samples studied were

of polyclonal origin. As with other solid tumors, this polyclonality may be caused by an imbalance of chromosomal alterations and increases the difficulty of using molecular targeted therapy in comparison to monoclonal tumors such as hematopoietic malignancies [63].

1.2.11. Tyrosine kinase receptors

The epidermal growth factor receptor (EGFR) is a transmembrane glycoprotein that has functional roles in regulating cellular survival, proliferation, and differentiation. It is related to a poor prognosis, decreased survival, and resistance to chemotherapy and radiotherapy in tumor cells [117].

Shalaby and associates studied the effect of EGFR in chordoma pathogenesis, using immunohistochemistry to analyze 173 chordomas from 160 patients. Nearly 40% of their samples showed a high-level copy number gain of the chromosome band 7p12, where EGFR is located. Furthermore, 69% of the samples were positive for total EGFR expression. These results suggest that it is logical to stratify chordoma patients as EGFR-positive and EGFR-negative for therapy [118].

In another study, immunohistochemical analysis of receptor tyrosine kinase signal transduction activity was monitored in 21 cases of chordoma. HER2, KIT, EGFR and PDGFR-beta were identified in 0%, 33%, 67%, and 100% of cases, respectively. Phosphorylated isoforms p44/42 mitogen-activated protein kinase, Akt, and STAT3, all of which indicate tyrosine kinase activity, were detected in the majority of cases [30]. Another study has reported EGFR expression in 81% of cases of chordoma [119].

A recent study examined the expression of PDGFR-alpha, c-MET, and EGFR in 52 primary and 104 recurrent lesions and noted their consistency with clinicopathological parameters. PDGFR-alpha, EGFR, and c-MET were expressed in 75%, 83%, and 77% of primary tumors, respectively. In addition, all of the investigated tyrosine kinase receptors were found to be expressed in 97% of the recurrent samples. A younger patient age was correlated with higher PDGFR-alpha and c-MET expression, while higher expressions of PDGFR-alpha and EGFR correlated with a poorer prognosis [120].

1.2.12. Apoptosis

The p53 tumor-suppressor protein plays a crucial role in almost all types of human cancers. Mutations in the p53 gene often result in increased levels of the protein because of an increased half-life [121]. An accumulation of p53 has also been observed in chordoma cells [3,122,123]. Functional studies focusing on the effects of abundant p53 in chordomas showed that recurrent and non-recurrent intracranial chordomas had different proliferative potentials. The MIB-1 staining index of recurrent tumors was higher than that of non-recurrent tumors and there was a high correlation between recurrence, a high MIB staining index, and positive staining of cell-cycle-related proteins, especially p53 and cyclin D1 [124]. Another study investigating the expression levels of G1-S checkpoint genes demonstrated that 10% to 45% of primary tumors had alterations in p53, MDM2, cyclin D1 and pRb protein levels. Among all of these G1-S checkpoint protein alterations, only p53 overexpression has been correlated with a reduced overall survival. In a recent study of sacral and skull-base chordomas, overexpression of CDK4, p53, and MDM2 were detected in 20%, 28%, and 56% of the tumors, respectively. The expression of CDK4 and p53 were both correlated with poor overall survival [125].

In a comparative study, Park and colleagues investigated the apoptosis index and proliferation potential of chordomas and notochordal cells, demonstrating that NGF and TrkA receptors were highly expressed in chordoma cells. This finding suggests a possible mechanism of malignant transformation of notochordal remnants to a chordoma by contradicting the apoptotic signal of the p75 receptor. In 10 sacral chordoma tissue samples taken after surgical treatment, the mean proliferation potential index was significantly higher than in notochordal cells, and the mean apoptosis index of chordoma cells was significantly lower compared with that of notochordal cells [126].

Survivin is an inhibitor of apoptosis that belongs to the inhibitor of apoptosis gene family. It augments a tumor’s resistance to various apoptotic stimuli and can block apoptosis either through caspase-dependent or caspase-independent mechanisms [127].

Chen and coworkers found survivin expression in 70% of 30 chordoma samples. Their study showed that survivin expression correlated with recurrence and might be considered as a potential therapeutic target [128].

1.2.13. Invasion and Metastasis

Although generally considered to be slow-growing tumors, in some chordoma tumors are aggressive and metastatic. The literature documents that these tumors metastasize to many locations, including the lungs, bones, and liver. Chordomas are highly invasive tumors locally, and metastasis generally occurs at later stages of the disease. Metastasis occurs in less than 10% of skull-base tumors and 20% to 40% of spinal tumors. Primary tumors usually metastasize to the lungs, bones, liver, and skin. Other sites of metastasis include muscle, retroperitoneum, pleura, and the adrenal glands, spleen, pancreas, heart, kidneys, and urinary bladder [129,23,22,130,20,131,19].

Extensive bone destruction has been observed in chordomas that are coupled with a high recurrence rate [22,132]. Chordomas are unusual bone tumors that have both epithelial and mesenchymal characteristics. Several studies show that the epithelial character of chordomas might be associated with invasiveness. In a study of the local invasiveness of chordomas, high levels of matrix metalloproteinase-1 (MMP-1), matrix metalloproteinase-2 (MMP-2), the tissue inhibitor of metalloproteinase-1 (TIMP-1), cathepsin-B and urokinase plasminogen activator (uPA) have been found. These molecular traits can be associated with tumor infiltration of host bone in most of the primary and recurrent skull-base chordomas. In addition, a poorer prognosis was correlated with higher expression levels of MMP-1 and uPA [133]. Similar results were obtained in another study by the same team, in which patients with spinal chordomas expressing higher MMP-2 had a worse prognosis. In the same study, the expression of low-molecular-weight cytokeratin (CAM5.2) was consistent with TIMP-1, cathepsin B and uPa in skull-base chordomas, and with MMP-1, MMP-2, and uPa in spinal chordomas [134].

Another study of 34 primary spinal chordomas showed a correlated expression with an epithelial marker CAM5.2, indicating an epithelial phenotype. Lesions with higher c-MET expression displayed elevated levels of MMP expression [135]. Chordomas have been reported to have a lower expression of matrix metalloproteinase and urokinase-type plasminogen activator than other primary and metastatic spinal cancers, suggesting probable roles in invasiveness for these enzymes. The roles of MMP-2 and MMP-9 in chordoma invasiveness were revealed in another study [136,137].

The expression of the epithelial marker E-cadherin has been reported repeatedly in chordomas. An immunohistochemical study of seven chordoma cases examined the expression of Ep-CAM, pan-cytokeratin, and E-cadherin, and found that E-cadherin was expressed particularly at the cell-cell adhesion areas, a phenomenon consistent with an invasive tumor phenotype. A similar study showed that expression of N-cadherin was upregulated in chordomas and was associated with reduced recurrence-free survival, which showed an inverse correlation with E-cadherin. The same study showed that the expression of E-cadherin was decreased and correlated with increased mortality. These findings suggest that the cadherins play a crucial role in the malignancy of chordomas [93,138,92,139,94].

Strong expression and proteolytic activity of tumor cell-derived cathepsin K, which is an important protein for invasiveness of tumors, has been observed in chordomas of the clivus [140]. In a study of sacral chordomas, the expression of insulin-like growth factor II mRNA-binding protein 3 (IMP3) was detected in 62.5% of cases, and this IMP3 presence was associated with local muscle invasion, high Ki-67 expression, and tumor recurrence [141].

MET is an integral plasma membrane protein, a tyrosine kinase receptor that has a role in signaling between the extracellular environment and cytoplasm. The elevated expression of MET is a mediator to stimulate tumor growth and metastasis, cell dissociation, and infiltration of tissues [142,143]. The role of HGF/c-MET signaling in tumorigenesis has been investigated many times, and findings suggest that this signaling is associated with tumorigenesis, a poor prognosis, and invasiveness in several sarcomas and carcinomas [143-145]. Two different studies have shown that c-MET expression can be observed in the majority of chordomas [146,82].

Several studies investigated a relationship between c-MET and malignancy. Naka and colleagues investigated the expression of c-MET and HGF in 46 primary and 25 recurrent chordomas to determine their clinicopathological significance, the association between HGF/c-MET signaling and proliferative ability, cell differentiation, prognosis, and the invasive ability of skull-base chordomas. They found that c-MET was expressed in 70% and 88% of primary and recurrent tumors, respectively. A higher expression of low molecular weight cytokeratin (CAM5.2) was correlated with a higher c-MET expression than those with lower CAM5.2 in both primary and recurrent lesions. Urokinase plasminogen activator (uPA) expression was also found to be associated with a higher c-MET expression in primary lesions; however, in recurrent lesions, a higher c-MET expression was found to be related to

the scores of uPA, MMP-1, MMP-2, and the tissue inhibitor of matrix metalloproteinase-1. Patients who had a higher c-MET expression had longer survival times [147].

Although the discoveries about invasion and metastasis are limited, advancements in this field are growing quickly with the development of molecular techniques. In the future, we will see much advancement in the diagnosis, prognosis, and therapeutic targeting of chordomas.

1.2.14. Cancer Stem Cells in Chordoma

The cancer stem-like cell theory originated from observations that tumors are composed of heterogeneous cells, a subset of which contains cells with properties similar to stem cells, such as self-renewal and differentiation. This subset of cells has been related to tumor growth, recurrence, metastasis, and chemoresistance.

The first study of cancer stem cells in chordomas was by Aydemir and associates and showed that skull-base chordoma cells and U-CH1 carried the stem-cell surface markers CD90 and CD105 in abundance. Oct4, klf4, c-myc, sox2, and the embryonic stem-cell markers SSEA-1 and NANOG expression were detected in the samples. In an osteogenic medium, the cancer stem-like cells exhibited significant morphological change and increased alkaline phosphatase activity. Cancer stem-like chordoma cells were observed to grow in non-adherent soft agar medium, which is related to the capability of self-renewal. Differentiating agents also slowed down the migration speed of the treated cells [5, 9]. Furthermore, coupling the chemotherapeutic agents etoposide and cisplatin with the differentiation agent retinoic acid increased the inhibition of cell growth in U-CH1 cells, suggesting that the chemoresistance of chordomas may be a result of the presence of cancer stem cells [148]. ALDH, a common marker for cancer stem cells, was observed in a very small portion of the MUG-Chor1 cell line population [149].

Hu and associates also reported the existence of cancer stem cells. After establishing a chordoma cell line that expressed brachyury, keratin, and S-100, as in classic chordomas, these investigators generated sarcospheres. These sarcospheres had a higher expression of the ALDH1 stem-cell marker, self-perpetuated, and differentiated into neuroepithelial and

mesodermal cell types. Injecting these sarcospheres into an athymic mouse model induced the formation of tumors with the phenotypic properties of chordomas [150].

Increasing data related to the importance of cancer stem cells in tumorigenesis and metastasis show that this cell population may be a powerful target for treatment, but further investigation focusing on the potential role of cancer stem cells in chordomas is required. Chordoma cancer stem-like cells will also be used routinely in basic research as disease models, and patient-derived models of chordoma will ensure advancement in drug screening studies.

1.3. TUMOR PROMOTING INFLAMMATION

The earliest known observation of leukocytes within tumors was presented by Virchow in late 19th century which gives first hints of the relationship of inflammation and cancer. However, accumulation of stronger evidence has occurred in the last decade and elucidation of molecular pathways behind the relationship between tumorigenesis and inflammation [151]. Cancers occur mostly due to mutations and environmental factors. A considerable portion of cancer related environmental factors are associated with inflammation such as chronic infection, tobacco, asbestos inhalation and obesity [152]. Tumor promoting inflammation is now considered as one of the emerging hallmarks of cancer [153].

1.3.1. Tumor Infiltration and Macrophages

In the presence of a tumor, lymphocytes accumulate towards the tissue and migrate inside the tumor mass. These lymphocytes are called tumor infiltrating lymphocytes (TILs). The infiltrating cells are composed of white blood cell types including natural killers, macrophages, B cells and T cells. This event has an obvious and anticipated effect of suppressing the tumor cells and cause good prognosis. However, in more recent studies a surprising effect of these cells have been discovered by which the inflammatory tumor microenvironment is supported by the cytokines secreted. Sites in the tumor, where chronic inflammation persists to exist, were defined as wounds that never healed, pointing out the dual effect of TILs [154]. Leukocytes that have been associated with tumorigenesis can be listed as macrophage subtypes, T cells, B cells, neutrophils and mast cells [155-157]. These

cells release pro-inflammatory molecules such as EGF, VEGF, FGF2, inflammatory chemokines and cytokines and pro-invasive molecules [158,159]. By using these effector molecules, tumor infiltrating inflammatory cells induce angiogenesis, cancer cell proliferation, tissue invasion, metastatic dissemination and seeding [155,157,160,158].

There are limited studies on the presence of TILs in chordoma. In a recent study, PD-L1was found to be highly expressed in chordoma and TILs exist in chordoma tumors. Additionally TILs were correlated with metastasis in chordoma patients [161].

Tumor-associated macrophages (TAMs) account for a major part of tumor infiltrating leukocytes. Although some positive effects could be observed, macrophage infiltration is mostly associated with poor prognosis in breast cancer, Hodgkin's lymphoma, T-cell lymphoma, cervical cancer and melanoma [162-165]. Macrophages are the first immune cells to infiltrate pre-invasive tumor locations by chemotaxis towards the inflammatory products such as CCL chemokines, VEGF and CSF-1, evolve into TAMs by factors such as LIF, TNF-α and IL-6 that are produced by tumor cells. Later, TAMs secrete factors that enhance angiogenesis, local invasion, metastasis and local immune suppression (Figure 1.3).

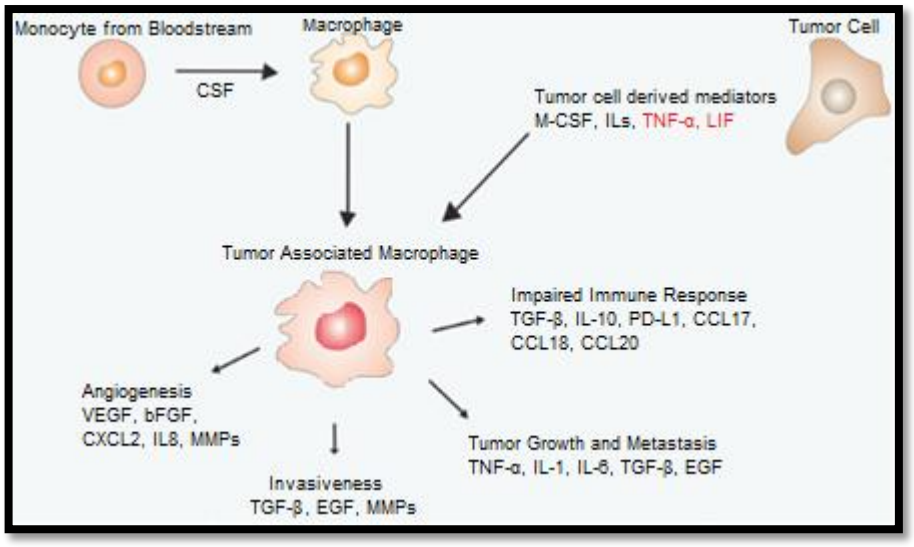

Figure 1.3 Chemotaxis, differentiation and effects of TAMs in the tumor microenvironment. Circulating monocytes are attracted into the tumor location by factors such as VEGF. Colony stimulating factor causes differentiation. Macrophages become TAMs by factors such as LIF and other interleukins and express molecules such as TNF-α, MMPs, VEGF to enhance angiogenesis, tumor growth and metastasis. TAMs also secrete factors that induce local immune suppression.

1.3.2. Tumor Necrosis Factor

EMT is a reversible trans-differentiation process. It plays an important role in embryonic development, sustaining of pluripotency of stem cells and cancer pathogenesis. During EMT, cell polarization occurs, cell-cell interactions weaken and cell motility increases. EMT is known to increase tumor aggressiveness by promoting drug resistance, metastasis and poor clinical outcome.

The EMT process can be monitored by following various cell properties. Most common signs of EMT are cell surface antigens where E-Cadherin, cytokeratins, epithelial membrane antigen (EMA) decrease. An increase in the levels of twist, slug, snail, vimentin, N-Cadherin and fibronectin is observed which fluctuate over the process of transition.

Tumor necrosis factor alpha (TNF-α) is s cytokine that is predominantly secreted by white blood cells, specifically the macrophage. Although the name implies a necrotic and/or apoptotic effect, the molecule may also promote increased survival, motility and invasive abilities. Two types of TNF-α receptors exist, which are called TNFR1 and TNFR2. TNFR1 receptor usually takes part in apoptotic cell signaling cascades in many cell types including tumor cells [166]. However binding of TNF-α to TNFR1 may not always have this effect for cancer cells since activation of the NF-kB pathway by TNF-α has been observed in some cancers which eventually leads to anti-apoptotic activity [167]. TNF-α plays a role inflammation, immunity and cancer progression [168]. TNF has been associated with tumor promoting inflammation and tumor progression. In ovarium cancer TNF-α which was intrinsically produced by cancer cells was shown to increase cell proliferation and tumor progression [169]. In vitro studies in renal carcinoma supported the notion that TNF-α can induce EMT [170]. In ovarium and breast cancers TNF-α increased the level of CD44 which is considered to be a cancer stem cell (CSC) marker [171,172].

The effects of TNF-α on EMT of cancer cells have been studied in breast and renal cancer. In a study on breast cancer, MCF-7 cells that are sensitive to TNF-α were exposed to it in a long term with increasing concentrations. The resulting cells were not only resistant to TNF-α induced apoptosis but also had increased NF-kB activity and a mesenchymal character. Moreover these cells had increased chemoresistance [173]. Similar results were observed in

renal carcinoma cells that have been treated with 50ng/mL TNF-α. The emerging cells were more invasive and showed a more aggressive character [174,175].

1.3.3. Leukemia Inhibitory Factor

During the evolution of a solid tumor, complex cell-to-cell interactions, orchestrated by physical and chemical mediators, occur in the tumor microenvironment [153]. As a member of the interleukin-6 cytokine family, the leukemia inhibitory factor (LIF) is a pleiotropic molecule acting on different types of cells under a variety of conditions. LIF binds to the LIF receptor to activate a number of pathways, such as JAK/STAT3, MAPK, Ras/Raf/MEK/ERK, and PI3K [176-179]. LIF also acts as a pro-inflammatory cytokine in conditions such as arthritis [180,181] and spinal cord injury [182]. Currently, the relationship between LIF and cancer is ambiguous, but LIF overexpression has been observed in a number of cancers including skin, pancreas and breast [183-185]. A relatively small number of studies reveal that LIF has a diverse effect on various types of cancer. LIF can suppress or promote the differentiation of cancer cells and may contribute to disease progression or reduce growth, depending on the tumor type [186-188]. LIF has been shown to promote epithelial-mesenchymal transition (EMT) through miR-21 induction [189], and create a pro-invasive tumor microenvironment in tumor-surrounding fibroblasts [190].

1.4. THE AIM OF THE STUDY

The aim of this project is to evaluate the effects of pro-inflammatory cytokines and miRNAs on expression of relevant genes and pathways for chordoma progression and initiation.

2. MATERIALS AND METHODS

Materials and methods will be explained in four parts.

2.1. INVESTIGATING THE ROLE OF MIR-31 IN CHORDOMA

2.1.1. Expression analysis for quantification of selected miRNAs

The expression levels of four miRNAs (hsa-miR-222, has-miR-140-3p, hsa-miR-148a and hsa-miR-31) differed according to microarray analysis between chordoma and nucleus pulposus samples. These differences were realtime polymerase chain reaction (PCR) using primers obtained from Exiqon (Vedbaek, Denmark). First, cDNA was synthesized from all miRNA samples according to the manufacturer's protocol (Exiqon, Denmark Cat. No.: 203300). All of the reagents, including the enzyme mix, miRNAs, and reaction buffer, were mixed and incubated at 42^{o}C for 60 min. These newly synthesized cDNAs were used as templates for gene-expression analysis through real-time PCR by simply combining the reaction buffer, primer mix, and cDNA in a 96-well plate (Roche, Switzerland Cat. No.: 04729692001).

2.1.2. Data analysis

The data were analyzed using the 2-^{dd}Ct method. During real-time PCR, spike-in control and primers were used to evaluate the efficacy of the procedure. For normalization, 5S RNA was used as a control. Statistical analysis was performed with Student's t test.

2.1.3. Transfection of hsa-miR-31

Ambion FAM3 Dye-Labeled Pre-miR Negative Control #1 (Life Technologies) was used to evaluate the ability of X-tremeGENE siRNA Transfection Reagent (Roche, Switzerland Cat. No.: 04476093001) to transfect U-CH1 cells. After transfection, cells were imaged with a fluorescence microscope. After this validation, hsa-miR-31 (Ambion Pre-miR miRNA

Precursors PM: 114065, USA) was transfected into U-CH1 cells with the X-tremeGENE siRNA Transfection Reagent (Roche,Cat.No. 04476093001) according to the manufacturer's protocol. To control the efficiency of transfection and to determine the intracellular availability of hsa-miR-31, total RNA isolation and miRNA reverse transcription was performed and followed by real-time PCR. The level of hsa-miR-31 was measured at 8, 16, 24, 48, and 72 h after transfection. The control groups were the X-treme-GENE group, in which only the transfection reagent and medium were delivered to cells, the scrambled miRNA group (Ambion Pre-miR miRNA Precursor Molecules—Negative Control #1, USA), and the negative control group, which contained only medium.

2.1.4. Proliferation assay

To evaluate the effect of hsa-miR-31 on proliferation, the CellTiter 96 AQueous One Solution Cell Proliferation Assay (Promega, Fitchburg, WI, USA) was used. MTS analysis was performed at 24, 48, 72 and 96 h after transfection of hsa-miR-31 on cells grown on six-well plates. The control groups were the X-tremeGENE group, in which only the transfection reagent and medium was delivered to cells, the scrambled miRNA group (Ambion Pre-miR miRNA Precursor Molecules—Negative Control #1, USA), and the negative control group, which contained only medium. Proliferation of U-CH1 cells was assessed by measuring the absorbance at 490 nm with an ELx800 Elisa micro-plate reader (Bio-Tek, Winooski, VT, USA). All means and standard deviations were calculated with the Microsoft Excel 2007 SR-2 software package.

2.1.5. Annexin V staining

To elucidate the apoptotic effects of hsa-miR-31 on chordoma cells, annexin V (Roche; Cat.No. 03703126001, Switzerland). staining was performed 48–96 h after transfection of hsamiR- 31 into U-CH1 cells. Staining was carried out according to the manufacturer's protocol.

2.1.6. Flow cytometry

To evaluate apoptosis and necrosis with flow cytometry, the hsa-miR-31 precursor (Ambion Pre-miR miRNA Precursors PM: 114065, USA) was transfected into U-CH1 cells in six-well plates using X-tremeGENE siRNA Transfection Reagent (Roche, Cat. No. 04476093001, Switzerland) according to the manufacturer's protocol. Incubation for 72 and 120 h was followed by staining with annexin V and propidium iodide according to the manufacturer's protocol (BD Pharmingen, Cat.No. 556547, USA). Samples were run on the FACSCalibur flow cytometry device (Becton–Dickinson, Cat. No. 342975, USA).

2.1.7. hsa-miR-31 target genes

To detect oncogene targets that potentially play important roles in chordoma initiation and progression in U-CH1 cells (PIK3C2A, MET, SEPHS1), a validated target (RDX) was selected using online miRNA databases, followed by refinement with Ingenuity Systems (Redwood City, CA). The expression level of the selected target genes was measured at 8, 16, 24, 48, and 72 h after transfection using two-step real-time PCR using TaqMan Gene Expression Assays (Applied Biosystems, Foster City, CA, USA). The control groups were the X-tremeGENE group, in which only the transfection reagent and medium were delivered to the cells, the scrambled miRNA group (Ambion Pre-miR miRNA Precursor Molecules—Negative Control #1), and the negative control group, which contained only medium. GAPDH was used to normalize samples. The data was analyzed with the $2^{-\Delta\Delta}$Ct method.

2.2. THE ROLE OF MIR-31, MIR-140, MIR-148A AND MIR-222 IN CHORDOMA

2.2.1. Cell culture

Chordoma cell lines U-CH1, U-CH2, and MUG-Chor1 available at ATCC bioresource center, were kindly provided by the Chordoma Foundation (Durham, NC, USA). The cell lines were cultured in culture flasks or well plates coated with 0.1% gelatin (SIGMA-ALDRICH cat. no. G1890-100G) with IMDM/RPMI (4:1) 10% FBS containing 10% fetal bovine serum and 1% antibiotics (100 ug/mL streptomycin and 10,000 units/mL penicillin).

Eight nucleus pulposus tissue samples obtained from patients with an acute disc hernia were used as the healthy controls.

2.2.2. Total RNA isolation

Cell lysates were acquired from 6-well plates and T75 flasks with the TRIzol method, according to the manufacturer's protocol, by directly adding the TRIzol reagent (Invitrogen) on monolayer cells or by pelleting after trypsinization with 0.05 trypsin EDTA solution (Life Technologies). RNA was quantified using a NanoPhotometer (IMPLEN).

2.2.3. Expression analysis for quantifying selected miRNAs

With a two-step real-time polymerase chain reaction (PCR) using miRNA PCR primers (Exiqon), the cell lines U-CH1, U-CH2, and MUG-Chor1 were checked for the relative level of the selected miRNAs compared with nucleus pulposus samples by using a LightCycler 480 Instrument II device (Roche). 5S RNA was used as the housekeeping control. The data was analyzed with the $2^{-\Delta\Delta Ct}$ method.

2.2.4. Transfection of miRNA and anti-miRNA mimics

Ambion FAM3 Dye-Labeled Pre-miR Negative Control #1 (Life Technologies) has been used in a previous study to evaluate the ability of X-tremeGENE siRNA Transfection Reagent (Roche) to transfect U-CH1 cells. We used the same method to evaluate the efficiency of transfection of U-CH2 and MUG-Chor1 cell lines. After transfection, cells were imaged with fluorescence microscopy. The pre-miRNA mimics hsa-miR-31 and hsa-miR-222-3p (Ambion Pre-miR miRNA Precursors) and anti-miRNA mimics anti-hsa-miR 140-3p and anti-hsa-miR-148a (Ambion Anti-miR miRNA Inhibitor) were transfected into U-CH1, U-CH2, and MUG-Chor1 cells with X-tremeGENE siRNA Transfection Reagent in 6-well plates, according to the manufacturer's protocol. To control the efficiency of transfection and to determine the intracellular availability of the ectopically expressed or downregulated miRNAs, total RNA isolation and miRNA reverse transcription was

performed, followed by real-time PCR after transfection. The miRNA levels were measured after 8 hours with miRNA real-time PCR.

2.2.5. Cell viability assay

To evaluate the effect of pre-miRNA mimics hsa-miR-31 and hsa-miR-222-3p, and anti-miRNA mimics anti-hsa-miR 140-3p and anti-hsa-miR-148a, on cell viability, chordoma cell lines U-CH1, U-CH2, and MUG-Chor1 were transfected. The CellTiter 96 AQueous One Solution Cell Proliferation Assay (Promega) was used according to the manufacturer's protocol. MTS analysis was done 24, 48, 72, and 96 hours after transfection. As the controls, the X-tremeGENE transfection reagent, the scrambled miRNA group (Ambion Pre-miR miRNA Precursor Molecules or Anti-miR Negative Control #1), and the negative control group, which contained only opti-MEM, were used. Results were obtained by detecting absorbance at 490 nm with an ELx800 Elisa microplate reader (BioTek)

2.2.6. Apoptosis detection with flow cytometry

To evaluate apoptosis and necrosis with flow cytometry, pre-miRNA mimics hsa-miR-31 and hsa-miR-222-3p, and anti-miRNA mimics anti-hsa-miR 140-3p and anti-hsa-miR-148a, were transfected into U-CH1, U-CH2, and MUG-Chor1 in six-well plates using X-tremeGENE siRNA Transfection Reagent according to the manufacturer's protocol. Only the miRNAs that decreased viability were chosen for each cell line. Cells were harvested 48 or 72 hours after transfection, followed by staining with annexin V and 7-AAD, according to the manufacturer's protocol, with the PE Annexin V Apoptosis Detection Kit I (BD Pharmingen) Flow cytometry was done using FACSAria III (BD Biosciences).

2.2.7. Cell cycle analysis

Cell cycle analysis was done 72 hours after transfection of each cell line. Cells were trypsinized, collected, and fixed in ethanol at -20 degrees Celsius for 1 hour. Cells were permeabilized by using Triton X-100 (Sigma) and treated with RNAse A (Qiagen).

Propidium iodide stain was used to visualize the amount of DNA content in the cells by using FACSAria III.

2.2.8. Expression analysis to quantify target and downstream genes

Several website databases (mirdb.org/miRDB/, mirtarbase.mbc.nctu.edu.tw, http://targetscan.org/, pictar.mdc-berlin.de, http://www.microrna.org/, diana.cslab.ece.ntua.gr) were used to choose validated and predicted targets of hsa-miR-31, hsa-miR-140-3p, hsa-miR-148a, and hsa-miR-222-3p (Table 2.1). The predicted targets were chosen to balance prediction match scores and the relevancy of the given genes in potential chordoma initiation and progression. The expression level of the selected target genes was measured 72 hours after transfection. Additionally, the CDH1, CK19, EMA, SNAI1, SNAI2, VIM and CDH2 levels were evaluated. All mRNA levels were measured through two-step real-time PCR with TaqMan Gene Expression Assays (Applied Biosystems, Foster City, CA, USA). The control group was the transfection reagent (X-Treme) group and GAPDH was used to normalize. The data was analyzed with the $2^{-\Delta\Delta}$Ct method.

Table 2.1 The validated and predicted targets of selected miRNAs

miRNA	**Validated Target Genes**	**Predicted Target Genes**
hsa-miR-31	RDX	MET
hsa-miR-140-3p	NRIP1	MAPK1, GOLT1B, CBL, SCAMP1
hsa-miR-148a	DNMT1, DNMT3B	BCL2L11, USP33
hsa-miR-222-3p	TRPS1, BIRC5, STAT5A, MMP1	KIT, CDKN1B

2.2.9. Statistical Analysis

All means and standard deviations were calculated with the Microsoft Excel 2007 SR-2 software package and Graphpad Prism. All results were evaluated by using the two-tailed student's t test.

2.3. LEUKEMIA INHIBITORY FACTOR AND ITS ROLES IN CHORDOMA

2.3.1. Human Chordoma and Nucleus Pulposus Tissue Samples

Over a period of 12 years (2005 through 2016), chordoma tissue samples were obtained from 20 patients at the time of surgery at the Department of Neurosurgery, Yeditepe University Medical School in Istanbul, Turkey. None of the patients had undergone chemotherapy. All chordoma tissues were immediately frozen and stored at -80 °C until RNA extraction. Nucleus pulposus primary cells, which were obtained as described previously[148] from patients with acute disc herniation, were used as a healthy control. To exclude fibrous cells, patients with chronic disc herniation were not included in the study.

Clinicopathological data including age, sex, tumor location, diagnosis, tumor origin, surgery margin, tumor location, recurrence, metastasis, and adjuvant therapy were collected retrospectively. The follow-up time was calculated from the date of surgery until the patient's death or last follow-up. Samples pathologically defined as chordoma were included, while samples with insufficient patient information or a follow-up time of less than 3 months were excluded from the study.

The study was approved by the Institutional Review Board of Yeditepe University Hospital (IRB 98-3943B and 101-4621B), and written informed consent was obtained from all participants.

2.3.2. Cell Culture and LIF Treatment

Chordoma cell lines U-CH1[58] and MUG-Chor1[191], available from the ATCC bioresource center, were kindly provided by the Chordoma Foundation (Durham, NC, USA). Cells were cultured in culture flasks or well plates coated with 0.1% gelatin (SIGMA-

ALDRICH cat. no. G1890-100G) and IMDM/RPMI (4:1) containing 10% fetal bovine serum and 1% antibiotics. Cell lines were checked routinely for molecular markers, polymerase chain reaction (PCR)-based mycoplasma screening and Sanger sequencing were used for short tandem repeat to verify retaining of chordoma character. Recombinant human leukemia inhibitory factor was obtained from Millipore (cat. no. LIF 1050) and administered to cells in medium in a 100 ng/mL concentration.

2.3.3. ICC and Flow Cytometry

LIF-treated cells were detached, washed, and re-suspended in PBS without Ca++ and Mg++. This procedure was followed with the addition of FcR-blocking human reagent (Miltenyi Biotech, cat. no. 120-000-442, Germany), and the cells were incubated for 5 minutes on ice. For each experimental group, cells were separated into one unstained and one stained group. Antibodies recognizing CD15 conjugated with FITC (Miltenyi Biotech, cat. no. 130-081-101, Germany), CD133/1 conjugated with APC (Miltenyi Biotech, cat. no. 130-090-826, Germany), and CD338 conjugated with PerCP-Cy5.5 (BD, cat. no. 561460) were incubated for 30 minutes, then washed with PBS without Ca++ and Mg++ to eliminate unbound antibodies. Both groups were stained with DAPI (Biolegend, cat. no. 422801, USA). Histograms were generated for the stained population, and signal intensity was recorded for each surface marker after the samples were run in FACS Aria III (BD Biosciences, USA). The unstained control was used to determine threshold values. DAPI was used to eliminate non-viable cells.

To visualize LIF receptors on chordoma cell surfaces, cells grown on gelatin-coated coverslips were fixed using the paraformaldehyde-methanol method after 1 and 8 weeks of LIF treatment. Fixed cells were incubated with LIFR conjugated with FITC (Santa Cruz, cat. no. sc-9995, USA) and washed twice with PBS. DAPI stain (Biolegend, cat. no. 422801, USA) was added to the specimen and visualization was done under the fluorescent microscope.

2.3.4. Cell Migration and Invasion Assays

Cell culture inserts of 8,0 µm (Millipore, cat. no. PIEP12R48, Germany) were used to determine the invasiveness and migration capacity of LIF-treated cells. For the invasion, assay chambers were coated with 100 µl of 250 ug/mL basement Matrigel (BD Biosciences, cat. no. 354234, USA) and incubated overnight at 37 degrees C. Cells treated with LIF for 1, 3, 5, and 8 weeks were seeded into the upper chambers at a density of 4x104 in 100-µl serum-free IMDM/RPMI (4:1) medium. The lower chambers were filled with 1 mL IMDM/RPMI (4:1) containing 10% fetal bovine serum. After 24 hours of incubation, the membranes were fixed with 3.7% formaldehyde for 4 minutes and made permeable with methanol for 20 minutes, then stained with crystal violet for 2 minutes. Migrating and invading cells were visualized and counted in four different fields of 400-fold magnification under the inverted microscope.

2.3.5. Colony Formation Assay

The self-renewal capacity of LIF-treated cells under non-adhesive conditions was determined with the colony-formation assay. Six-well plates were coated with 1 mL of IMDM/RPMI (4:1) containing 10% fetal bovine serum and 1% antibiotics with 1% low-melting agarose (Sigma, cat. no. A9045, Germany). After 20 minutes of incubation at 37 degrees C, 1x104 cells were mixed with 1 mL of IMDM/RPMI (4:1) containing 10% fetal bovine serum and 1% antibiotics with 0.7% low-melting agarose. The medium was changed every 3 days. After 3 weeks in culture, the plates were stained with 0.05% crystal violet for quantifying colonies. Colonies containing more than 20 cells were counted under an inverted light microscope.

2.3.6. Tumorosphere Formation Assay

LIF-treated cells (4x105 at 1, 3, 5 and 8 weeks) were seeded in 25-cm2 culture flasks coated with 2% agarose and 0,9% NaCl. The media used for sphere formation was IMDM/RPMI (4:1) with 1% antibiotics, 20 ng/ml human FGF-2 (BD Biosciences), 20 ng/ml EGF (BD Biosciences), 1X N2 supplement (Gibco, USA), and 1X B27 supplement (Gibco) during the

culturing of cells at 37 degrees C in a 5% CO2 incubator. Clusters formed by MUG-Chor1 cells were checked routinely and were dispersed by gentle pipetting. After 3 weeks, spheroid bodies were transferred to 96-well plates and quantified under an inverted microscope (Leica, Germany) at 400X magnification.

2.3.7. Chemoresistance Assay

To evaluate the effect of LIF on chemoresistance, 2.5x104 cells were seeded into 24-well plates in duplicates after 1, 2, 5 and 8 weeks of LIF administration. Freshly prepared 0.012 μM paclitaxel and 0.012 μM bortezomib in chordoma medium was added to the cells and changed every 2 days. An MTS assay was conducted after 7 days to assess the relative viability of LIF-treated cells and controls.

2.3.8. Microarray

For microarray analysis, total RNA isolated with Trizol (Thermo Fisher Scientific, cat. no. 15596026, USA) from U-CH1 and MUG-Chor1 cells treated with LIF for 3 weeks was used for whole transcriptome analysis with the Human Gene 2.1 ST Array (Affymetrix, GeneAtlas system, USA) according to the manufacturer's protocol. The resulting data were analyzed with Transcriptome Analysis Console 3 software (Affymetrix, USA).

2.3.9. Quantitative Gene Expression Analyses

Twenty fresh-frozen primary clival chordoma tissues were homogenized by using liquid nitrogen with a mortar and pestle, followed by the immediate addition of TRIzol according to the manufacturer's protocol. Cell lysates of 6 cultured nucleus pulposus cells from patients with acute disc herniation were used to acquire total RNA with the TRIzol method, as described previously [148]. RNA was quantified using a NanoPhotometer (Implen, Germany). Total RNA was isolated from LIF-treated cells and their controls with the TRIzol method, according to the manufacturer's protocol. All mRNA levels were measured through two-step real-time PCR with TaqMan Gene Expression Assays (Applied Biosystems, Foster

City, CA, USA). Relative mRNA levels were detected with the $2^{-\Delta\Delta Ct}$ method with GAPDH as the housekeeping gene. Analyses were conducted by normalizing with the control groups.

2.3.10. Statistical Analysis

The microarray data were analyzed with one-way repeated measures of ANOVA (paired) by using two controls and two LIF-treated samples. Clinicopathological features age, sex, tumor location, recurrence, metastasis, and survival were analyzed for their correlation with LIF expression level. Correlations were evaluated with Spearman's rank correlation test (n=12). The overall survival graph was sketched by using Kaplan-Meier survival analysis with the Mantel-Cox test (n=20). All other p values were obtained with two-tailed Student's t-test using at least triplicates (n>3) for each experiment. A value of $p<0.05$ was considered statistically significant. The high and low LIF groups of patients were separated into groups of equal number according to the relative median LIF levels. Significant outliers were evaluated for each experiment and removed from analysis.

2.4. TUMOR NECROSIS FACTOR AND CHORDOMA

2.4.1. Cell Culture and TNF-α Treatment

Chordoma cell lines U-CH1 [58] and MUG-Chor1 [191] and U-CH2 available from the ATCC bioresource center, were provided by the Chordoma Foundation (Durham, NC, USA). Cells were cultured in culture flasks or well plates coated with 0.1% gelatin (SIGMA-ALDRICH cat. no. G1890-100G) and IMDM/RPMI (4:1) containing 10% fetal bovine serum and 1% antibiotics. Routine checking was made for molecular markers, polymerase chain reaction (PCR)-based mycoplasma screening and Sanger sequencing were used for short tandem repeat to verify retaining of original cell line characteristics. Human recombinant TNF-α was obtained from SIGMA (cat. no. T0157). TNF-α was administered to cells in 10 ng/mL in short-term experiments. U-CH1 and MUG-Chor1 cells was administered with TNF-α for 12 months to obtain long term TNF-a treated cells (LT-TNF) cell lines with TNF-α concentration gradually increasing from 2.5 and 5 to10 ng/mL. The cell lines were grown in 10 ng/mL TNF-α thereon. NF-kB inhibitor QNZ

(Sigma-Aldrich Cat. SML0579 Germany) was administered to cells alongside TNF-α as the TNF+QNZ control for long term treatment. To see prolonging effects of long-term TNF-α treatment LT-TNF U-CH1 and MUG-Chor1 cell lines were deprived of TNF-α for 6 months and another control group was established as the TNF-α deprivation group. PI3K inhibitor wortmannin (Sigma-Aldrich Cat. W1628 Germany) was used as a controls for the PI3K-Akt pathway.

2.4.2. ICC and Flow Cytometry

Cells were detached, washed, and re-suspended in PBS without Ca++ and Mg++. This procedure was followed with the addition of FcR-blocking human reagent (Miltenyi Biotech, cat. no. 120-000-442, Germany). Cells were incubated for 5 minutes on ice. CD338 conjugated with PerCP-Cy5.5 (BD, cat. no. 561460) was incubated for 30 minutes, then washed with PBS without Ca++ and Mg++ to eliminate unbound antibodies. Both groups were stained with DAPI to eliminate dead cells (Biolegend, cat. no. 422801, USA).
To visualize the behavior of NF-kB molecules, LT-TNF cells grown on gelatin-coated coverslips were fixed using the 4% paraformaldehyde method. Fixed cells were treated with 1% BSA for blocking and incubated overnight with primary anti-NF-kB p65 antibody (Abcam, cat. no. ab16502, USA), then washed with 1.5% PBS-Tween. Alexa Fluor 488 labeled goat anti-Rabbit IgG was added and incubated for 1 hour (Thermo-Fisher, cat. No. A-11034, USA). DAPI stain (Biolegend, cat. no. 422801, USA) was added to the specimen and visualization was done under the fluorescent microscope.

2.4.3. Cell Migration and Invasion Assays

Cell culture inserts of 8.0 μm (Millipore, cat. no. PIEP12R48, Germany) were used to determine the invasiveness and migration capacity of TNF-treated cells. For the invasion, assay chambers were coated with 100 μl of 250 μg/mL basement Matrigel (BD Biosciences, cat. no. 354234, USA) and incubated overnight at 37^{o}C. Cells were seeded into the upper chambers at a density of $4x10^{4}$ in 100-μl serum-free IMDM/RPMI (4:1) containing TNF-α (10 ng/mL). The lower chambers were filled with 1 mL IMDM/RPMI (4:1) containing 10% fetal bovine serum. LT-TNF cells were seeded into chambers with medium lacking TNF-α.

For short term effect analysis U-CH1 and MUG-Chor1 cells were seeded with serum-free complete medium, serum-free complete medium+TNF, serum-free complete medium+TNF+QNZ and serum-free complete medium+TNF+wortmannin groups. After 24 hours of incubation, the membranes were fixed with 3.7% formaldehyde for 4 minutes and made permeable with methanol for 20 minutes, then stained with crystal violet for 2 minutes. Migrating and invading cells were visualized and counted in four different fields of 400-fold magnification under the inverted microscope.

2.4.4. Colony Formation Assay

The self-renewal capacity of LT-TNF cell lines under non-adhesive conditions was determined with the colony-formation assay. Six-well plates were coated with 1 mL of IMDM/RPMI (4:1) containing 10% fetal bovine serum and 1% antibiotics with 1% low-melting agarose (Sigma, cat. no. A9045, Germany). After 20 minutes of incubation at 37^{o}C, 1x10^{4} cells were mixed with 1 mL of IMDM/RPMI (4:1) containing 10% fetal bovine serum and 1% antibiotics with 0.7% low-melting agarose. The medium was changed every 3 days. After 3 weeks in culture, the plates were stained with 0.05% crystal violet for quantifying colonies. Colonies containing more than 20 cells were counted under an inverted light microscope.

2.4.5. Tumorosphere Formation Assay

LT-TNF cells (4x10^{5}) were seeded in 25-cm2 culture flasks coated with 2% agarose and 0.9% NaCl. The media used for sphere formation was IMDM/RPMI (4:1) with 1% antibiotics, 50 ng/ml human FGF-2 (BD Biosciences), 50 ng/ml EGF (BD Biosciences), 1X N2 supplement (Gibco, USA), and 1X B27 supplement (Gibco) during the culturing of cells at 37^{o}C in a 5% CO2 incubator. Cell clusters were routinely dispersed by using serological pipette. After 4 weeks, spheroid bodies were transferred to 96-well plates and quantified under an inverted microscope (Leica, Germany) at 400X magnification.

2.4.6. Chemoresistance Assay

To evaluate the effect of TNF-α on chemoresistance, 2.5x104 cells were seeded into 24-well plates in duplicates after. Freshly prepared 0.012 μM paclitaxel and 0.012 μM bortezomib in chordoma medium was added to the cells and changed every 2 days. An MTS assay was conducted after 7 days to assess the relative viability of LT-TNF treated cells and controls.

2.4.7. Microarray

For microarray analysis, total RNA isolated with Trizol (Thermo Fisher Scientific, cat. no. 15596026, USA) from U-CH1 and MUG-Chor1 cells treated with TNF-α for 1 week (n=2), for 12 months (n=4) and untreated cells (n=6) were used for whole transcriptome analysis with the Human Gene 2.1 ST Array (Affymetrix, GeneAtlas system, USA) according to the manufacturer's protocol. The resulting data were analyzed with Transcriptome Analysis Console 3 software (Affymetrix, USA). Additional analysis was made using Ingenuity Pathway Analysis (Qiagen, USA) and DAVID internet database.

2.4.8. Quantitative Gene Expression Analyses

RNA was quantified using a NanoPhotometer (Implen, Germany). Total RNA was isolated from TNF-α treated cells and their controls with the TRIzol method, according to the manufacturer's protocol. All mRNA levels were measured through two-step real-time PCR with TaqMan Gene Expression Assays (Applied Biosystems, Foster City, CA, USA). Relative mRNA levels were detected with the $2^{-\Delta\Delta Ct}$ method with GAPDH as the housekeeping gene. Analyses were conducted by normalizing with the control groups.

2.4.9. Statistical Analysis

The microarray data were analyzed with one-way between subjects ANOVA (unpaired). All other p values were obtained with two-tailed Student's t-test using at least triplicates (n>3) for each experiment. A value of $p<0.05$ was considered statistically significant. Significant outliers were evaluated for each experiment and removed from analysis.

3. RESULTS

3.1. INVESTIGATING THE ROLE OF MIR-31 IN CHORDOMA

This section has been published as "MicroRNA expression profiling reveals the potential function of microRNA-31 in chordomas." J Neurooncol. 2013 Nov;115(2):143-51. doi: 10.1007/s11060-013-1211-6. Epub 2013 Aug 3.

3.1.1. hsa-miR-31 transfection

The transfection capability of the X-tremeGENE siRNA Transfection Reagent, when used with U-CH1 cells, was evaluated by using Ambion FAM3 Dye-Labeled Pre-miR Negative Control #1. Fluorescence microscopy showed that the FAM-labeled miRNA constructs were successfully transfected into cells (Figure 3.1). Therefore, transfections were carried out with the X-tremeGENE siRNA Transfection Reagent. After transfection, real-time PCR was performed to show the presence and processability of the transfected hsa-miR-31. RNA samples were isolated from U-CH1 cells, eight, 16, 24, 48, and 72 h after transfection by hsa-miR- 31. Results showed that the hsa-miR-31 expression level was highest eight hours after transfection. The hsa-miR- 31 expression level then decreased gradually until day four (Figure 3.2).

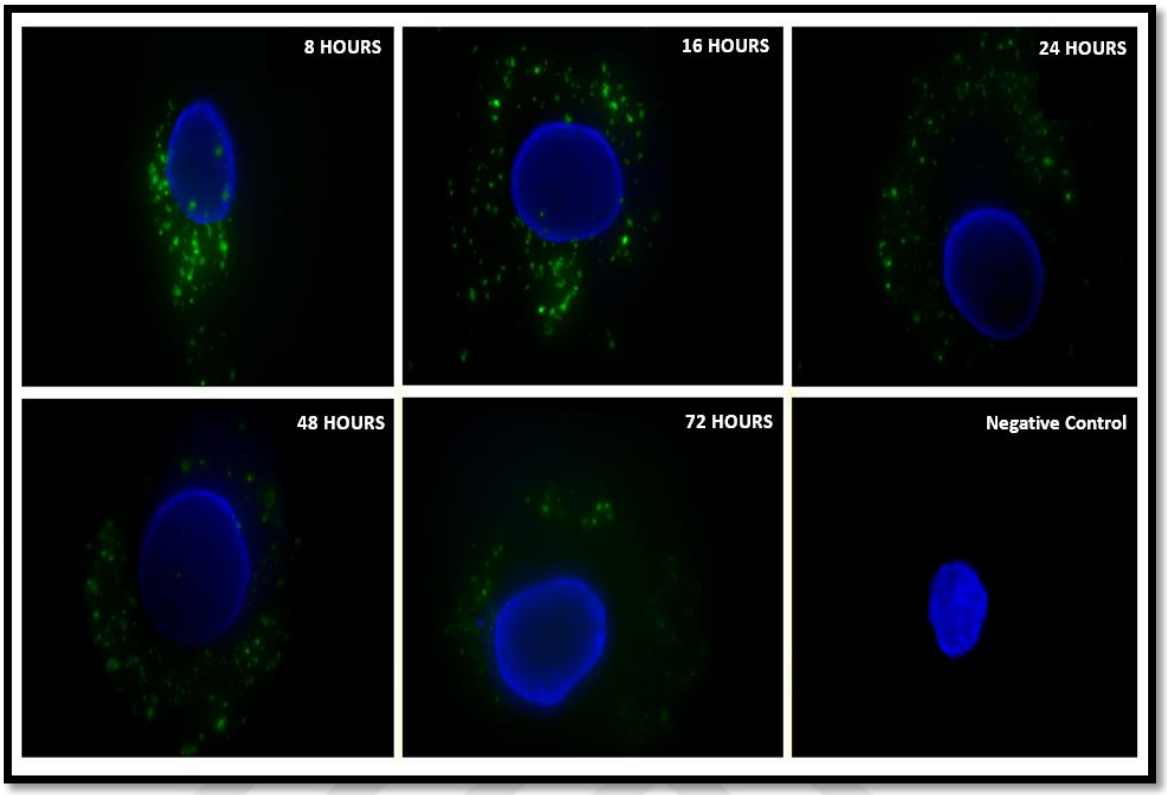

Figure 3.1 FAM-conjugated scrambled miRNA molecules were transfected into U-CH1 cells for direct observation of cellular uptake. The green spots represent FAM-labeled miRNAs and the nucleus is stained with DAPI (blue)

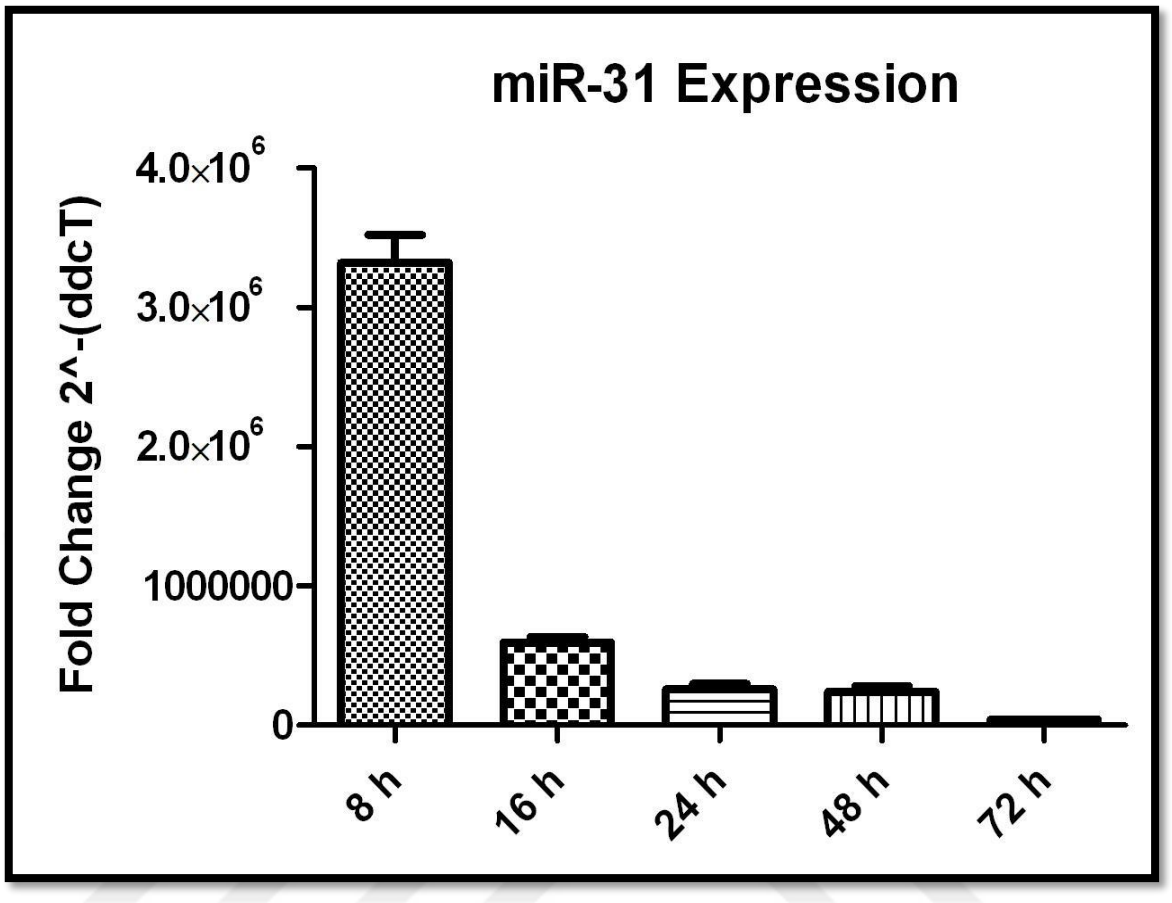

Figure 3.2 Expression of hsa-miR-31 at 8, 16, 24, 48 and 72 h after transfection into U-CH1 cells.

3.1.2. hsa-miR-31 and the proliferation of U-CH1 cells

To investigate the effect of hsa-miR-31 on the proliferation of U-CH1 cells, MTS tests were performed. Seventy-two hours after hsa-miR-31 transfection, U-CH1 cell viability was reduced by 27 % (Figure 3.3).

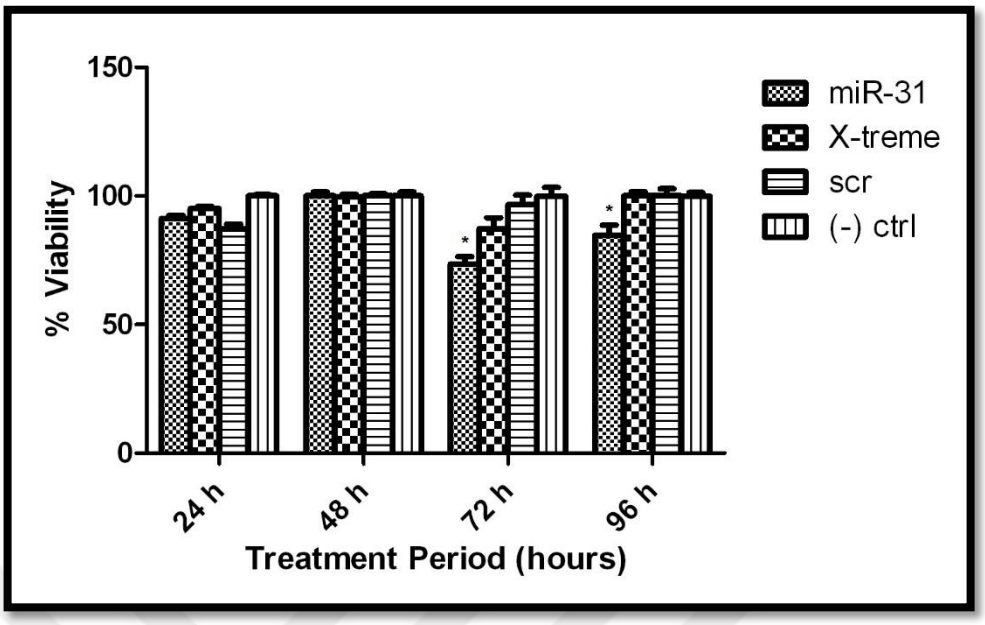

Figure 3.3 MTS cell proliferation results following transfection of hsa-miR-31 into U-CH1 cells. '*' indicates $p<0.05$

3.1.3. hsa-miR-31 and apoptosis in U-CH1 cells

To further examine the decreased proliferation of U-CH1 cells after hsa-miR-31 transfection, hsa-miR-31-transfected U-CH1 cells were stained with annexin V to evaluate the apoptotic effects of hsa-miR-31. Flow cytometry revealed that hsamiR-31-transfected cells have a significantly higher apoptosis rate after 72 and 120 h compared to non-transfected cells (Figure 3.4).

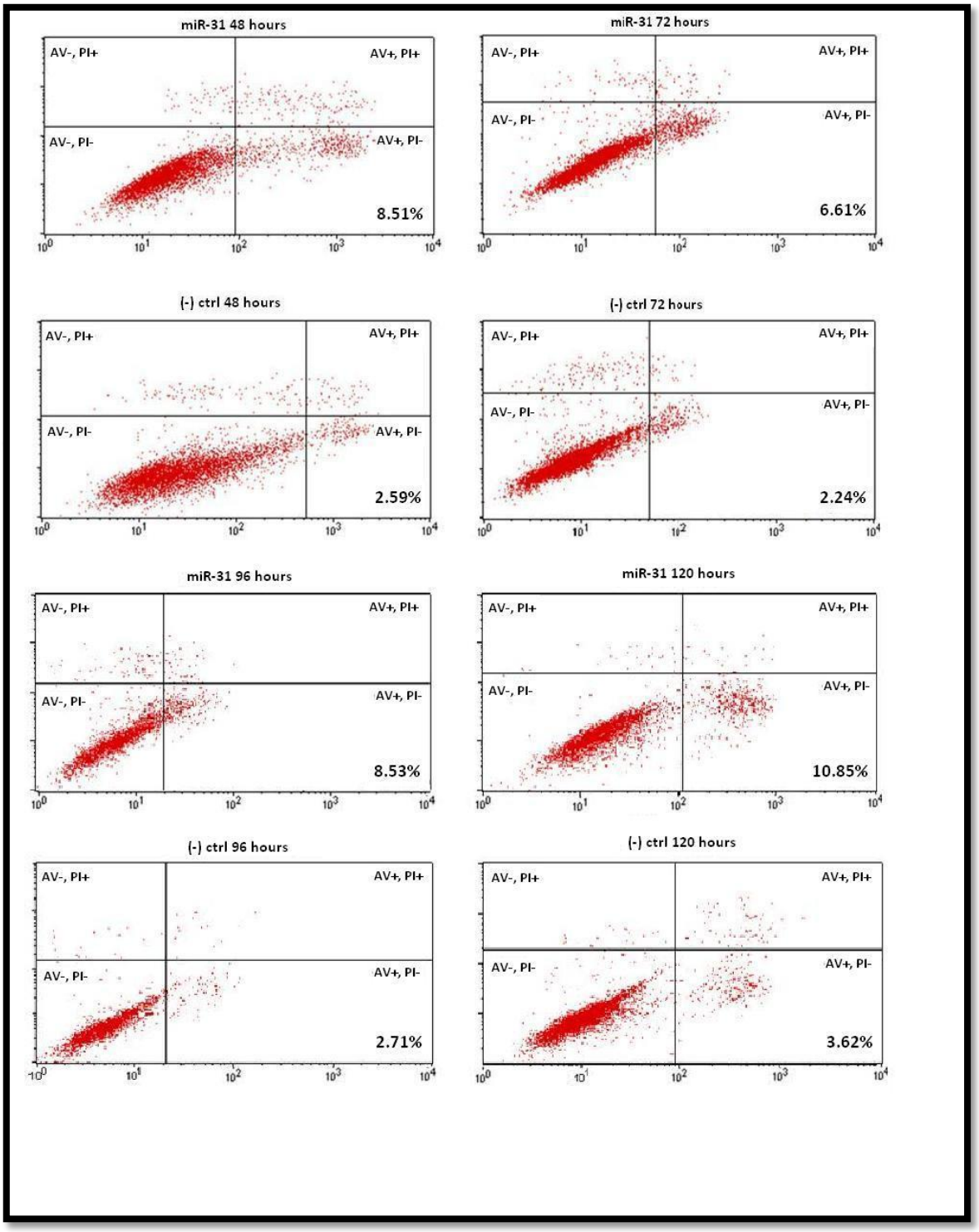

Figure 3.4 Dot plot showing Annexin/PI staining of U-CH1 cells grown on six-well plates

3.1.4. hsa-miR-31 and the expression of c-MET and radixin

RT-PCR analysis revealed that hsa-pre-miR-31 transfection decreases the relative expression of its predicted target, c-MET, and its confirmed target, radixin, in U-CH1 cells. Relative c-MET expression was lowest after 48 h (44 %) and relative radixin expression was as low as 75 % after 16 and 24 h. The changes in PIK3C2A and SEPHS1 expression were insignificant (Figure 3.5).

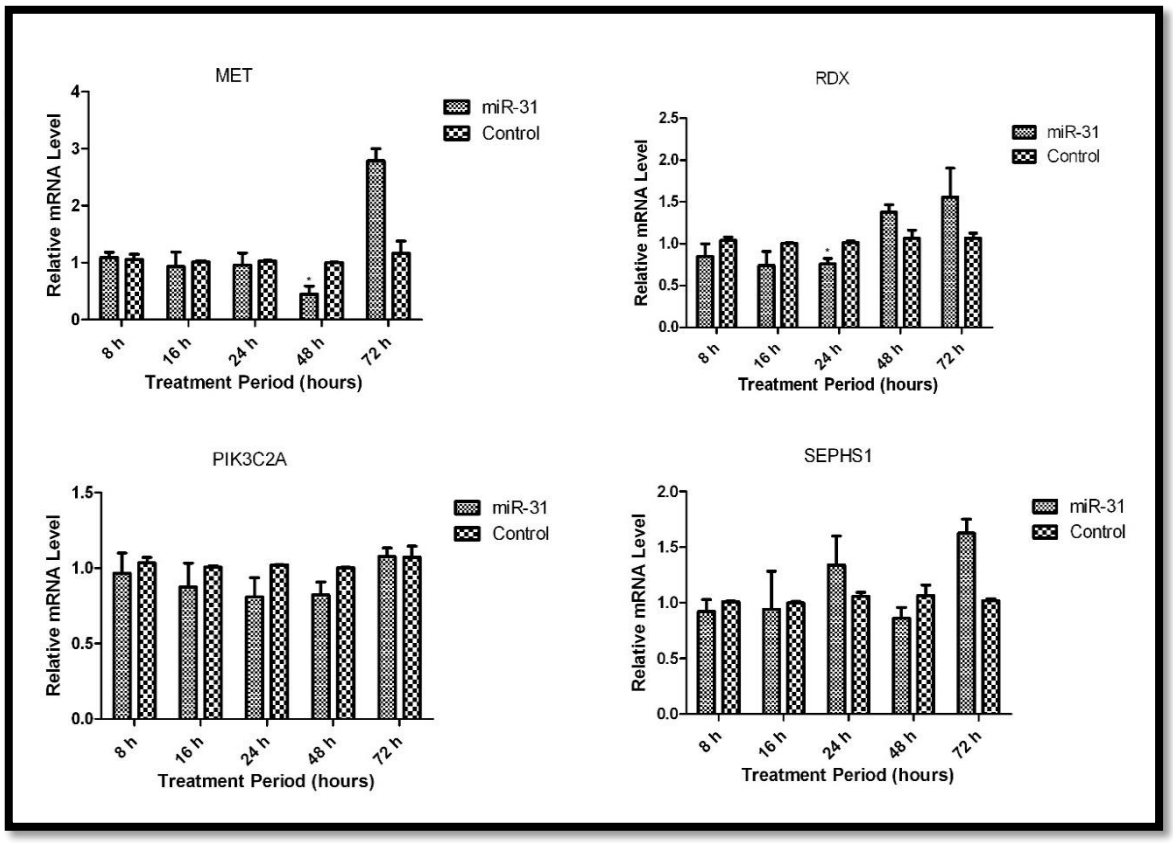

Figure 3.5 Relative mRNA levels of predicted and confirmed targets of miR-31 by RT-PCR at 8, 16, 24, 48 and 72 h after transfection.

3.2. THE ROLE OF MIR-31, MIR-140-3P, MIR-148A AND MIR-222 IN CHORDOMA

This section has been published as "The potential function of microRNA in chordomas." Gene. 2016 Jul 1;585(1):76-83. doi: 10.1016/j.gene.2016.03.032. Epub 2016 Mar 23.

3.2.1. Differential expression of miRNAs in chordoma cell lines

Levels of hsa-miR-31, hsa-miR-140-3p, hsa-miR-148a, and hsa-miR-222 were compared with real-time PCR by using total RNA from U-CH1, U-CH2, and MUG-Chor1 cell lines. The expression of miR-148a and miR140-3p selected miRNAs had a similar pattern in all three cell lines (Figure 3.6 b,c), whereas miR-31 was more abundant in U-CH2 than in the nucleus pulposus control (Figure 3.6 a). miR-222-3p was downregulated in U-CH1 compared to nucleus pulposus, and upregulated in U-CH2 and MUG-Chor1 (Figure 3.6 d).

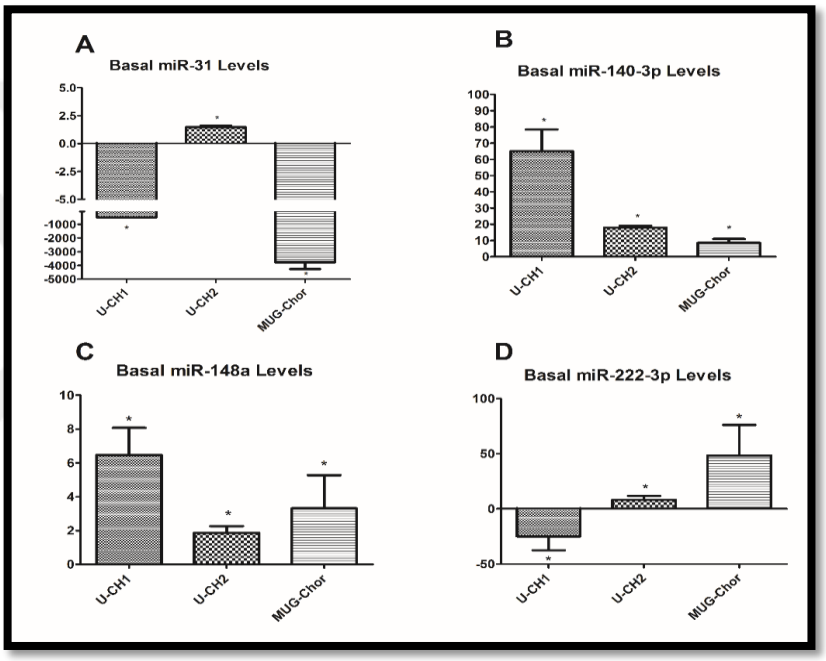

Figure 3.6 A mixed pattern of miRNA expression has been observed in the 3 chordoma cell lines. (A) miR-31 is highly downregulated in U-CH1 and MUG-Chor1 but it is slightly upregulated in U-CH2. (B,C) miR-140-3p and miR-148a are upregulated in all three cell lines. (D) miR-222-3p is downregulated in U-CH1 and upregulated in U-CH2 and MUG-Chor1. '*' indicates $p<0.05$.

3.2.2. Pre-miR and anti-miR mimics were successfully transfected into cell lines

We assessed the transfection capability of the X-tremeGENE siRNA Transfection Reagent, the processibility of pre-miR mimics into mature miRNA, and the ability of the anti-miR mimics to suppress their target miRNAs. Transfection into U-CH1 has been previously optimized [114]. For U-CH2 and MUG-Chor1, we used Ambion FAM3 Dye-Labeled Pre-

miR Negative Control #1 to visualize the presence of miRNA molecules inside the cell after transfection. Fluorescence microscopy showed that the FAM-labeled miRNA constructs were successfully transfected into U-CH2 (Figure 3.7 a) and MUG-Chor1 (Figure 3.7 b). No green fluorescence was detected in the control group (Figure 3.7 c). Pre-miR and anti-miR mimics were transfected into U-CH1, U-CH2, and MUG-Chor1, and followed by real-time PCR after 8 hours. Results showed that the pre-miR mimics significantly increased the level of their mature miRNA counterparts, while the anti-miR mimics significantly decreased theirs (Figure 3.7 d).

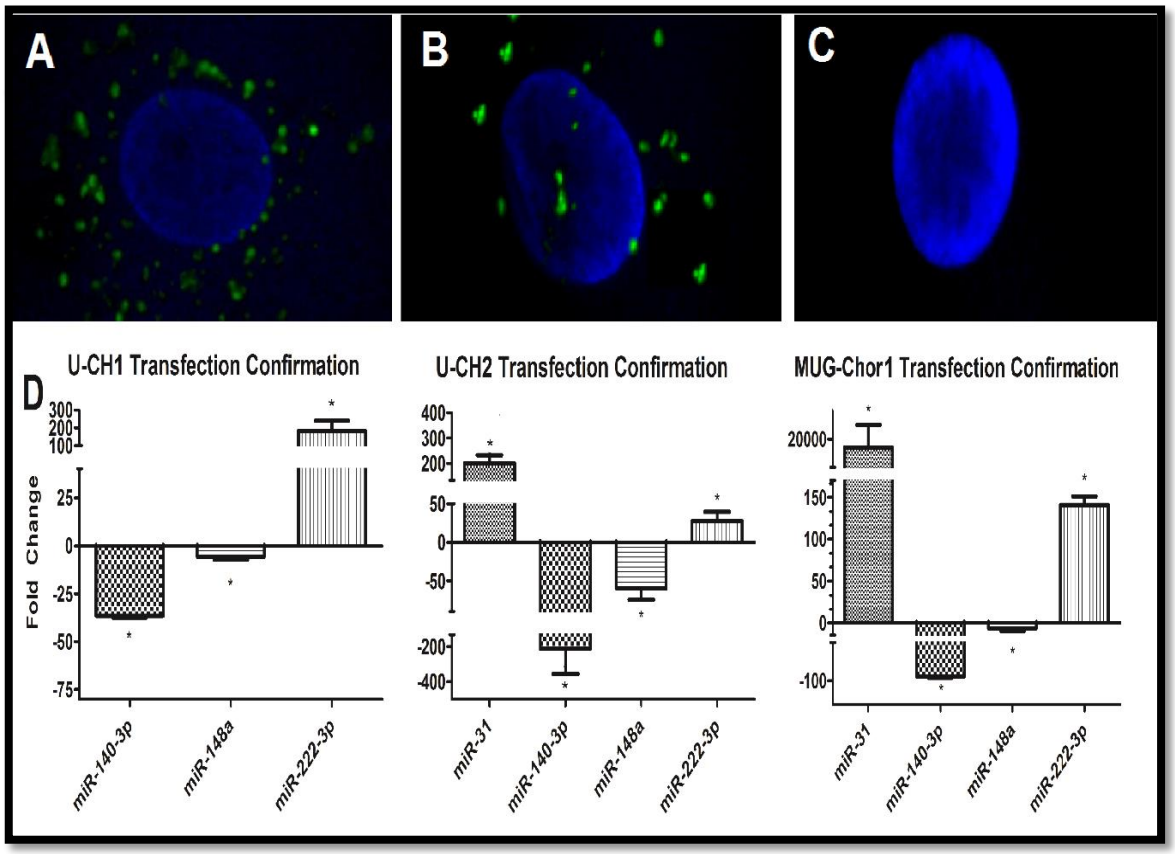

Figure 3.7 The miRNA levels were successfully controlled by transfection. Cell were transfected with FAM-labeled miRNA mimic (green) and nuclear DAPI staining (blue) visualized under fluorescent microscope captured under 100X objective. (A) U-CH2 (B) MUG-Chor1 (C) U-CH2 X-Treme control. (D) U-CH1, U-CH2 and MUG-Chor1 transfected with Anti-miRNA and Pre-miRNA mimics. Anti-miRNA mimics for miR-140-3p and miR-148a caused a decrease in their target miRNA level while Pre-miR mimics for miR-31 and miR-222 increased the abundance of the miRNA in the cell. '*' indicates $p<0.05$

3.2.3. Effects of miRNA level on cell viability

To assess how the abundance of each miRNA plays a role in the viability of chordoma cells, MTS tests were done 24, 48, 72, and 96 hours after transfection. Pre-miR-31 and anti-miR-148a were found to significantly decrease viability in all three cell lines after 72 and 96 hours. Anti-miR-140-3p decreased viability in U-CH1 after 72 and 96 hours, and U-CH2 after 72 hours, but had no effect on MUG-Chor1 cell viability. We also observed a decreased viability effect of pre-miR-222 on U-CH2 (Figure 3.8).

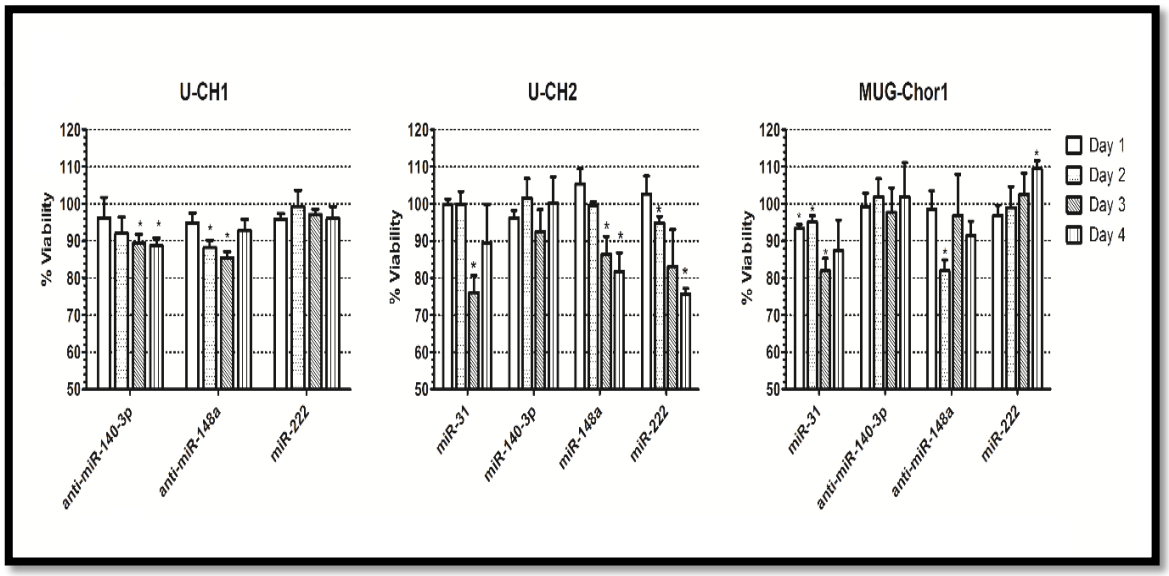

Figure 3.8 . miRNAs showed anti-proliferative effect on chordoma cell lines. Percentile viability was measured by normalizing the light signal from the MTS assay using the transfection reagent control group. '*' indicates $p<0.05$.

3.2.4. Effects of the selected miRNAs on apoptosis

Pre-miR and anti-miR molecules that had an effect on cell viability were transfected into cell lines to verify whether the decrease in cell viability was due to apoptosis. In flow cytometry analysis, the population for apoptotic cells was chosen as the Annexin V positive and 7AAD negative cells to eliminate any confusion of late apoptotic and necrotic cells which are positive for both Annexin V and 7AAD. Results showed that the selected miRNA mimics and anti-miRNA molecules significantly increased apoptosis after 72 hours by 40% (U-CH2 and anti-miR-148a) to 125% (MUG-Chor1 and miR-31-3p) when compared with the X-Treme control (Figure 3.9).

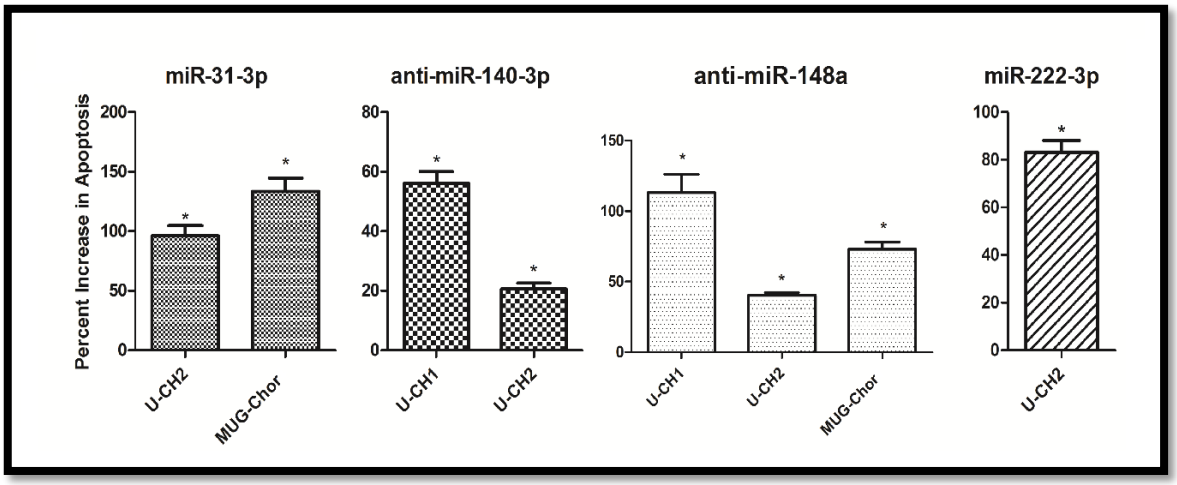

Figure 3.9 The decrease in cell viability is potentially caused by apoptosis. Each miRNA and cell line combination that had decreased viability in the MTS assay was checked for the apoptosis rate. The results indicate the percent increase in the number of the early apoptotic population in the apoptosis assay by flow cytometry, namely the Annexin V+/ 7AAD- negative cells. '*' indicates $p<0.05$.

3.2.5. Effects of the selected miRNAs on the cell cycle

For cell cycle analysis, we selected the miRNAs for each cell line that showed a significant effect on cell viability. Cell cycle histograms were analyzed to obtain the percentage of G0/G1, S, and G2/M populations for U-CH1, U-CH2, and MUG-Chor1. The gene transfection reagent was used as a control for each cell line (X-Treme). We found that miR-31-3p increased the S-phase cell population from 15.16% to 19.43% in U-CH1, from 10.53% to 20.97% in U-CH2, and from 16.70% to 21.29% in MUG-Chor1. The number of cells in the G2/M decreased as the S-phase arrest increased, while no significant changes were observed in the G0/G1 populations. Similar results were observed with the other selected miRNAs but to a lesser extent (Fig 3.10).

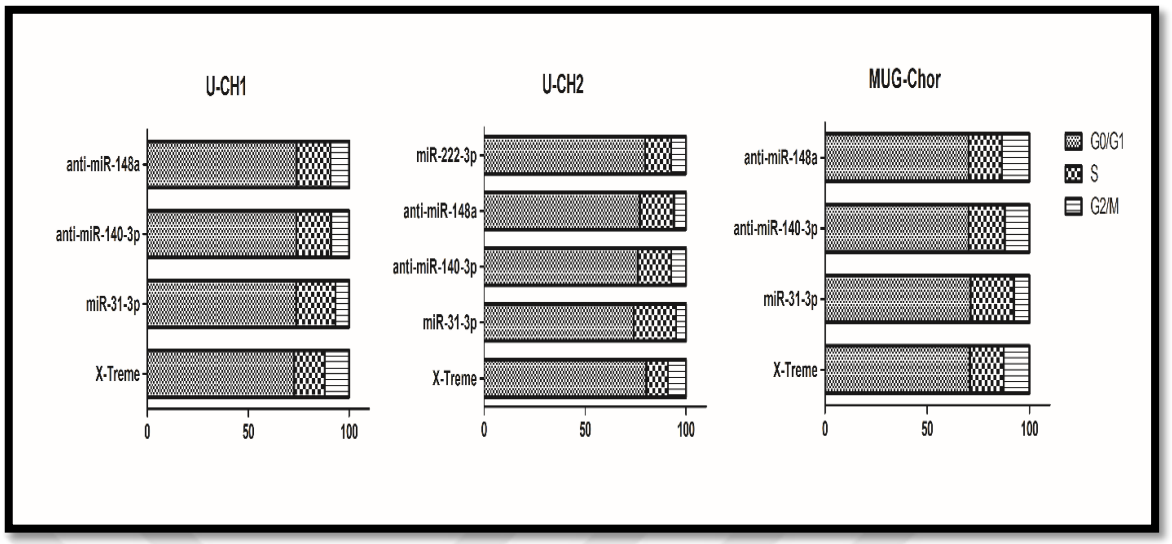

Figure 3.10 Cell cycle analysis by flow cytometry. Percentages of cells in the G0/G1, S and G2/M phases indicated in the bar graph reveal that the selected miRNAs slow down cell growth by increasing the number of cells in the S phase. miR-31 has been observed to have the biggest potential of S phase arrest capability among the other selected miRNAs for each of the cell lines.

3.2.6. Target gene expression

Among the selected miRNA targets, the expression level of the MMP1 gene could not be evaluated with real-time PCR and was excluded from the results. The results of miR-31 targets in the U-CH1 cell line have been published in a previous study, in which the validated target *RDX* and the predicted target *MET* levels downregulated after miR-31-3p transfection into the U-CH1 cell line [114]. All results were normalized with the GAPDH housekeeping gene and analyzed with the $2^{-\Delta\Delta cT}$ method by using the X-Treme gene transfection control group as the negative control.

The level of *RDX* expression decreased significantly in U-CH2 and MUG-Chor1 cell lines ($p<0.05$ and $p<0.01$, respectively) upon transfection with miR-31-3p. Similarly, the predicted target *MET* gene expression was also found to be downregulated by miR-31 in both cell lines (Figure 3.11 a,b).

miR-140-3p targeting did not retain a convincing result, since a consistent increase in the target gene expression level after anti-miR-140-3p admission in each of the three cell lines was expected but failed. Among the results, *MAPK1* is the most promising as a considerable

increase in the level of expression in the gene was noticed in U-CH1 and U-CH2, with an insignificant decrease in the MUG-Chor1 cell line.

The validated target genes, *DNMT1* and *DNMT3B*, selected for miR-148a were significantly upregulated in all three cell lines after administration of the anti-miR-148a antagomiR (Figure 3.11 c,d). The predicted target gene expression levels for *BCL2L11* and *USP33* showed a mixed response in our experiments; therefore, we cannot report any targeting for all three cell lines in the mRNA level.

Among the selected miR-222-3p targets, we obtained convincing results for the validated targets *TRPS1* and *BIRC5* (Figure 3.11 e,f) and for the predicted target *KIT* (Figure 3.11 g). As expected, the magnitude of decrease in the target gene expression level in the samples had an inverse relationship with their basal miR-222-3p level. The predicted target *KIT* gene expression considerably decreased after transfection, which could mean that *KIT* can be a direct or indirect target of hsa-miR-222-3p.

Since miR-222-3p overexpression decreases the *TRPS1* level, we decided to compare the levels of downstream epithelial-to-mesenchymal transition (EMT) and mesenchymal-to-epithelial transition (MET) markers in non-transfected MUG-Chor1 cells, which show 73 times more miR-222-3p expression compared to U-CH1. The levels of the markers in U-CH1 cells were used to normalize the data (Figure 3.11 h). We observed that the gene expression levels of MET markers *CDH1, CK19,* and *EMA* are lower in MUG-Chor1 compared to U-CH1**,** whereas the EMT markers *SNAI2*, *SNAI1*, *VIM* and *CDH2* gene expression levels are higher in MUG-Chor1 when compared to U-CH1.

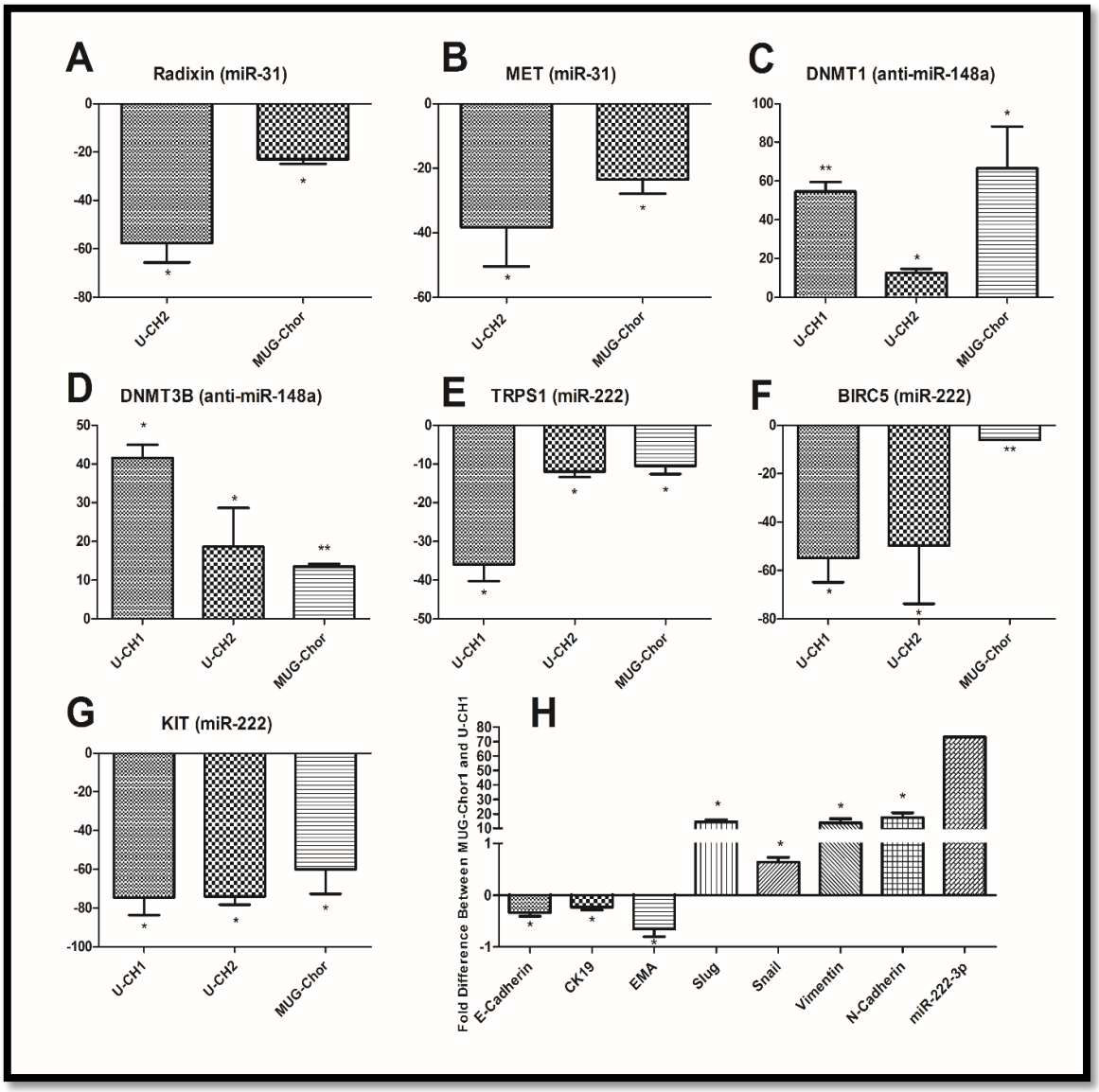

Figure 3.11 The effects of regulating miRNA levels on the predicted and validated target genes. The fold change in the target gene expression levels in U-CH1, U-CH2 and MUG-Chor1 relative to X-Treme control. (A) Radixin, the validated target of miR-31-3p. (B) MET, the predicted target of miR-31-3p. The gene expression levels of validated miR-148a targets after transfection with anti-miR-148-a (C) DNMT1 and (D) DNMT3B. (E,F) Validated targets of miR-222-3p: TRPS1, BIRC5. (G) The predicted target of miR-222-3p: KIT. (H) The correlation between the level of EMT markers and miR-222-3p in MUG-Chor1 and U-CH1. The columns represent the fold increase or decrease of each gene in MUG-Chor1 compared with U-CH1. '*' indicates $p<0.05$. '**' indicates $p<0.01$.

3.3. LEUKEMIA INHIBITORY FACTOR AND ITS ROLES IN CHORDOMA

This section has been published as “Leukemia Inhibitory Factor Promotes Aggressiveness of Chordoma.” Oncol Res. 2017 Feb 28. doi: 10.3727/096504017X14874349473815. [Epub ahead of print]

3.3.1. Surface LIFR Increases in a Time-dependent Manner upon LIF Treatment

Fluorescence microscopy images revealed that chordoma cell lines U-CH1 and MUG-Chor1 have cell surface LIF receptors (Figure 3.12), and these receptors increased as cells were exposed to LIF in a paracrine manner. LIF receptors were more abundant in week 8 compared to week 1, which indicates a time-dependent increase of cellular response to LIF exposure.

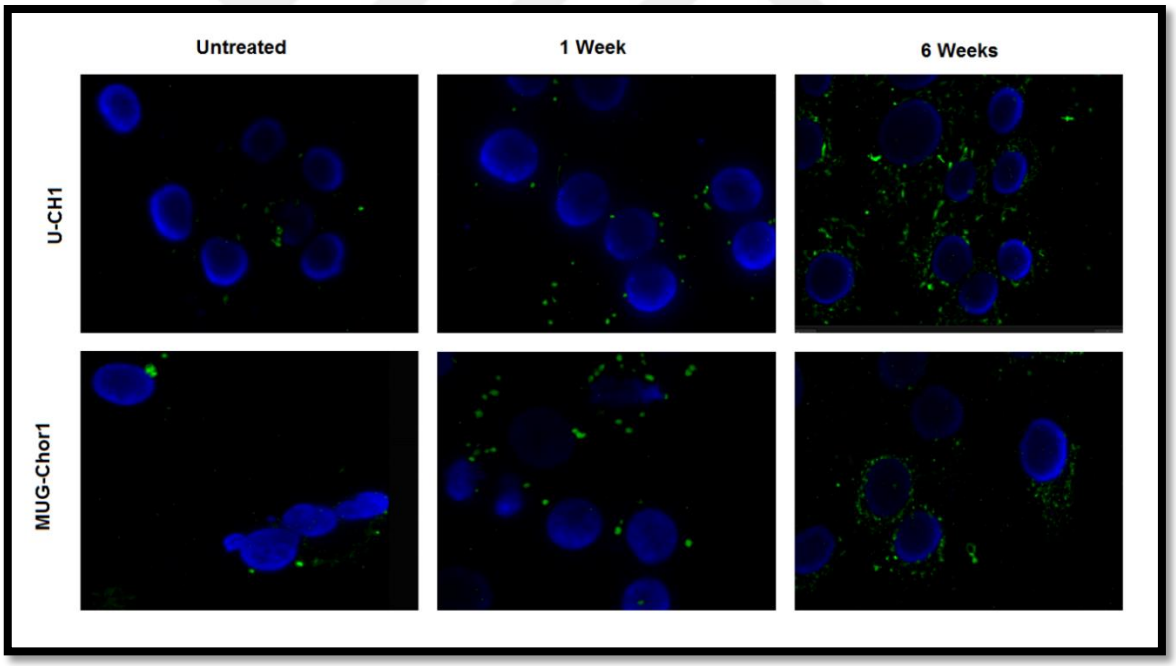

Figure 3.12 LIF treatment increases LIF receptors on chordoma cell surface. Anti-LIFR antibody (green) was used to visualize the LIFR level of U-CH1 and MUG-Chor1 after LIF treatment of 1 and 8 weeks. The control group was treated with complete chordoma medium.

3.3.2. LIF Treatment Increases Invasion and Migration Ability and Induces EMT-related Genes

We used trans-well chamber inserts to investigate the effect of LIF on migration and invasion. As representative images from week 1 indicate (Figure 3.13), LIF treatment drastically improved the migration and invasion ability (Figure 3.14) of both cell lines. This effect decreased over time and was neutralized at week 8. The effects of LIF treatment on EMT gene expression levels were also monitored. E-Cad and CK19 were suppressed by LIF treatment whereas the EMT marker ZEB2 expression had a significant peak at either week 3 or week 5. EMT marker levels at the corresponding weeks were consistent with the migration and invasion abilities. The expression level of MET, which plays an important role in local invasion by chordoma cells, also escalated in weeks 1 and 3 (Figure 3.15). No significant transformation of cells to a mesenchymal morphology was observed. LIF treatment did not significantly affect T gene expression in chordoma cell lines.

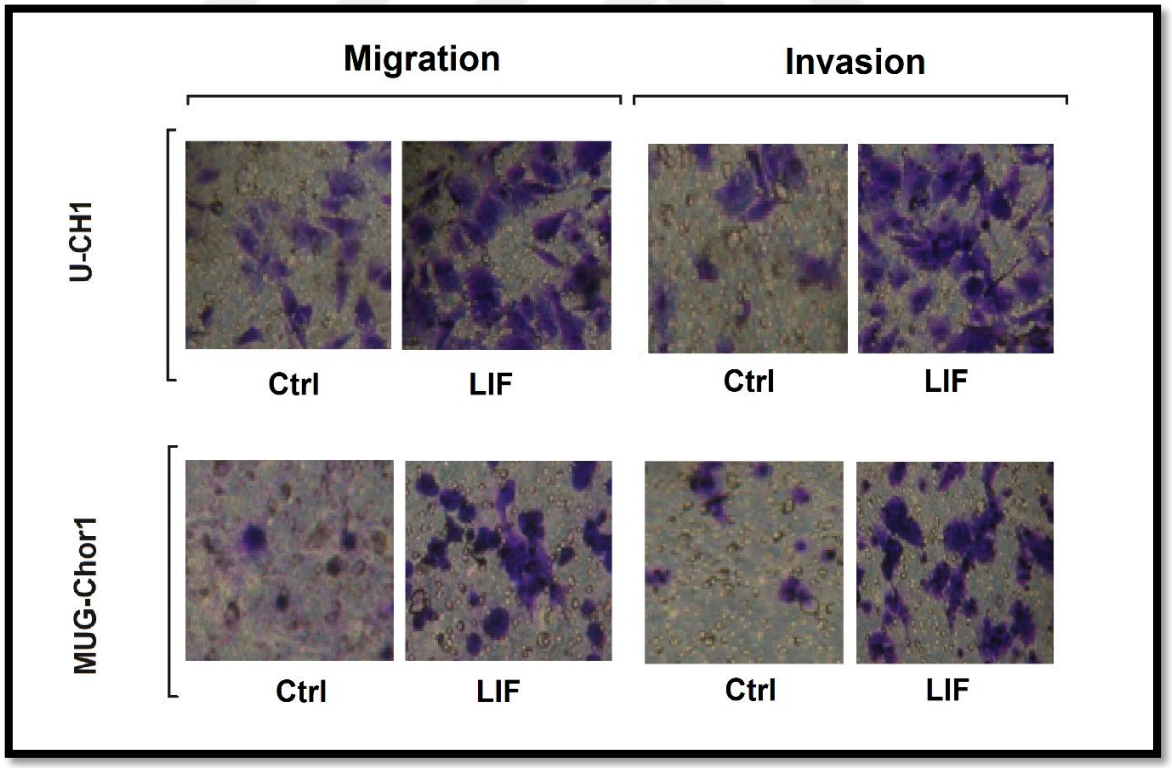

Figure 3.13 Representative images of migration and invasion assays at week 1.

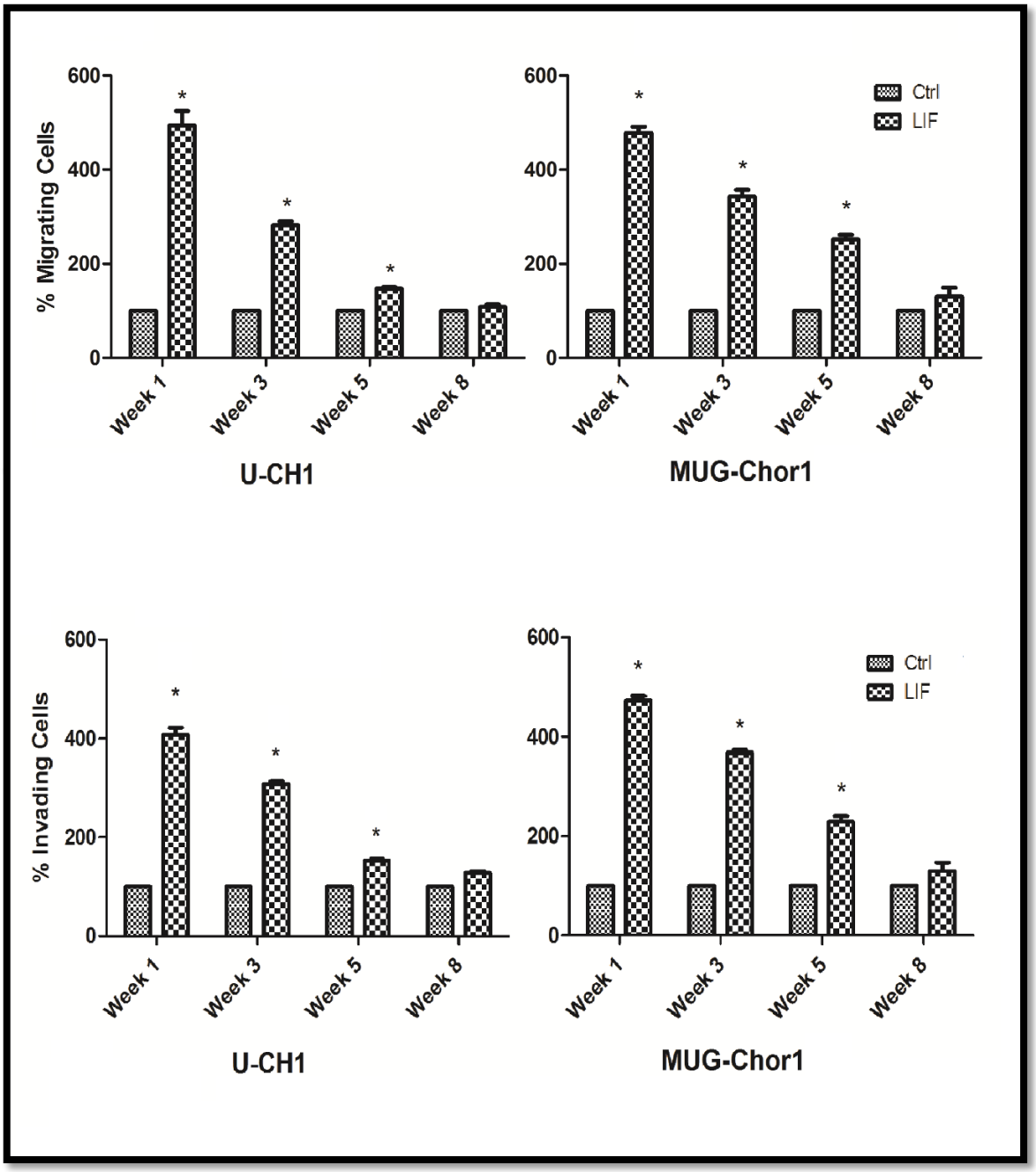

Figure 3.14 LIF promoted the migration and invasion ability of U-CH1 and MUG-Chor1. Data was normalized with the control group. The highest rate occurred at week 1 and steadily decreased thereafter. * $p<0.05$.

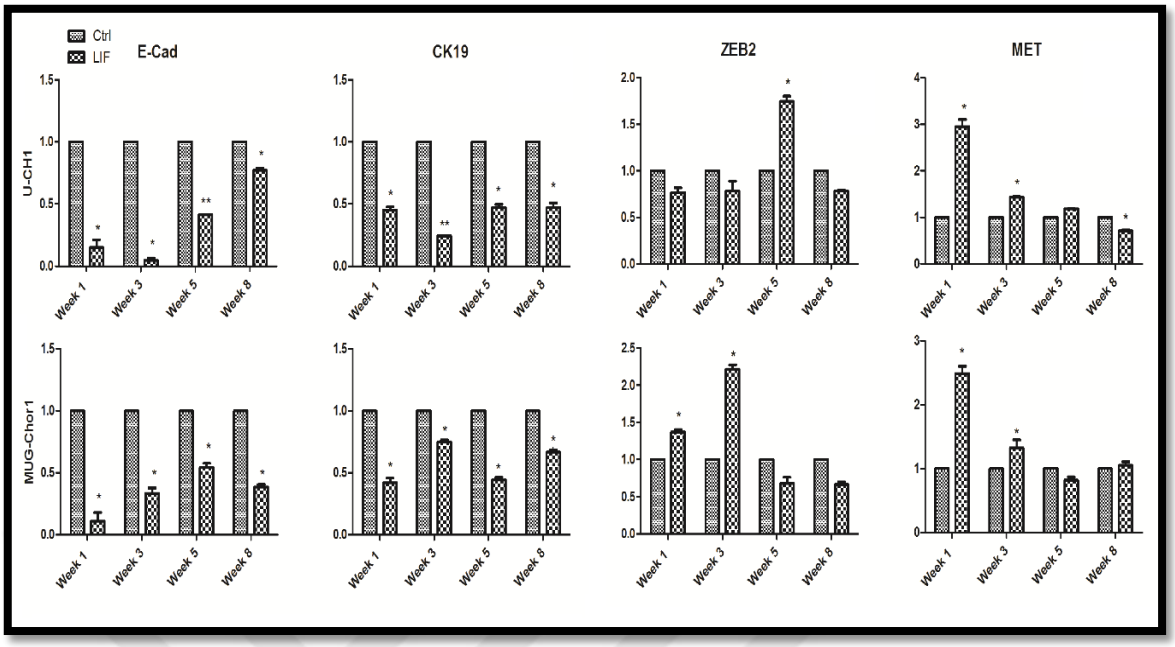

Figure 3.15 LIF treatment decreased the relative levels of epithelial markers E-Cad and CK19 while increasing the expression level of late EMT-marker ZEB2 level at weeks 1 and 3 for MUG-Chor1 and at week 5 for U-CH1 normalized with the control. Pro-invasive MET was significantly increased at weeks 1 and 3, a pattern consistent with the invasive character of the cells at the same time interval. * $p<0.05$; ** $p<0.01$.

3.3.3. LIF Promotes Anchorage-independent Growth, Tumorosphere-forming ability, and Chemoresistance of Chordoma Cells, Indicating an Increase in CSC Character

LIF promoted the anchorage-independent growth of chordoma cells in soft agar, as LIF treatment increased the number of colonies formed by U-CH1 and MUG-Chor1 cells after 5 and 8 weeks in a time-dependent manner (Figure 3.16). Furthermore, LIF-exposed cells formed a significantly higher number of tumorospheres when compared to cells grown in medium without LIF (Figure 3.17). The highest number of tumorospheres were formed after 8 weeks of LIF treatment, and no significant increase was observed at week 1 in either cell line. LIF treatment increased the chemoresistance of U-CH1 and MUG-Chor1 against bortezomib and paclitaxel from the third week onwards (Figure 3.18).

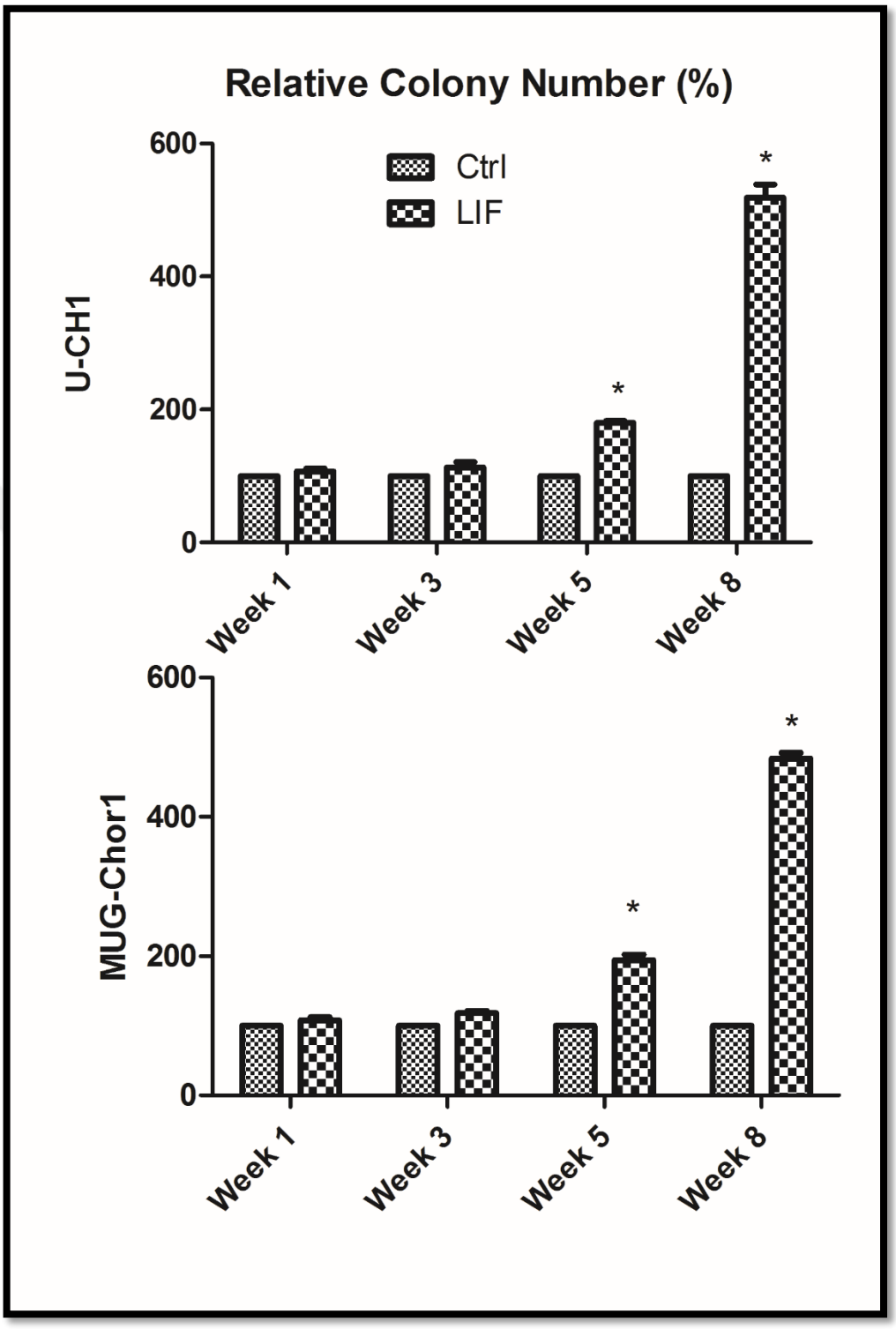

Figure 3.16 LIF treatment promoted anchorage-independent growth of U-CH1 and MUG-Chor1 cells in soft agar at weeks 5 and 8. The figure shows the relative number of colonies formed as a percentage of the control group.

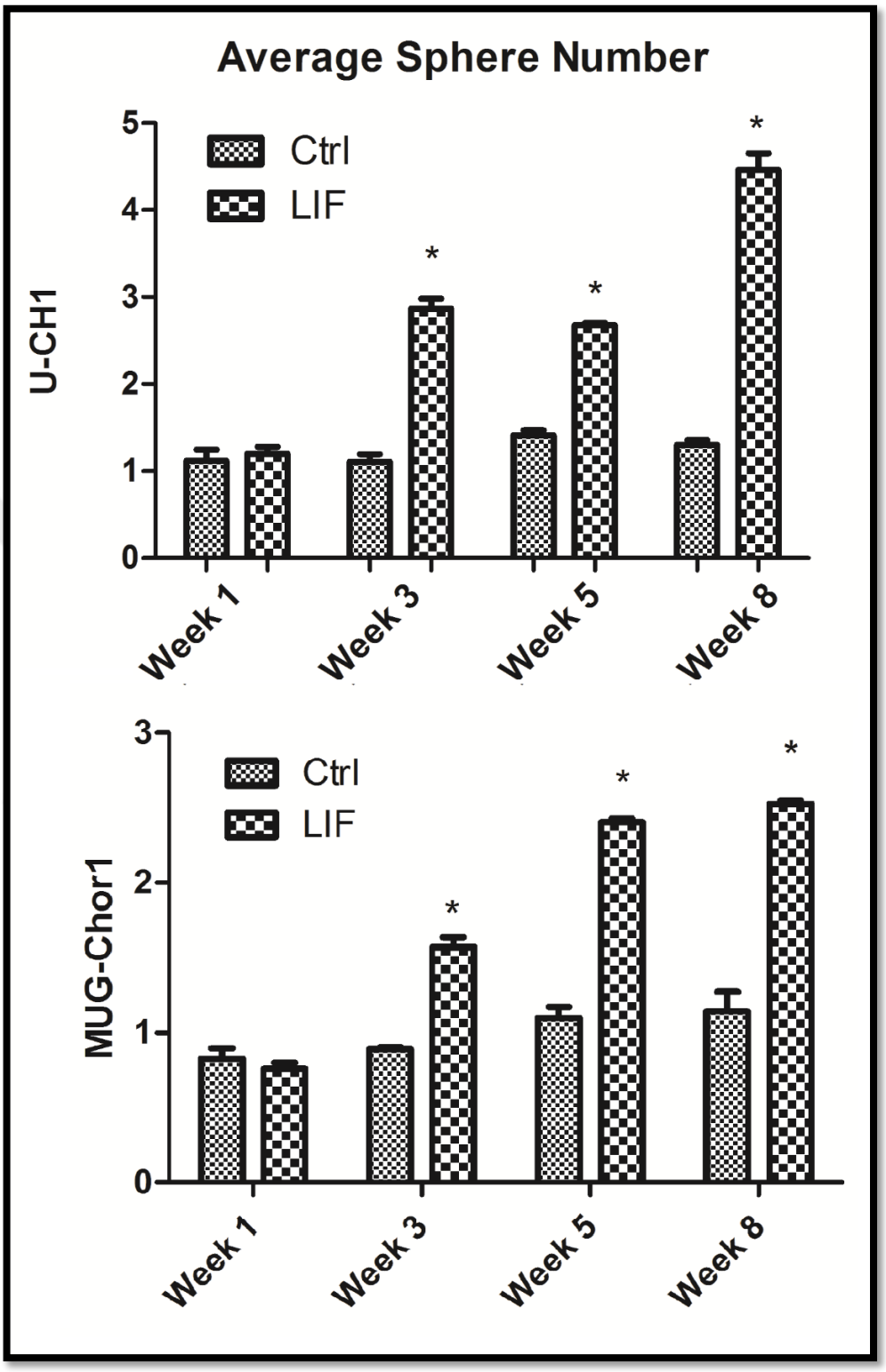

Figure 3.17 The tumorosphere formation abilities of U-CH1 and MUG-Chor1 cells on attachment-free conditions increased after week 3 and peaked at week 8. Graph columns represent the average tumorosphere number per well in a 96-well plate.

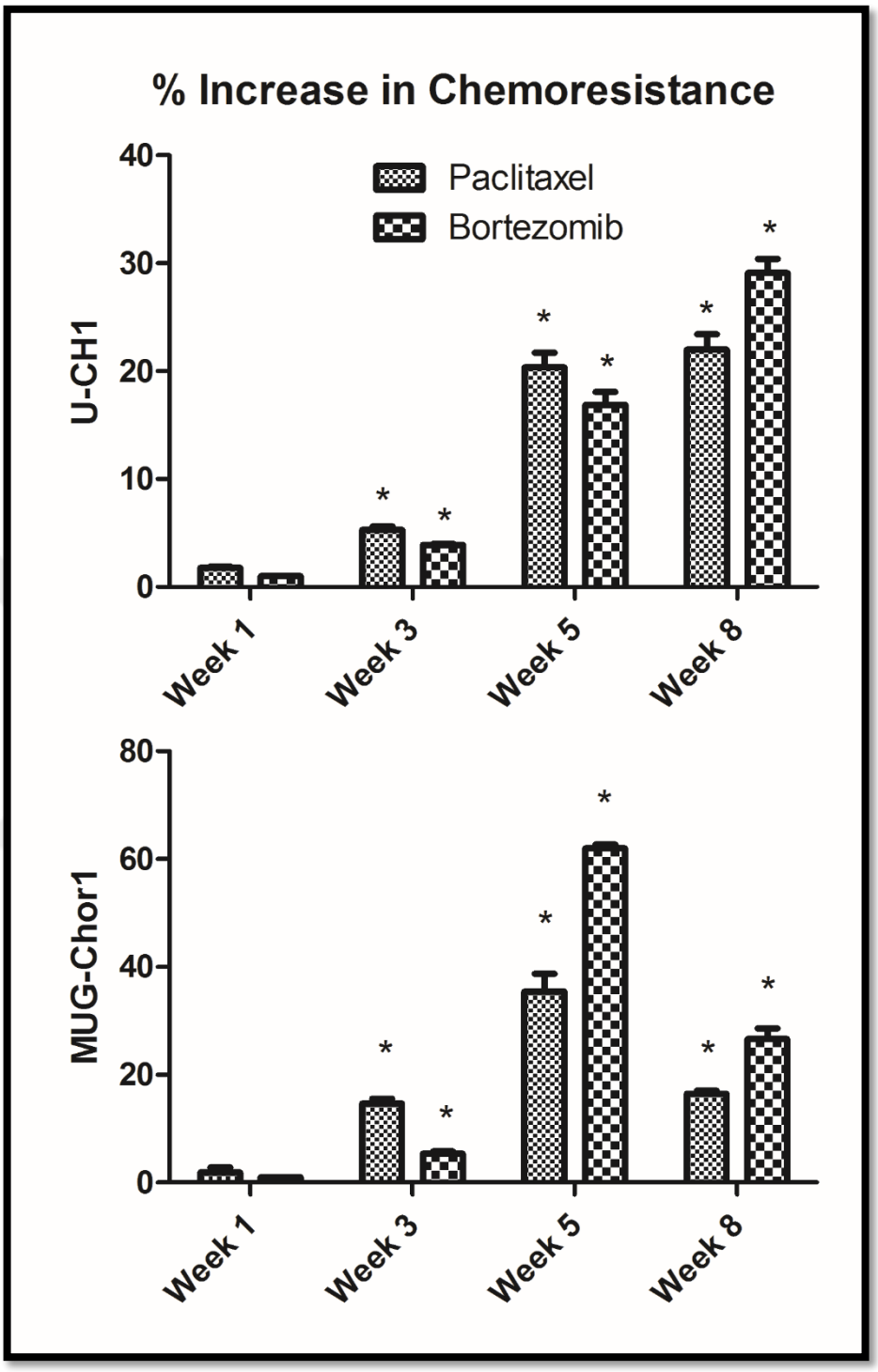

Figure 3.18 LIF treatment increased the chemoresistance of chordoma cells against paclitaxel and bortezomib at weeks 5 and 8. Chemoresistance was calculated as the percentage viability of LIF-treated cells over untreated cells for each week and each cell line.

As these functional tests implicate an increase in stem-like behavior, CSC and drug transport markers were increased in our experimental group, as indicated by real-time PCR. LIF

treatment increased the levels of CSC markers NANOG, Oct4, and Klf4 predominantly at week 5 (Figure 3.19).

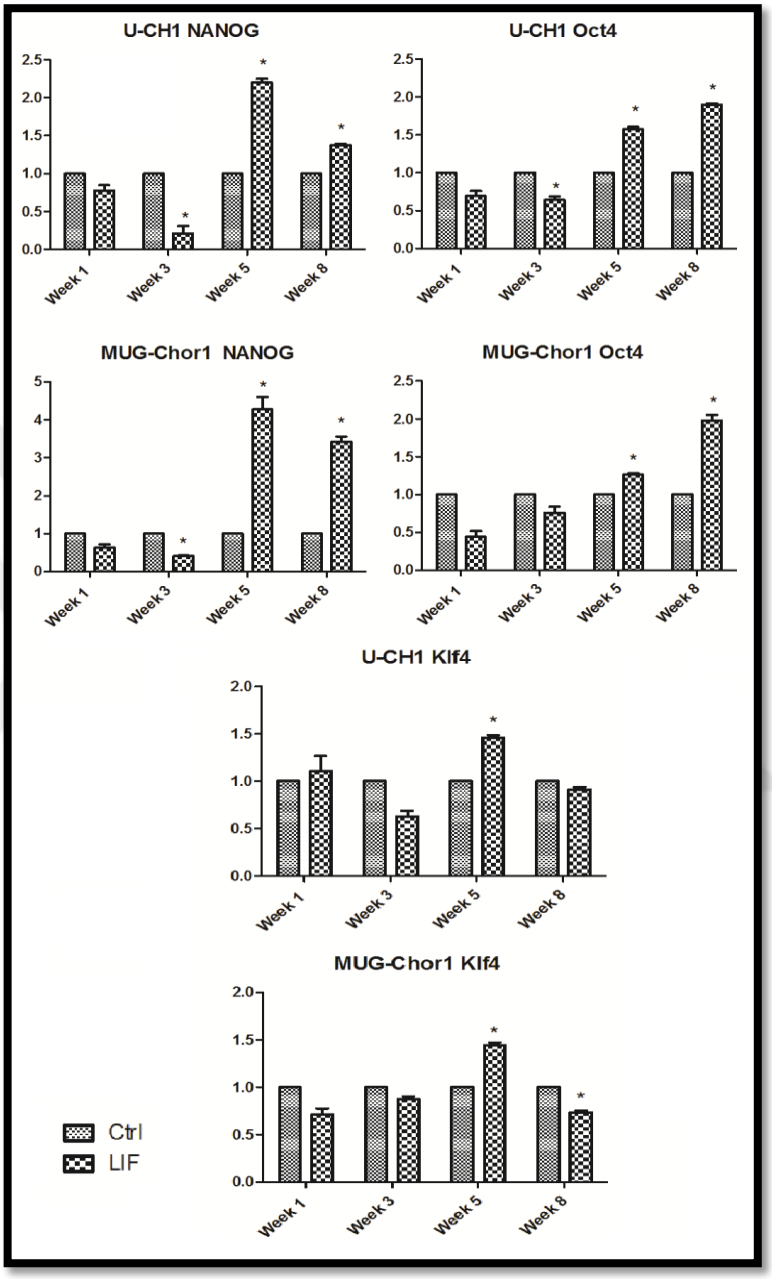

Figure 3.19 Relative CSC marker levels against the control group were determined with real-time PCR. The timing of increased CSC-marker expression was consistent with the results of the functional tests.

Potential chordoma CSC cell surface markers CD 133 and CD15 and the drug transporter CD338 (ABCG2) levels were consistent with our findings that LIF treatment transforms chordoma cells into a more stem-like state. CD 133, CD 15, and ABCG2 levels increased in

both cell lines at weeks 4 and 8 (Figure 3.20 and Figure 3.21). There was no significant increase in any of the three markers at week 1 (data not shown). No significant change was observed in the surface markers.

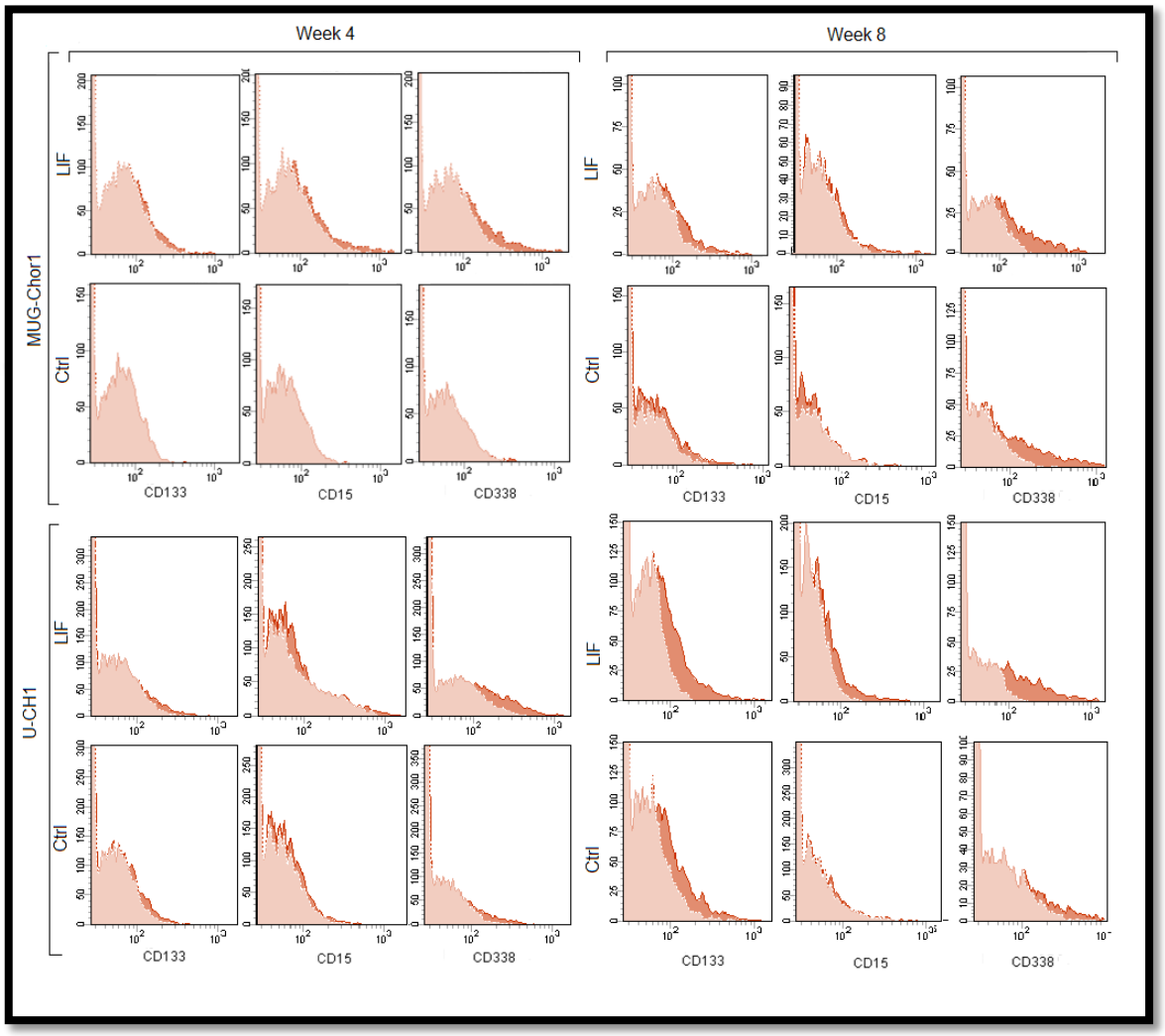

Figure 3.20 Flow cytometry results of CSC markers CD133, CD15, and the drug efflux protein ABCG2. In the histograms, pale red represents unstained cells whereas dark red represents stained cells.

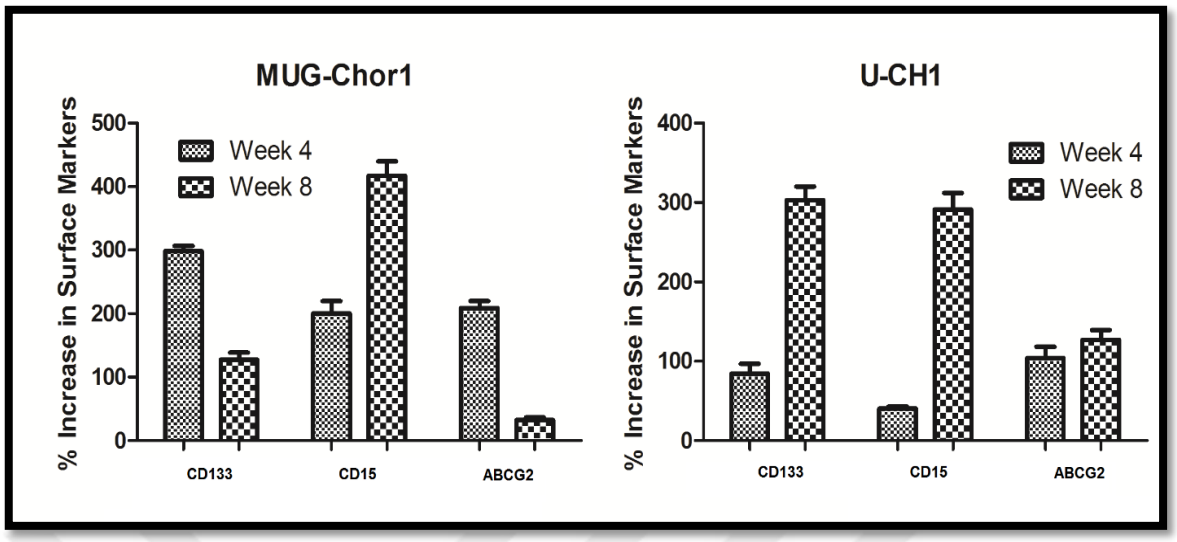

Figure 3.21 Flow cytometry results of CSC markers CD133, CD15, and the drug efflux protein ABCG2. The columns indicate the percentage increase of these surface markers after LIF treatment compared with the control group.

3.3.4. LIF Escalates Tumor Inflammatory and Anti-apoptotic Pathways

As a result of microarray analysis, a total of 31 genes were upregulated and 16 genes were downregulated in LIF-treated U-CH1 and MUG-Chor1 cell lines after 3 weeks. Of the 31 upregulated genes, 21 are related to inflammatory mechanisms (Fig. 3.22 a). In addition, 6 anti-apoptosis genes were upregulated in the apoptosis pathway. Gene networks related to inflammation, such as the Toll-like receptor signaling pathway, TNF-α, TWEAK signaling, IL-1 signaling, IL-6 signaling, and RANKL/RANK pathways, were effected with numerous genes that were dysregulated as a result of LIF treatment (Table 3.1). The pro-inflammatory gene TNFAIP2 expression level was checked in LIF-treated cells and was found to be consistent with the invasion and migration abilities, as well as EMT markers, which declined after week 3 (Fig. 3.22 b).

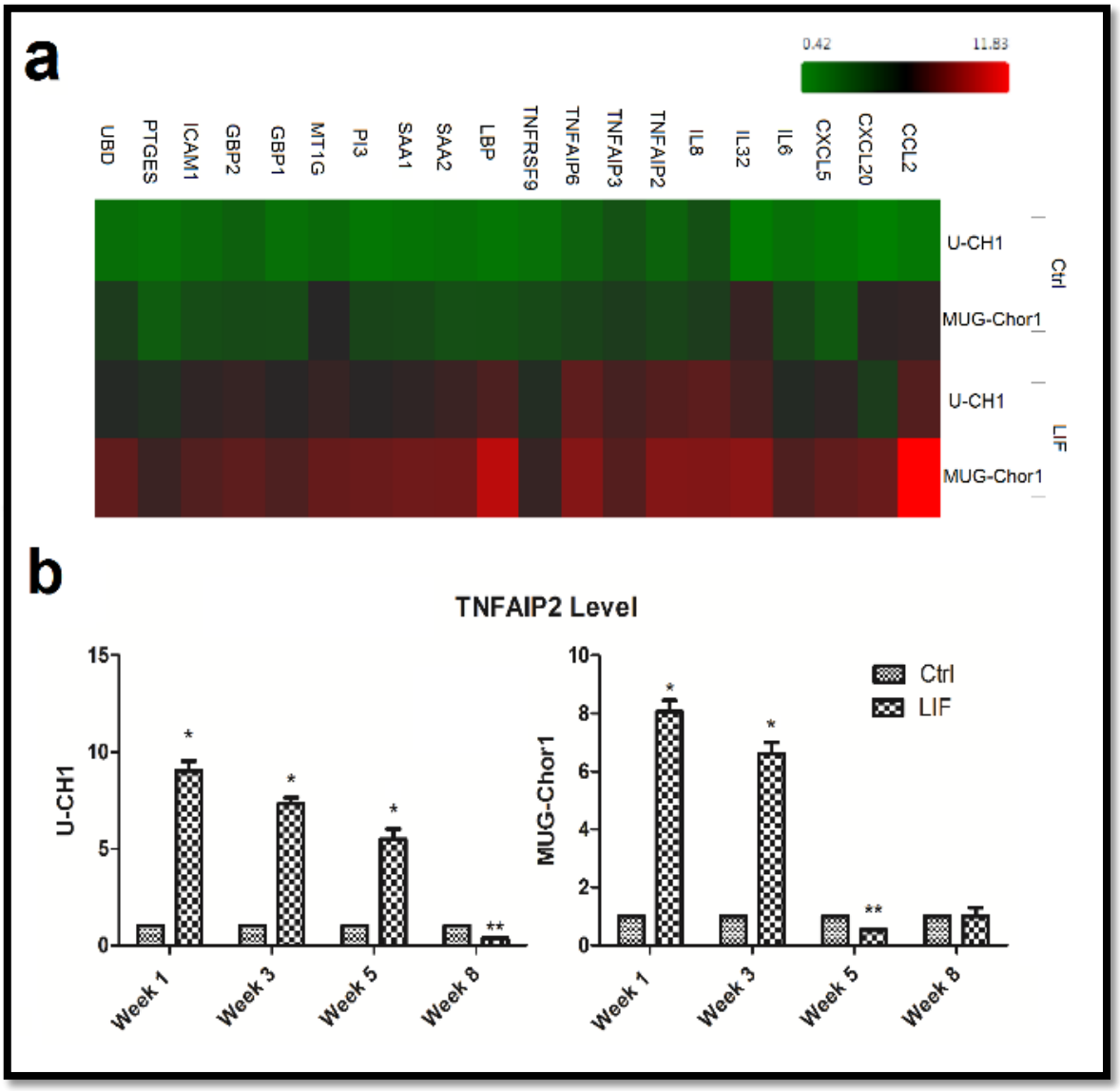

Figure 3.22 LIF escalates tumor inflammatory and anti-apoptotic pathways in chordomas. (A) A heat map representing the differential expression of 21 inflammation-related genes after 3 weeks of LIF treatment. (B) TNFAIP2 levels were checked as a marker of activated inflammation after LIF treatment in chordoma cells by using real-time PCR. * $p<0.05$, ** $p<0.01$.

Table 3.1 Pathways Regulated by LIF in Chordomas. Table shows the number of dysregulated genes in the respective pathways that positively regulate the pathway. Data was obtained by using Transcriptome Analysis suite (Affymetrix).

Pathway	**Number of Positive Regulators**
Inhibition of apoptosis	6
Toll-like receptor signaling pathway	8
Photodynamic therapy-induced NF-kB survival signaling	7
TNF-α signaling pathway	7
TWEAK signaling	5
IL-1 signaling pathway	5
IL-6 signaling pathway	3
RANKL/RANK	3
JAK/STAT	3

3.3.5. LIF Correlates with TNFAIP2, KLF4, and MET Gene Expression and Overall Survival and Tumor Size

Patient chordoma and nucleus pulposus samples were checked for LIF mRNA levels, and the chordoma samples had a higher LIF-level average than nucleus pulposus samples but the result was insignificant (Figure 3.23).

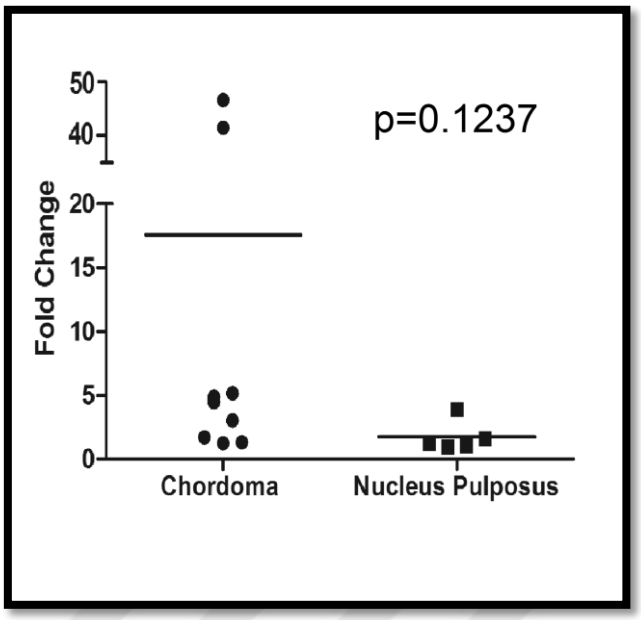

Figure 3.23 Dot plot comparing the level of LIF expression in chordoma tumor samples against that in nucleus pulposus samples. The horizontal bar represents the average value.

Moreover, tumor size was positively correlated with LIF level ($p<0.05$) (Figure 3.24).

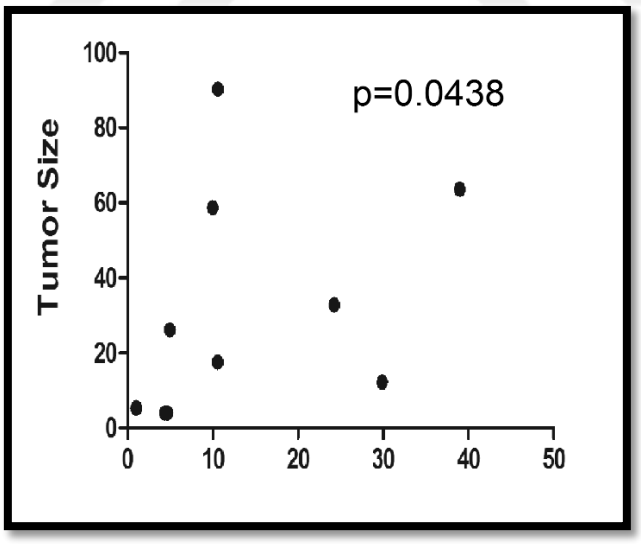

Figure 3.24 Correlation of LIF level (x-axis) versus tumor size

Sample cohort was checked for a Spearman's rank correlation between LIF and genes that were affected in the LIF-treatment experiments on cell lines. E-Cad (R= -0.308), CK19 (R= -0.235), ZEB2 (R= 0.341), TNFAIP2 (R= 0.653), KLF4 (R= 0.574), and MET (R= 0.793) showed a consistent correlation with our results with U-CH1 and MUG-Chor1. Among these, TNFAIP2 (p= 0.0114), KLF4 (p= 0.0320), and MET (p= 0.0007) were statistically

significant (Figure 3.25). Unlike in vitro treated cell lines, NANOG and Oct4 genes exhibited inconsistent results as they were inversely related to LIF levels, but the results were statistically insignificant (p= 0.1692 and p=0.5426, respectively).

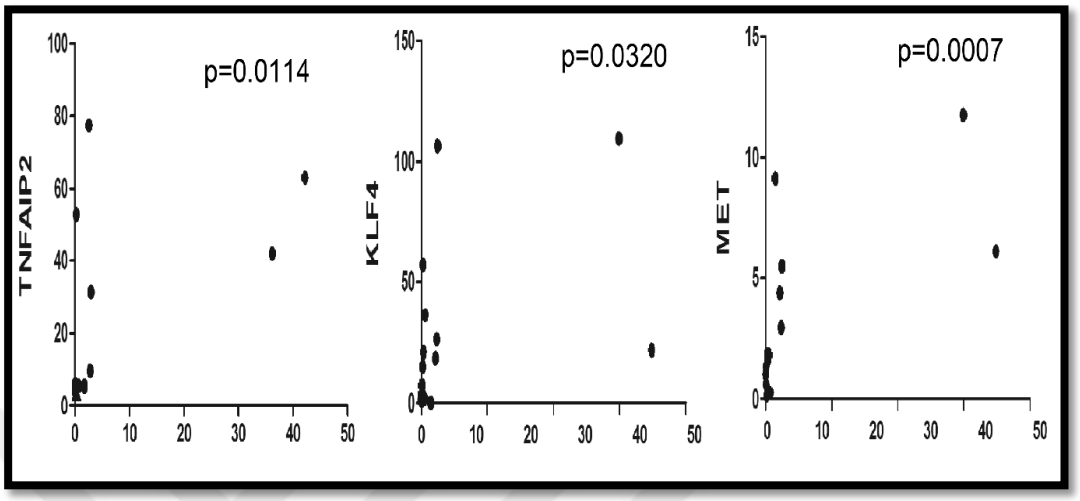

Figure 3.25 Correlation of LIF level (x-axis) versus TNFAIP2, KLF4, and MET.

Kaplan-Meier survival analysis revealed that patients with higher LIF levels in their tumors had a lower chance of overall survival than the low LIF group ($p < 0.05$) (Figure 3.26). In our cohort, the LIF level did not correlate with age, metastasis, or recurrence.

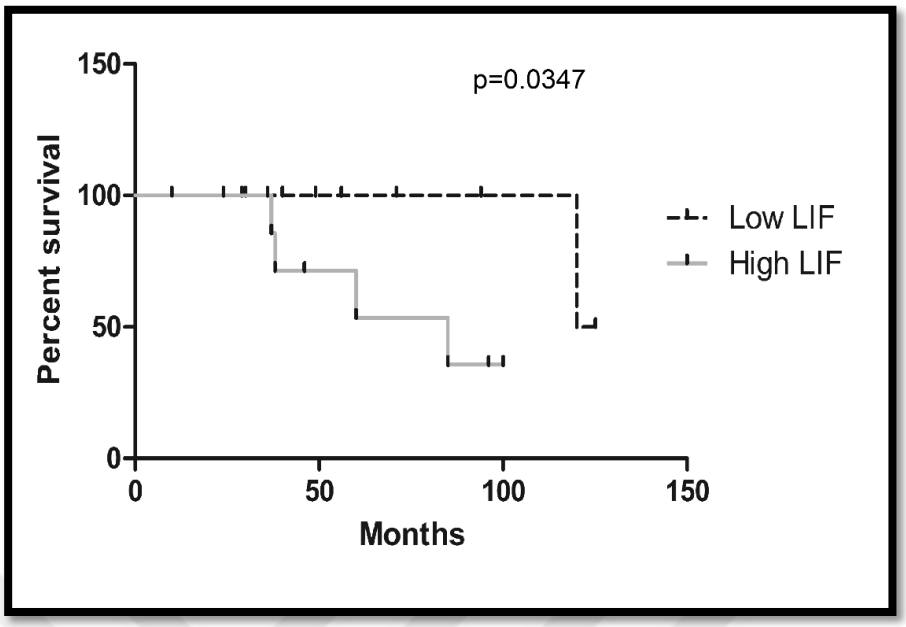

Figure 3.26 Kaplan-Meier survival plot of our patient cohort. High and low LIF groups were defined according to the relative LIF expression levels. The high LIF group had a poorer overall survival.

3.4. THE EFFECTS OF TUMOR NECROSIS FACTOR ON CHORDOMA

3.4.1. Chordoma cell lines respond to TNF-α treatment morphologically

The cell lines U-CH1 and MUG-Chor1 changed in morphology to a more mesenchymal state with the space between cells increasing and a more spindle-like cell structure forming which implicates that TNF-α treatment can cause EMT in chordoma cells (Figure 3.27).

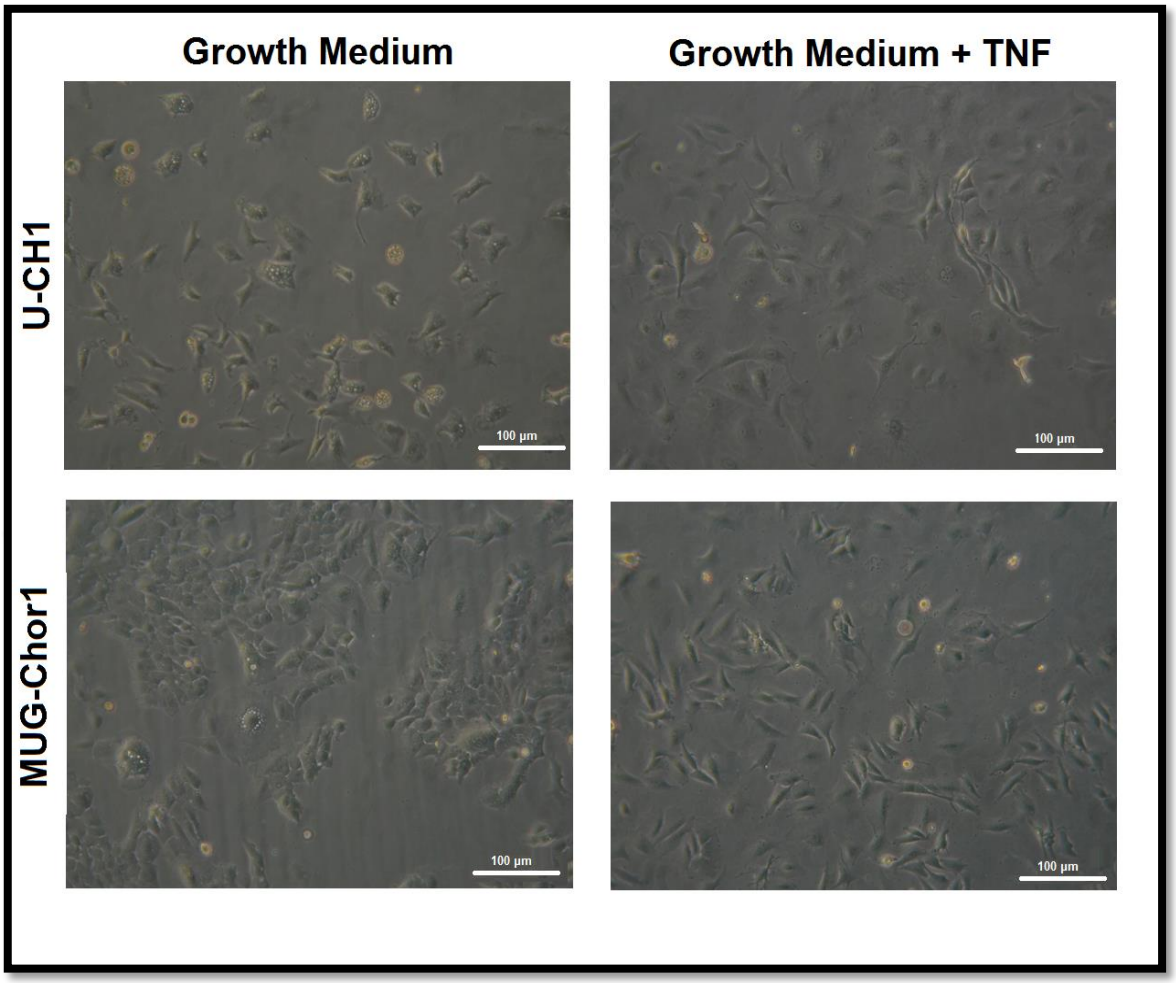

Figure 3.27 Inverted light microscopy image of LT-TNF chordoma cell lines U-CH1 and MUG-Chor1 at 100X magnification.

3.4.2. The NF-kB Complex Abundance Increases and is Activated after TNF-α Treatment

Fluorescence microscopy images revealed that chordoma cell lines U-CH1 and MUG-Chor1 possess NF-kB and its abundance is dramatically increased after long-term TNF-α exposure. Moreover the NF-kB inhibitor QNZ decreased the presence in vitro. Deprivation of TNF-α in the LT-TNF cells did not cause a difference in NF-kB abundance (Figure 3.28).

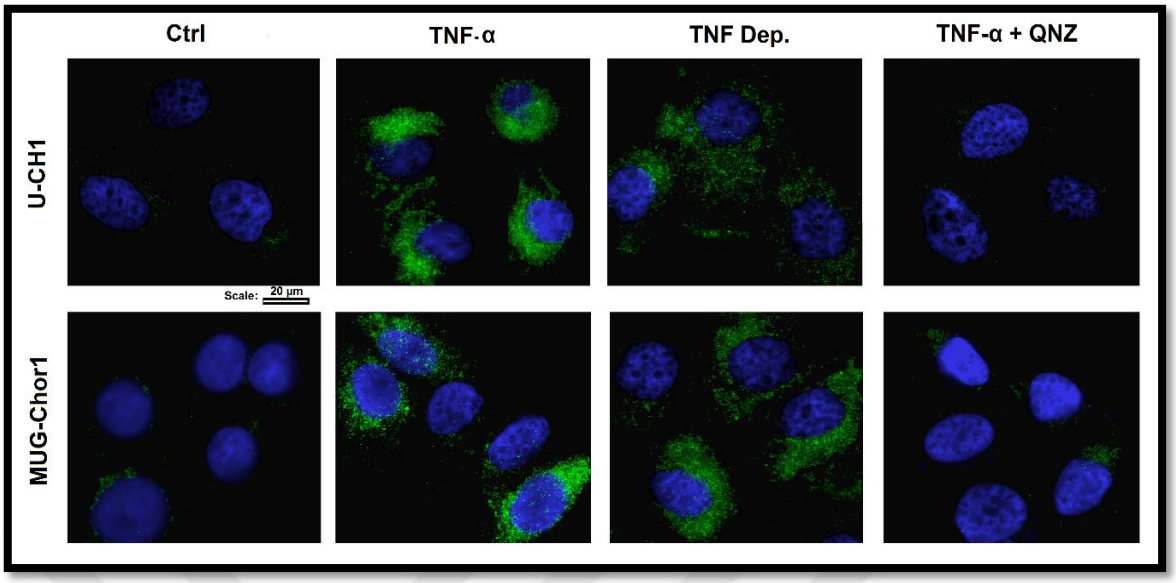

Figure 3.28 Long-Term TNF-α Treated Chordoma Cells exhibit activated NF-kB pathway both with increased staining of the p65 subunit (green) and localization near the nucleus (blue). Deprivation of TNF-α from Long-Term TNF treated Chordoma cells did not change activation of NF-kB pathway, whereas QNZ exposure reduced NF-kB abundance.

3.4.3. TNF-α Treatment Increases Invasion and Migration Ability and Induces EMT-related Genes

We used trans-well chamber inserts to investigate the effect of TNF-α on migration and invasion. TNF-α treatment significantly increased migration and invasion ability of both cell lines in both short term (Figure 3.29) and long term treatment. QNZ and wortmannin both decreased invasion and migration ability independently in short-term TNF-α treatment groups. TNF-α treatment significantly increased both migration and invasion and QNZ treatment significantly decreased these abilities ($p<0.05$). TNF-α deprivation did not cause any changes in the LT-TNF group (Figure 3.30).

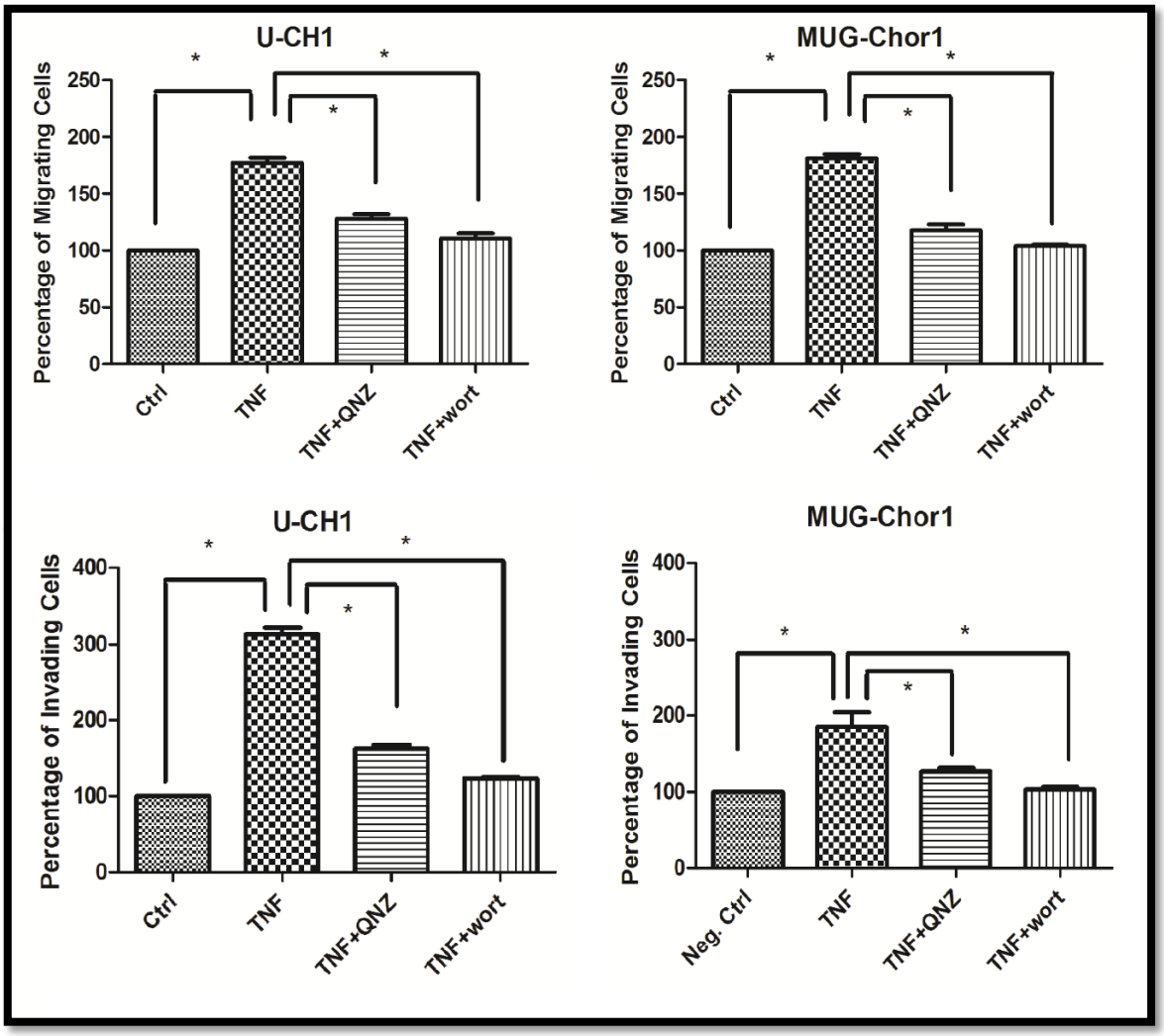

Figure 3.29 The effect of short-term TNF-α treatment on chordoma cells. U-CH1 and MUG-Chor1 was used. Wortmannin was used to see the effect of PI3K-Akt pathway on migration. '*' indicates $p<0.05$ between columns connected by the lines.

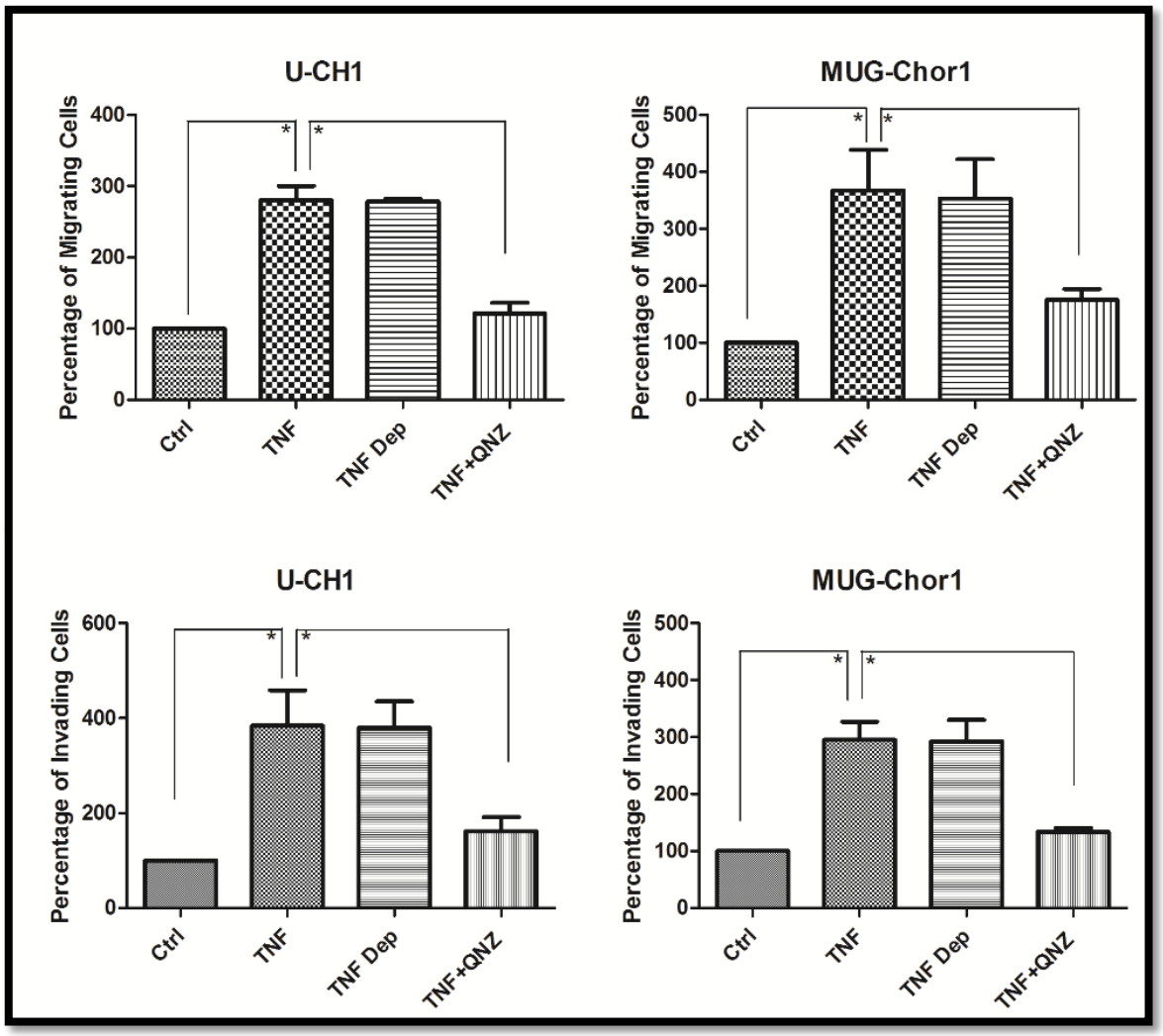

Figure 3.30 The effects of long-term TNF-α treatment on chordoma invasion and migration. '*' indicates $p<0.05$ between columns connected by the lines

The effect of TNF-α on EMT marker gene expression levels was determined in short-term treatment samples. CK19 was suppressed by TNF-α treatment whereas the EMT marker Vimentin, Slug, Twist, N-Cadherin were upregulated at day 1. At Day 4 E-Cadherin,CK19 and Brachyury expression diminished whereas Zeb2 expression increased. QNZ treatment of cells resulted in opposite or neutral effects in all but ZEB2 U-CH1 sample at day 1 (Figure 3.31). In LT-TNF-A U-CH1 and MUG-Chor1 cells, drastic suppression of epithelial markers E-cadherin, CK19 and EMA was observed while the late mesenchymal marker ZEB2 was upregulated. QNZ treatment decreased the effects of TNF-α but failed to neutralize it to the level of control cells (Figure 3.32).

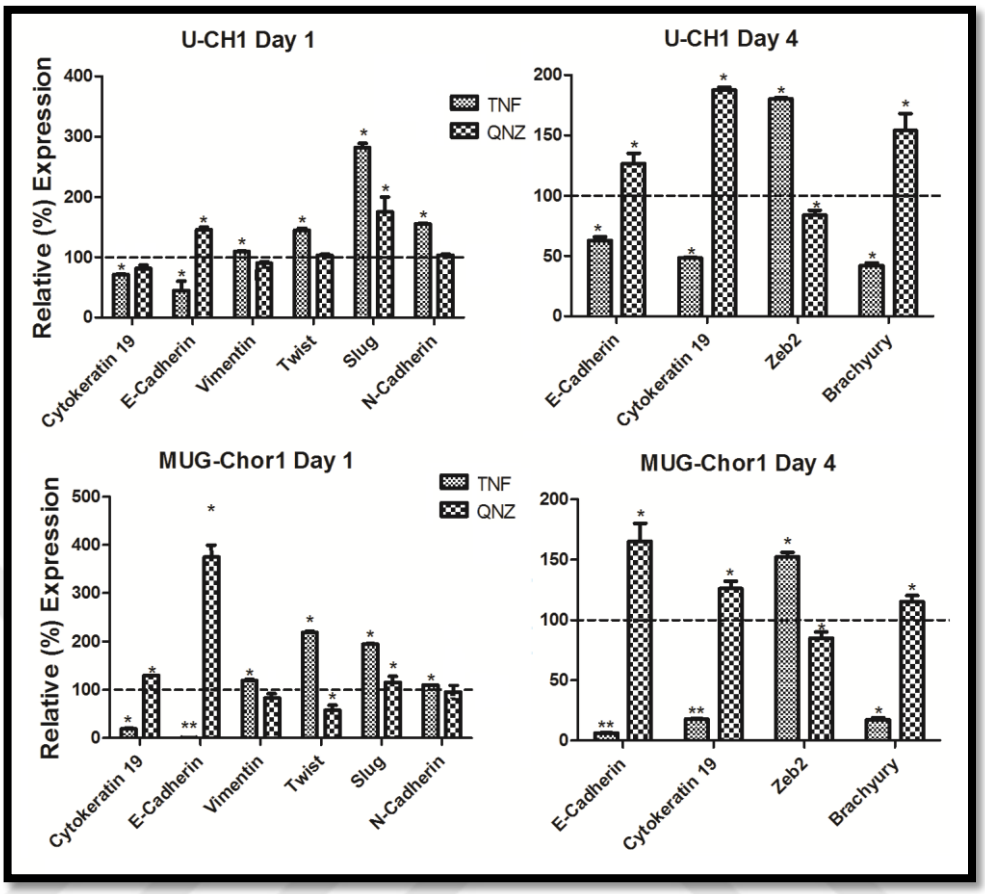

Figure 3.31 Relative percent quantification of EMT markers in chordoma cells after short-term TNF-α treatment. At Day 1, TNF-α decreased the relative level of epithelial markers CK19 and E-Cad while increasing Vimentin, Twist, Slug and N-Cadherin levels. At Day 4 E-Cad and CK19 levels remained low, while the late mesenchymal marker ZEB2 took over. Brachyury level have also decreased at Day 4. QNZ treatment reversed the effects of TNF-α. The threshold line represents 100 which is the value for controls of each group *: $p<0.05$.

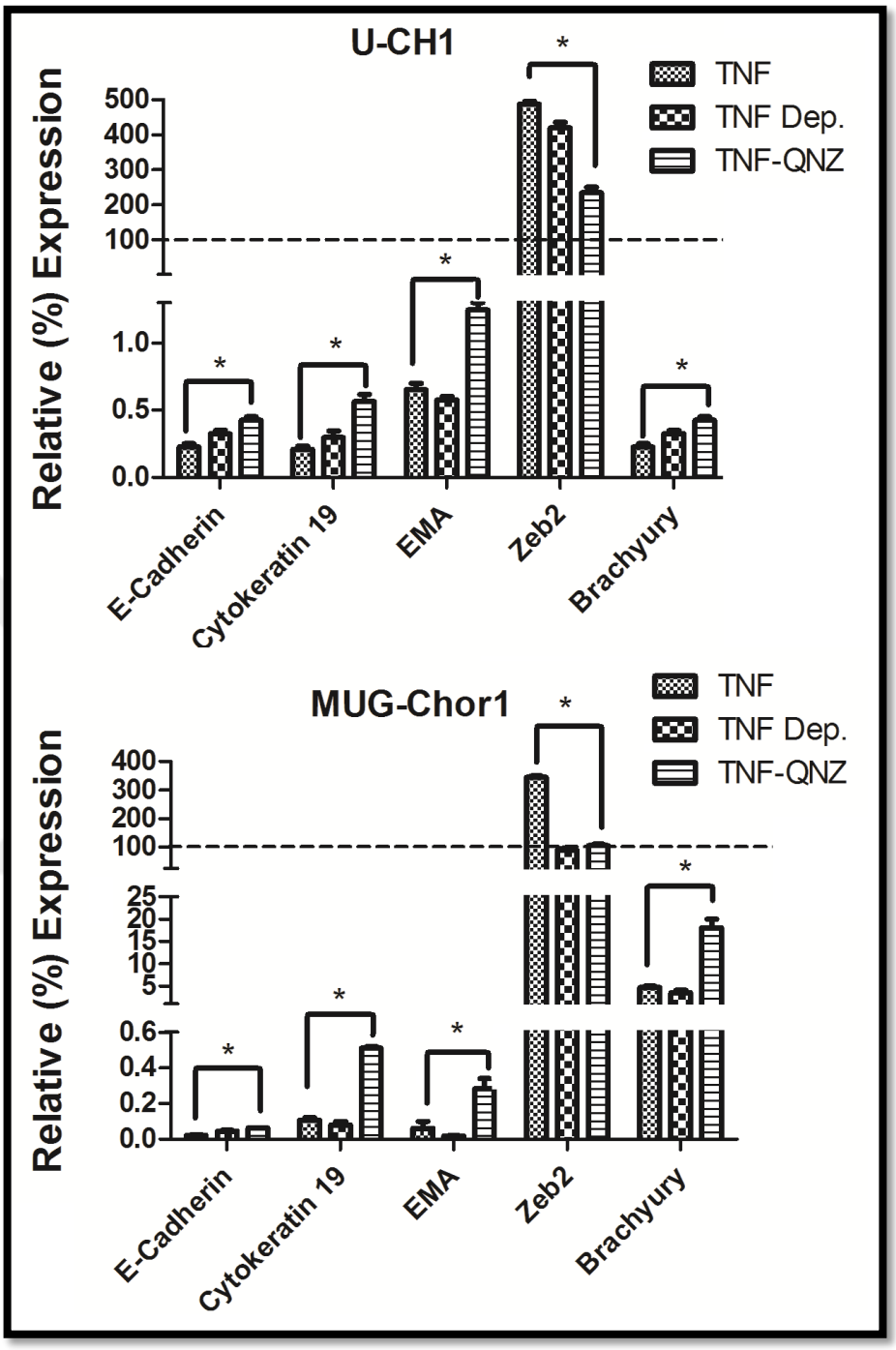

Figure 3.32 Relative percent quantification of EMT markers in chordoma cells for LT-TNF cells. TNF-α treatment decreased the relative level of epithelial markers E-Cad, CK19 and EMA levels while increasing the late mesenchymal marker Zeb2 levels. Brachyury level also decreased in LT-TNF cells. The threshold line represents 100 which is the value for controls of each group *: $p<0.05$.

3.4.4. TNF-α Promotes Anchorage-independent Growth, Tumorosphere-forming ability, and Chemoresistance of Chordoma Cells

Long-Term TNF-α treatment increased colony formation in U-CH1 and MUG-Chor1 cells. QNZ administration to Long-Term TNF-α treated chordoma cells decreased colony formation ability (Figure 3.33).

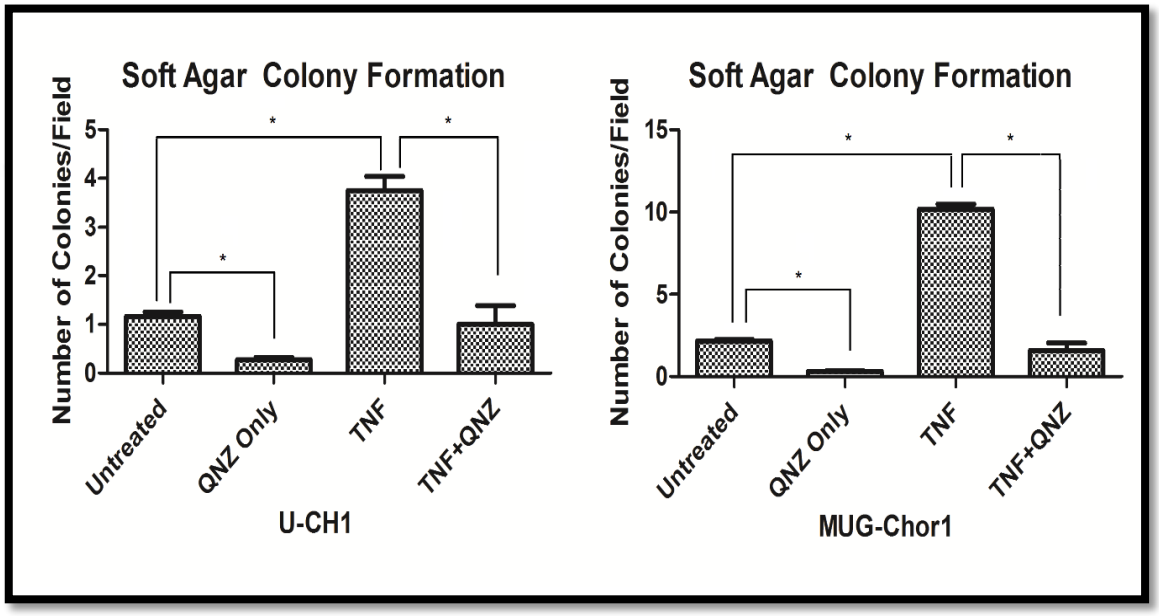

Figure 3.33 Long-Term TNF-α treatment promoted anchorage-independent growth of U-CH1 and MUG-Chor1 cells in soft agar. The figure shows the relative number of colonies formed as a percentage of the control group.

TNF-α treatment has increased in vitro tumorosphere formation in chordoma cells. Tumorosphere forming ability of LT-TNF group was significantly higher than the control group ($p<0.05$) (Figure 3.34).

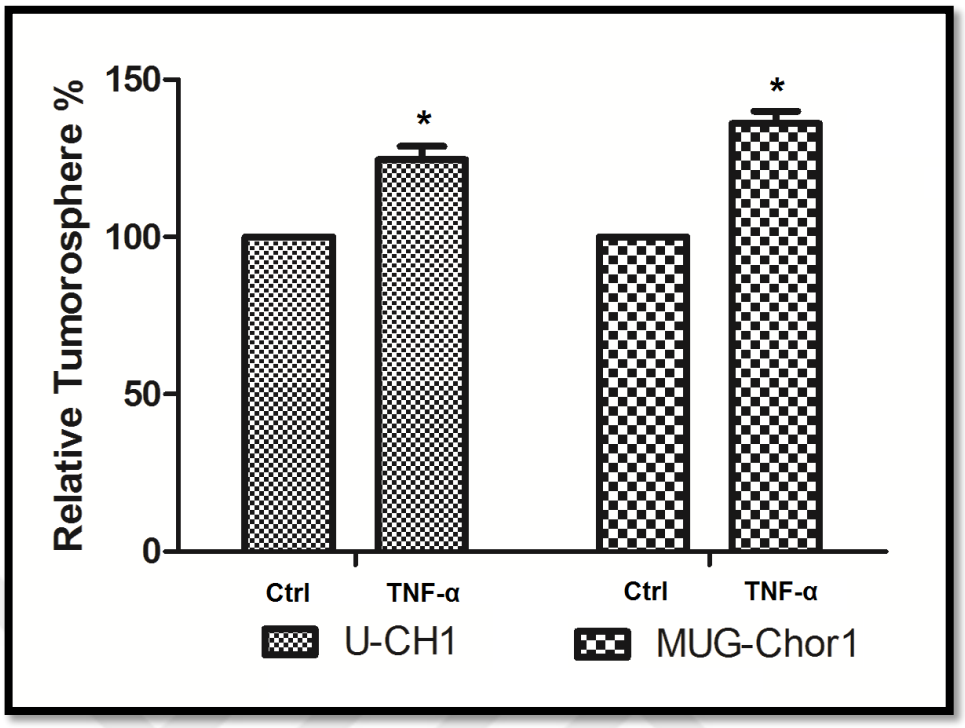

Figure 3.34 The tumorosphere formation abilities of U-CH1 and MUG-Chor1 cells on attachment-free conditions increased LT-TNF chordoma cells. Graph columns represent the relative percentage of the controls for each group.

Chemoresistance of LT-TNF cells significantly increased when compared to controls Bortezomib and Paclitaxel were used for chemoresistance assay. (Figure 3.35).

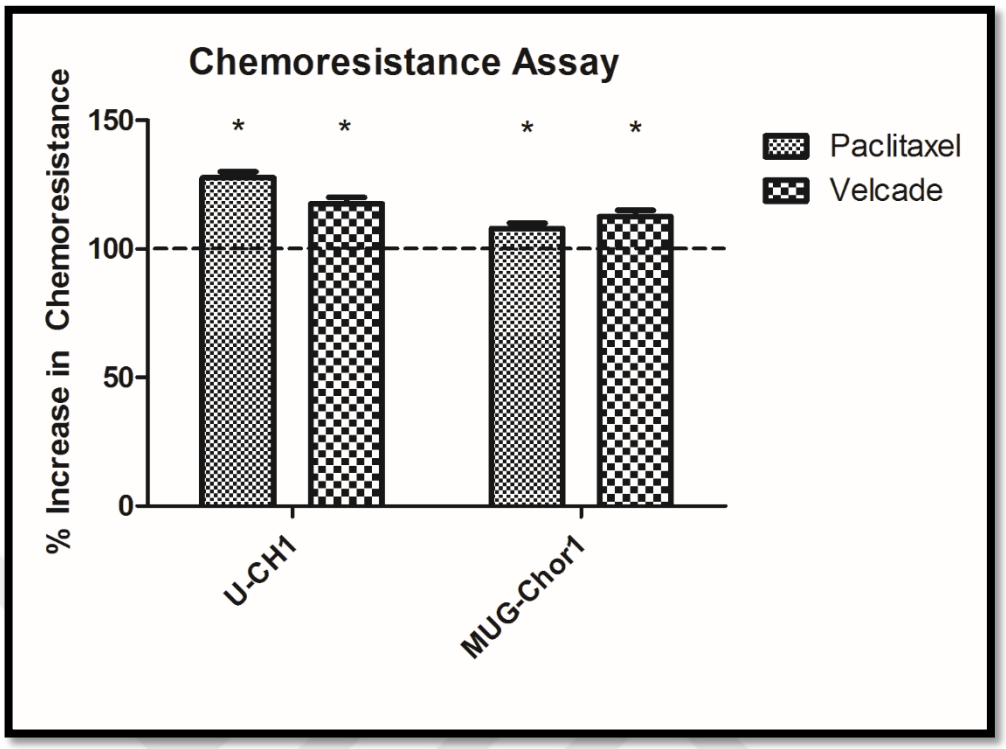

Figure 3.35 Long-Term TNF-α treatment increased the chemoresistance of chordoma cells against paclitaxel (0.012 μM) and bortezomib (0.012 μM) . Chemoresistance was calculated as the percentage viability of TNF-α-treated cells over untreated cells for each week and each cell line.

The drug transporter CD338 (ABCG2) levels were consistent with our findings that Long-Term TNF-α treatment transforms chordoma cells into a more chemoresistant state. (Figure 3.36).

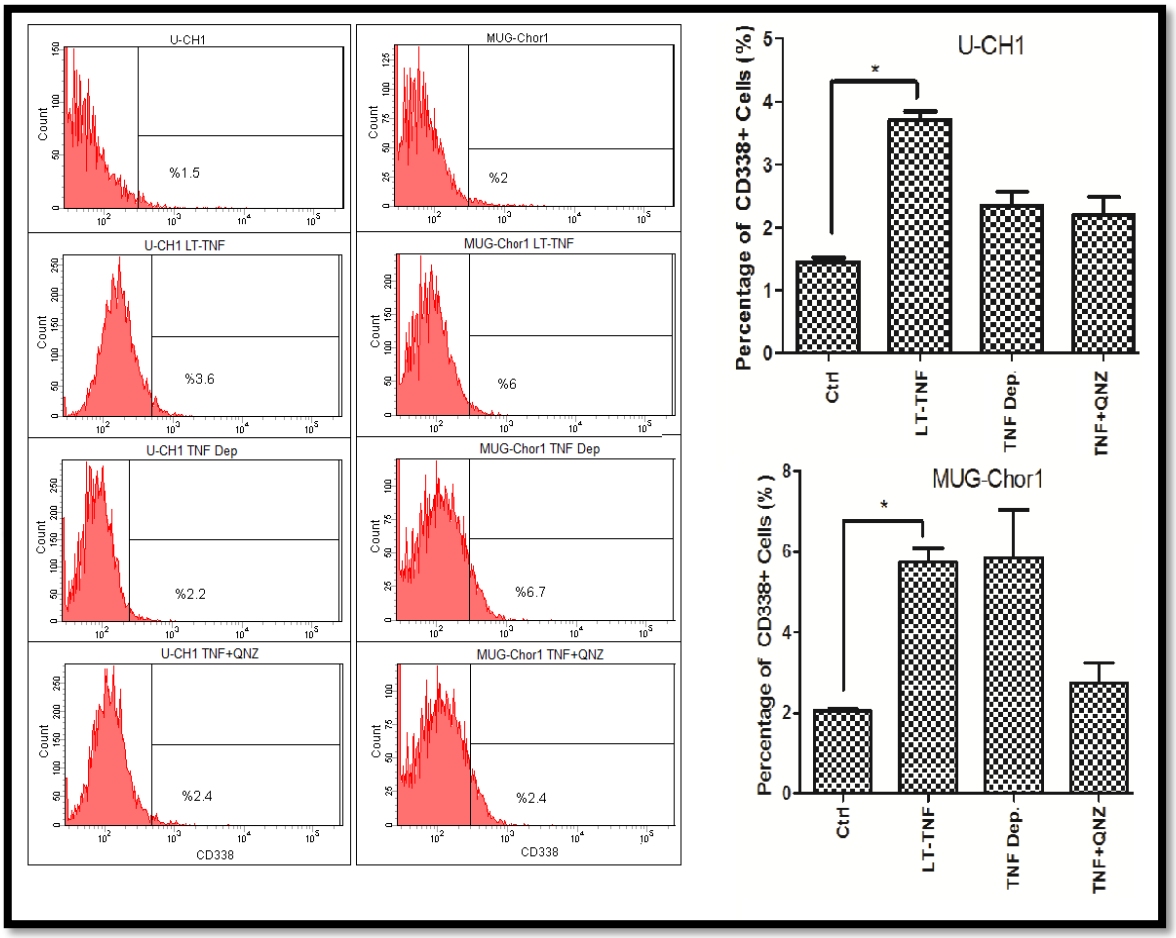

Figure 3.36 Representative histograms and column graph results of drug efflux protein CD338 surface abundance in LT-TNF cells. The columns indicate the percentage of detected cells as percentage of whole population '*' indicates $p<0.05$.

3.4.5. TNF-α Escalates Tumor Inflammatory and Metastatic Pathways in Chordoma

As a result of microarray analysis, 702 genes were shown to be upregulated and 539 genes were shown to be downregulated in LT-TNF samples against the control group. 351 genes were upregulated and 200 genes were downregulated in the samples that have been treated for with TNF-α for one week. KEGG pathway enrichment analysis presented an increase in the pro-inflammatory pathways both in long-term and short-term treatment groups. Gene networks related to inflammation and metastasis, such as the TLR signaling, TNF-α, NF-kB and CAMs were effected with numerous genes that were dysregulated as a result of one week TNF-α treatment (Table 3.2). In LT-TNF samples crucial pathways such as Ras signaling, PI3K-Akt, HIF-1, CAMs were found to be dysregulated (Table 3.3).

Table 3.2 Notable pathways in One week TNF-α treated samples against controls. Gene count represents the number of dysregulated genes in each pathway. Notable genes were selected and listed with additional information of fold change against the control after the '/' symbol. P-Value of the KEGG enrichment and relevant functions of the pathways has been provided. Finally list of cancers pathways of which were found to be related is listed.

Notable Pathways	**Gene Count**	**Notable Genes/ Fold Change**		**P-Value**	**Function**
TNF signaling pathway	18	VCAM1/8.71	NFKB1/2.2	3.66E-11	Inflammation, Metastasis
		MMP9/3.98	CSF1/4.74		
		CCL2/40.35	CCL5/22.46		
		CXCL10/15.72	ICAM1/13.57		
		CFLAR/2.01	TNFAIP3/9.87		
		TRAF3/2.72	BIRC2/2.5		
		BIRC3/ 13.04			
Toll-like receptor signaling pathway	12	TLR1/2.1	TLR2/2.25	1.05E-05	Inflammation, Metastasis
		TLR6/2.05	CCL5/22.46		
		CXCL10/15.72	CXCL11/3.49		
		FOS/-15.51	TRAF3/2.72		
		NFKB1/2.2			
NF-kappa B signaling pathway	10	NFKB1/2.2	NFKB2/2.69	7.04E-05	Inflammation, Metastasis
		VCAM1/8.71	CFLAR/2.01		
		RELB/2.61	TRAF3/2.72		
		BIRC2/2.5	ICAM1/13.57		
Cell adhesion molecules (CAMs)	9	VCAM1/8.71	L1CAM/2.07	0.00903	Invasion, Metastasis
		CD226/-2.33	ALCAM/-2.54		
		CLDN1/4.73	ICAM1/13.57		
		SDC2/-2.58			
Apoptosis	5	CFLAR/2.01	BIRC2/2.5	0.03893	Apoptotic Evasion
		BIRC3/ 13.04	NFKB1/2.2		
		NGF/2.1			
MAPK signaling pathway	10	RELB/2.61	FOS/-15.51	0.08163	Cell Growth
		MAP2K6/-5.08	PLA2G4C/4.5		
Associated Cancer	6	Small cell lung cancer		0.03098	Cancer

Table 3.3 Notable pathways in LT-TNF samples. Gene count represents the number of dysregulated genes in each pathway. Notable genes and their fold change values were listed with additional information of fold change against the control after the '/' symbol. P-Value of the KEGG enrichment and relevant functions of the pathways has been provided. Finally list of cancers pathways of which were found to be related is listed.

Notable Pathways	**Gene Count**	**Notable Genes/ Fold Change**		**P-Value**	**Function**
Proteoglycans in cancer	24	WNT5A/11.31	FGF2/7.09	3.54E-05	Metastasis
		IGF1R/2.78	TWIST2/3.77		
		VEGFA/3.07	SDC2/-3.73		
Ras signaling pathway	25	KITLG/2.96	FGF2/7.09	8.76E-05	Chordoma Progression
		IGF1R/2.78	PDGFRB/11.76		
		PDGFA/2.37	VEGFA/3.07		
		RASA4B/-2.01			
Rap1 signaling pathway	23	KITLG/2.96	FGF2/7.09	0.00021	Cell survival, Metastasis
		CDH1/-9.16	EFNA4/2.36		
		PDGFRB/11.76	PDGFA/2.37		
PI3K-Akt signaling pathway	31	KITLG/2.96	COL1A1/4.16	0.00044	Chordoma Pathogenesis and Progression
		COL4A1/4.59	FGF2/7.09		
		VEGFA/3.07	PDGFA/2.37		
Focal adhesion	21	COL1A1/4.16	COL4A1/4.59	0.00108	Invasion, Chemoresistance
		COL4A2/5.54	COL12A1/123.72		
		PAK2/2.43			
Pathways in cancer	30	KITLG/2.96	WNT5A/11.31	0.00658	Cancer Progression
		CDH1/-9.16	FGF2/7.09		
		FGFR3/-2.25	PDGFA/2.37		
		VEGFA/3.07			
HIF-1 signaling pathway	11	EDN1/19.52	IGF1R/2.78	0.01341	CSCs, Metastasis, Chemoresistance
		INSR/2.63	TFRC/2.9		
		VEGFA/3.07			
ErbB signaling	10	CBLB/3.83	PAK2/2.43	0.01707	Inhibiton of Apoptosis
		PRKCA/5.62			
Cell adhesion molecules (CAMs)	13	VCAM1/19.28	CD226/-3.11	0.02824	Metastasis
		L1CAM/8.18	ALCAM/-2.56		
		CDH1/-9.16	CNTNAP2/2.02		
		OCLN/-9.13	SDC2 /-3.73		
ABC transporters	6	ABCA6/3.27	ABCA9/2.64	0.04839	Tumorigenesis, Chemoresistance
		ABCC4/2.83	ABCC5/2.73		

Signaling pathways regulating pluripotency	12	SKIL/3.00, WNT5A/11.31, FGF2/7.09	0.04921	CSCs
Related Cancers	36	Melanoma, Glioma, Renal Cell Carcinoma, Prostate Cancer	$p<0.05$	Cancer

Ingenuity pathway analysis revealed that TNF-α acts on a wide spectrum of genes important for tumor progression. In one week treated group, the canonical pathways TNFR2 Signaling, Macrophage activation, NF-kB Signaling, Toll-like receptor signaling and IL-10 Signaling were affected. TNF-α, IL1B, NF-kB complex, RELA and TGFB1 have been reported as top upstream regulator genes. Notable diseases listed were inflammatory response, cancer, and inflammatory disease. Cell survival, cellular movement, and proliferation are the top molecular functions (Figure 3.37).

In long term treated samples, in addition to the TNF-α downstream and inflammatory pathways, pro-angiogenic pathways were found to be escalated. Top upstream regulators were TGFB1, TNF, IL1B, ERBB2 and WNT3A. Notable, top disease pathways affected were cancer, and inflammatory disease. Top molecular functions and cellular listed were cellular movement, cellular development, cellular growth and proliferation, cell-cell interaction, and cellular assembly (Figure 3.38).

For further analysis, networks with high consistency of gene regulation were investigated. In short term TNF-α samples 3 networks were generated. Legend for figures 3.40, 3.41, 3.42, 3.43, 3.44 and 3.45 can be found in Figure 3.39 (Figure 3.39). The first figure includes genes related to elevated inflammatory response with functions such as activation of antigen presenting cells, myeloid cells recruitment of phagocytes and immune response of cells (Figure 3.40). Second chart is focused on elevated pathways of cell movement, migration, invasion and leukocyte infiltration (Figure 3.41). The third chart is focused on recruitment of macrophages (Figure 3.42). For long term TNF-α treatment, first chart was designed to focus on escalated gene interactions in invasion of tumor cell lines and branching of endothelial cells which potentially mimics the late metastatic processes in which intravasation and/or extravasation occurs (Figure 3.43). Second chart focused on cell movement in cancer. The dysregulated gene levels are associated with pathways in breast

cancer cell movement (Figure 3.44). The last figure (Figure 3.45) focuses on downstream pathways of VEGFA which leads to vascularization and fibroblast mobilization.

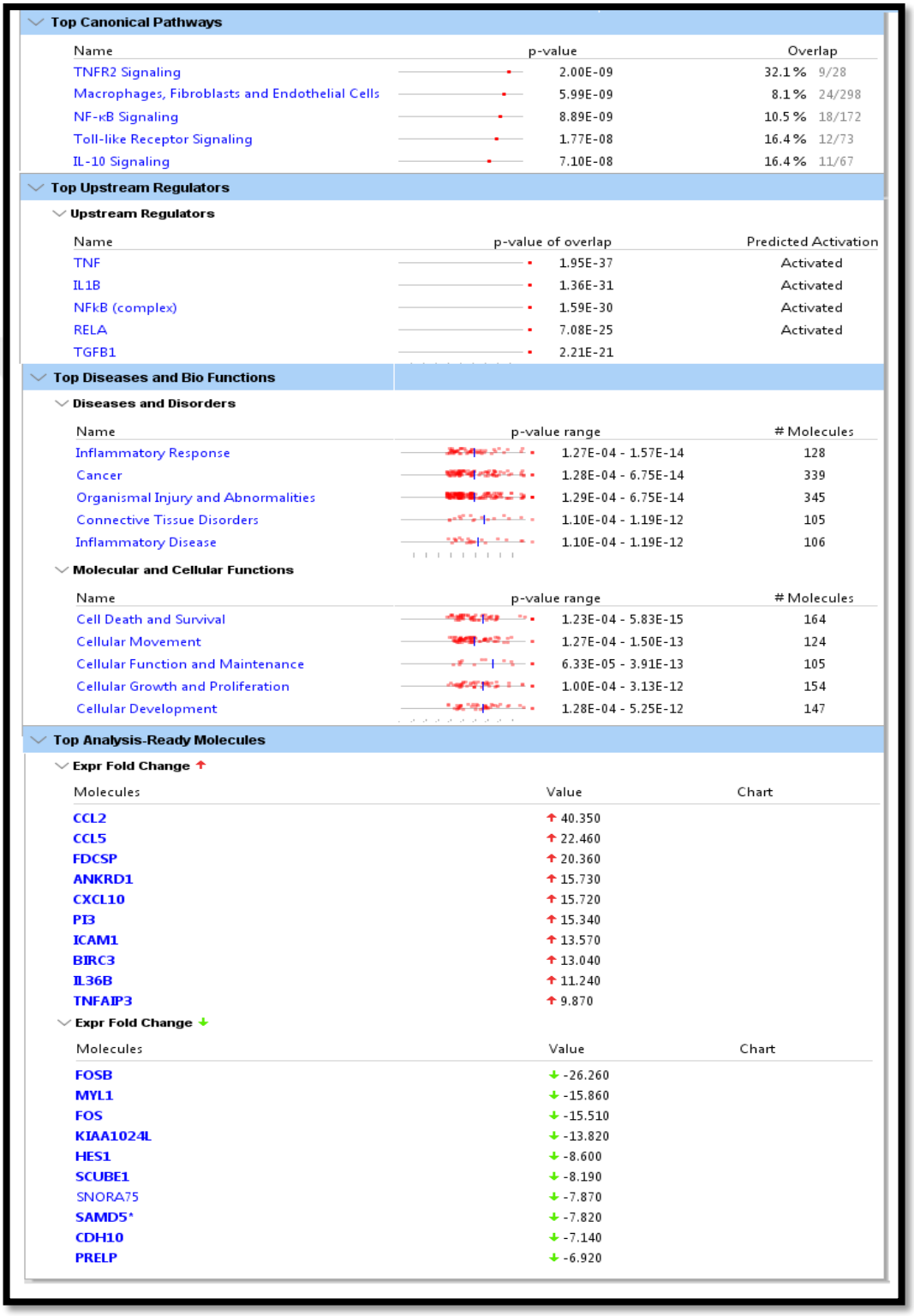

Top Canonical Pathways

Name	p-value	Overlap
TNFR2 Signaling	2.00E-09	32.1 % 9/28
Macrophages, Fibroblasts and Endothelial Cells	5.99E-09	8.1 % 24/298
NF-κB Signaling	8.89E-09	10.5 % 18/172
Toll-like Receptor Signaling	1.77E-08	16.4 % 12/73
IL-10 Signaling	7.10E-08	16.4 % 11/67

Top Upstream Regulators

Upstream Regulators

Name	p-value of overlap	Predicted Activation
TNF	1.95E-37	Activated
IL1B	1.36E-31	Activated
NFkB (complex)	1.59E-30	Activated
RELA	7.08E-25	Activated
TGFB1	2.21E-21	

Top Diseases and Bio Functions

Diseases and Disorders

Name	p-value range	# Molecules
Inflammatory Response	1.27E-04 - 1.57E-14	128
Cancer	1.28E-04 - 6.75E-14	339
Organismal Injury and Abnormalities	1.29E-04 - 6.75E-14	345
Connective Tissue Disorders	1.10E-04 - 1.19E-12	105
Inflammatory Disease	1.10E-04 - 1.19E-12	106

Molecular and Cellular Functions

Name	p-value range	# Molecules
Cell Death and Survival	1.23E-04 - 5.83E-15	164
Cellular Movement	1.27E-04 - 1.50E-13	124
Cellular Function and Maintenance	6.33E-05 - 3.91E-13	105
Cellular Growth and Proliferation	1.00E-04 - 3.13E-12	154
Cellular Development	1.28E-04 - 5.25E-12	147

Top Analysis-Ready Molecules

Expr Fold Change ↑

Molecules	Value	Chart
CCL2	↑ 40.350	
CCL5	↑ 22.460	
FDCSP	↑ 20.360	
ANKRD1	↑ 15.730	
CXCL10	↑ 15.720	
PI3	↑ 15.340	
ICAM1	↑ 13.570	
BIRC3	↑ 13.040	
IL36B	↑ 11.240	
TNFAIP3	↑ 9.870	

Expr Fold Change ↓

Molecules	Value	Chart
FOSB	↓ -26.260	
MYL1	↓ -15.860	
FOS	↓ -15.510	
KIAA1024L	↓ -13.820	
HES1	↓ -8.600	
SCUBE1	↓ -8.190	
SNORA75	↓ -7.870	
SAMD5*	↓ -7.820	
CDH10	↓ -7.140	
PRELP	↓ -6.920	

Figure 3.37 General summary of the Inegnuity pathway analysis for one-week TNF-α treated chordoma cells versus control.

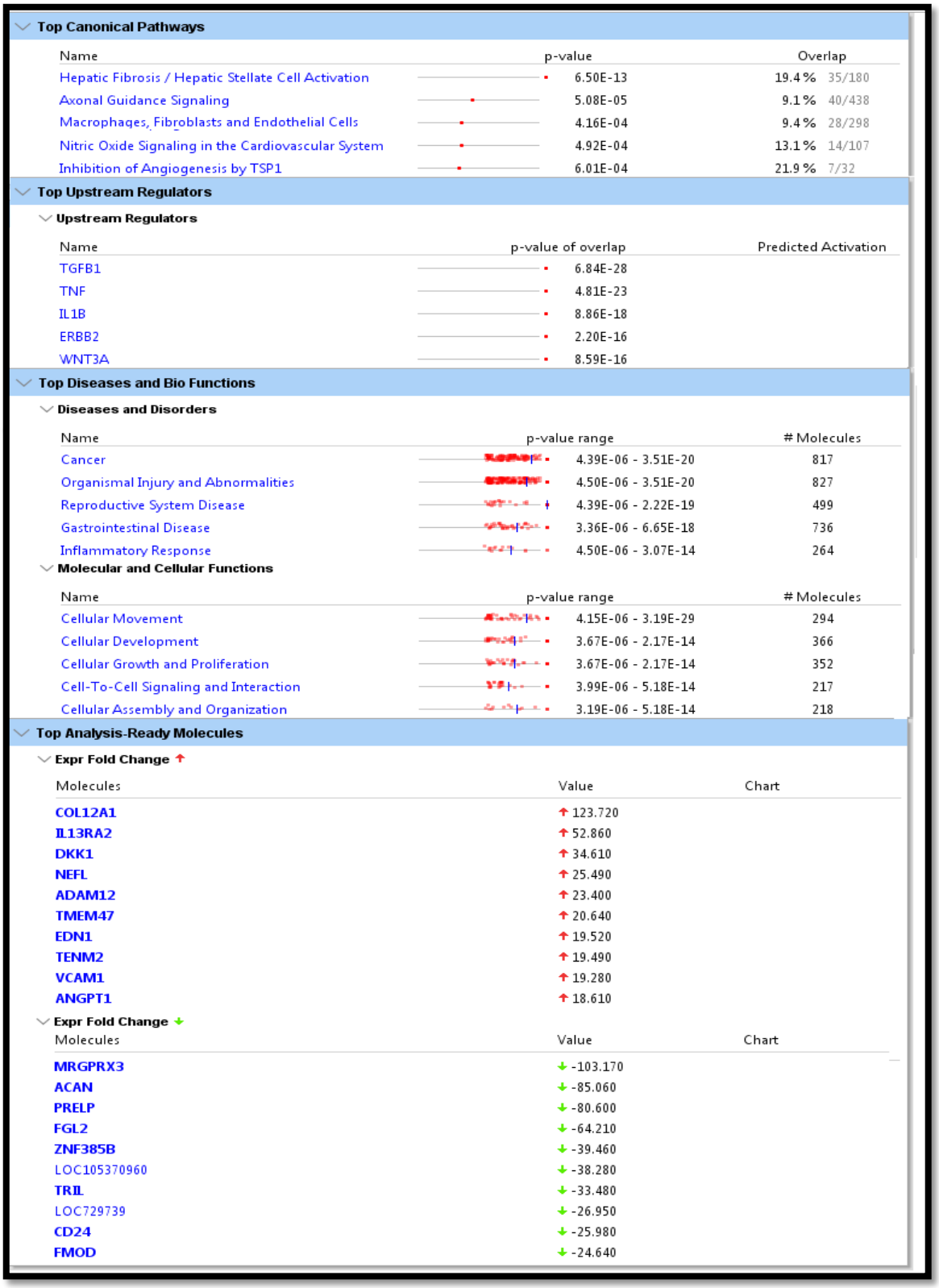

Top Canonical Pathways

Name	p-value	Overlap
Hepatic Fibrosis / Hepatic Stellate Cell Activation	6.50E-13	19.4 % 35/180
Axonal Guidance Signaling	5.08E-05	9.1 % 40/438
Macrophages, Fibroblasts and Endothelial Cells	4.16E-04	9.4 % 28/298
Nitric Oxide Signaling in the Cardiovascular System	4.92E-04	13.1 % 14/107
Inhibition of Angiogenesis by TSP1	6.01E-04	21.9 % 7/32

Top Upstream Regulators

Upstream Regulators

Name	p-value of overlap	Predicted Activation
TGFB1	6.84E-28	
TNF	4.81E-23	
IL1B	8.86E-18	
ERBB2	2.20E-16	
WNT3A	8.59E-16	

Top Diseases and Bio Functions

Diseases and Disorders

Name	p-value range	# Molecules
Cancer	4.39E-06 - 3.51E-20	817
Organismal Injury and Abnormalities	4.50E-06 - 3.51E-20	827
Reproductive System Disease	4.39E-06 - 2.22E-19	499
Gastrointestinal Disease	3.36E-06 - 6.65E-18	736
Inflammatory Response	4.50E-06 - 3.07E-14	264

Molecular and Cellular Functions

Name	p-value range	# Molecules
Cellular Movement	4.15E-06 - 3.19E-29	294
Cellular Development	3.67E-06 - 2.17E-14	366
Cellular Growth and Proliferation	3.67E-06 - 2.17E-14	352
Cell-To-Cell Signaling and Interaction	3.99E-06 - 5.18E-14	217
Cellular Assembly and Organization	3.19E-06 - 5.18E-14	218

Top Analysis-Ready Molecules

Expr Fold Change ↑

Molecules	Value	Chart
COL12A1	↑ 123.720	
IL13RA2	↑ 52.860	
DKK1	↑ 34.610	
NEFL	↑ 25.490	
ADAM12	↑ 23.400	
TMEM47	↑ 20.640	
EDN1	↑ 19.520	
TENM2	↑ 19.490	
VCAM1	↑ 19.280	
ANGPT1	↑ 18.610	

Expr Fold Change ↓

Molecules	Value	Chart
MRGPRX3	↓ -103.170	
ACAN	↓ -85.060	
PRELP	↓ -80.600	
FGL2	↓ -64.210	
ZNF385B	↓ -39.460	
LOC105370960	↓ -38.280	
TRIL	↓ -33.480	
LOC729739	↓ -26.950	
CD24	↓ -25.980	
FMOD	↓ -24.640	

Figure 3.38 General summary of the Inegnuity pathway analysis for LT-TNF treated chordoma cells versus control.

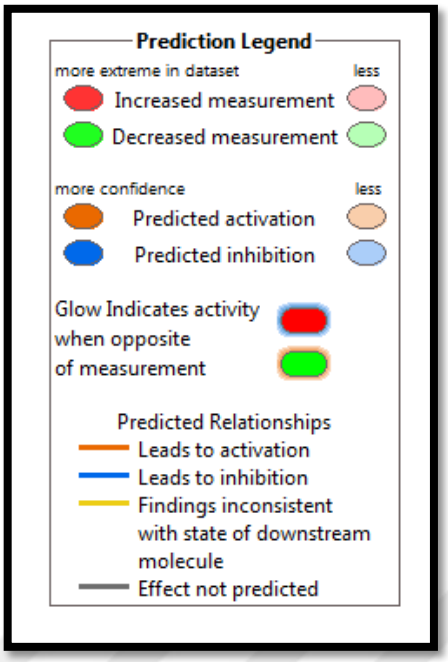

Figure 3.39 Prediction legend for the following casual networks created.

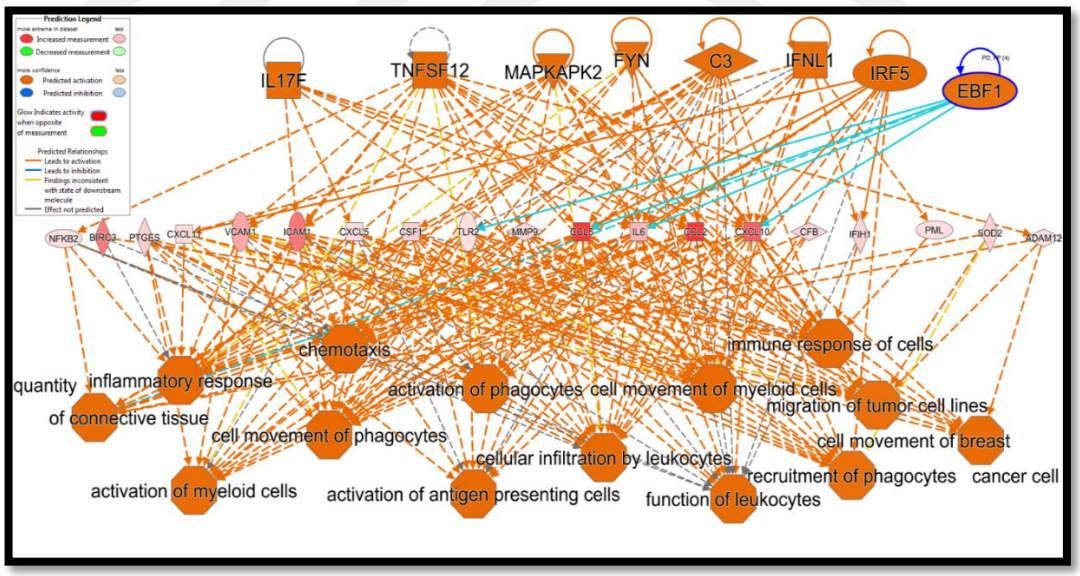

Figure 3.40 Gene expression network related to elevated inflammatory response with functions such as activation of antigen presenting cells, myeloid cells recruitment of phagocytes and immune response of cells in short term TNF treated cells. Orange color means predicted activation and pink to red color means increased expression in an increasing magnitude.

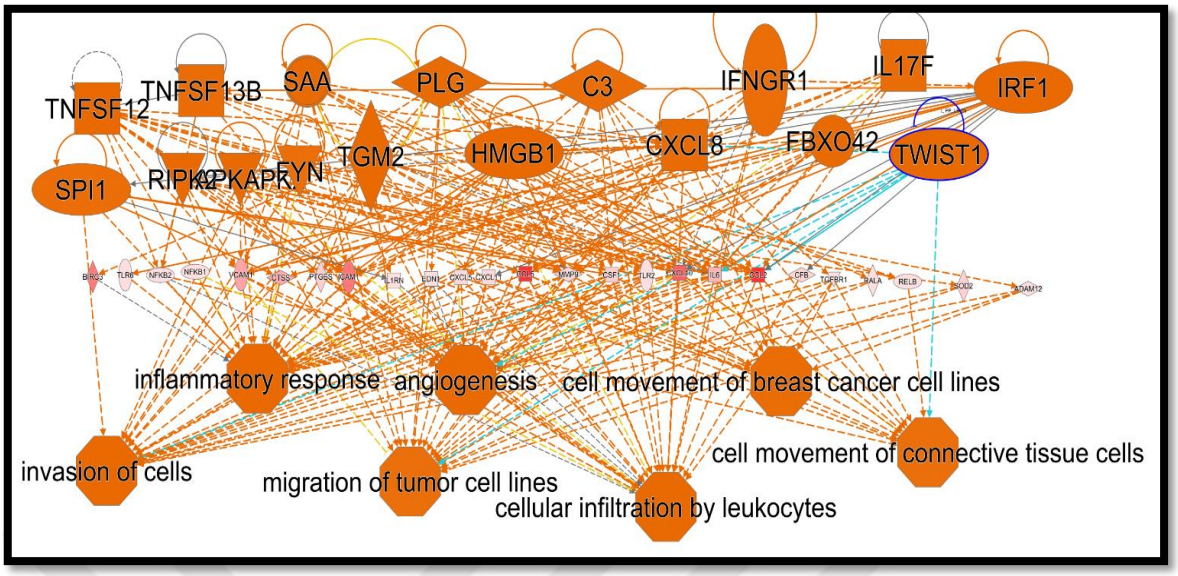

Figure 3.41 Gene expression network related to elevated pathways of cell movement, migration, invasion and leukocyte infiltration in short term TNF treated cells. Orange color means predicted activation and pink to red color means increased expression in an increasing magnitude.

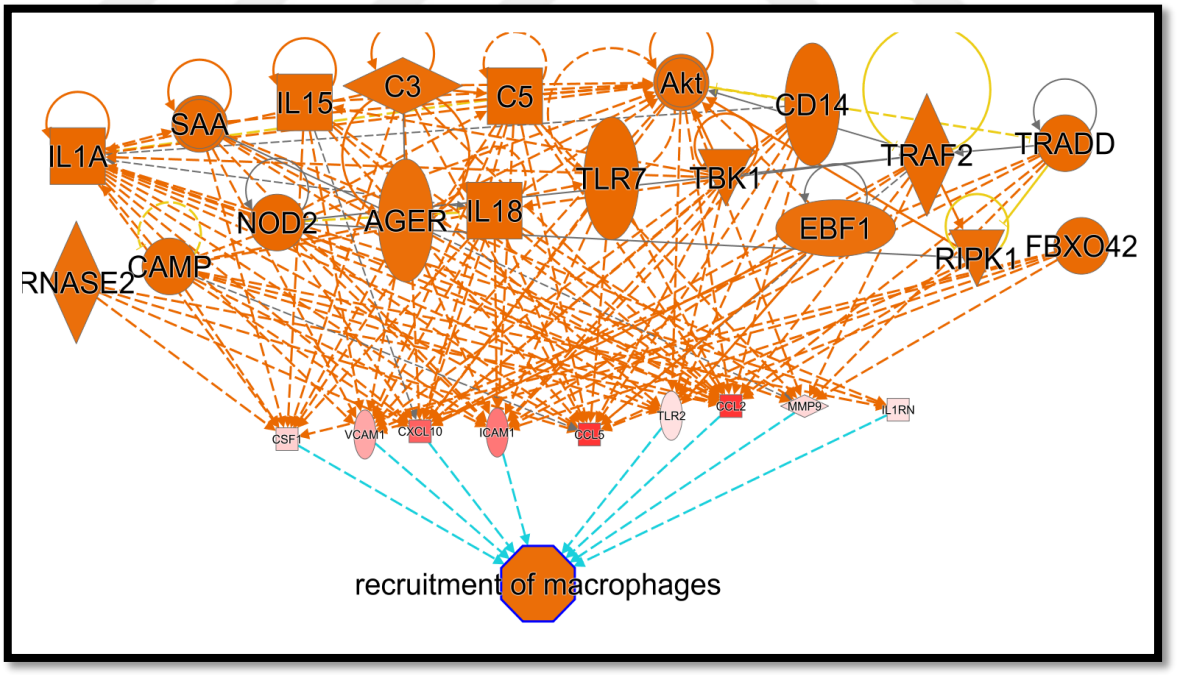

Figure 3.42 Gene expression network related to macrophage recruitment in short term TNF treated cells. Orange color means predicted activation and pink to red color means increased expression in an increasing magnitude.

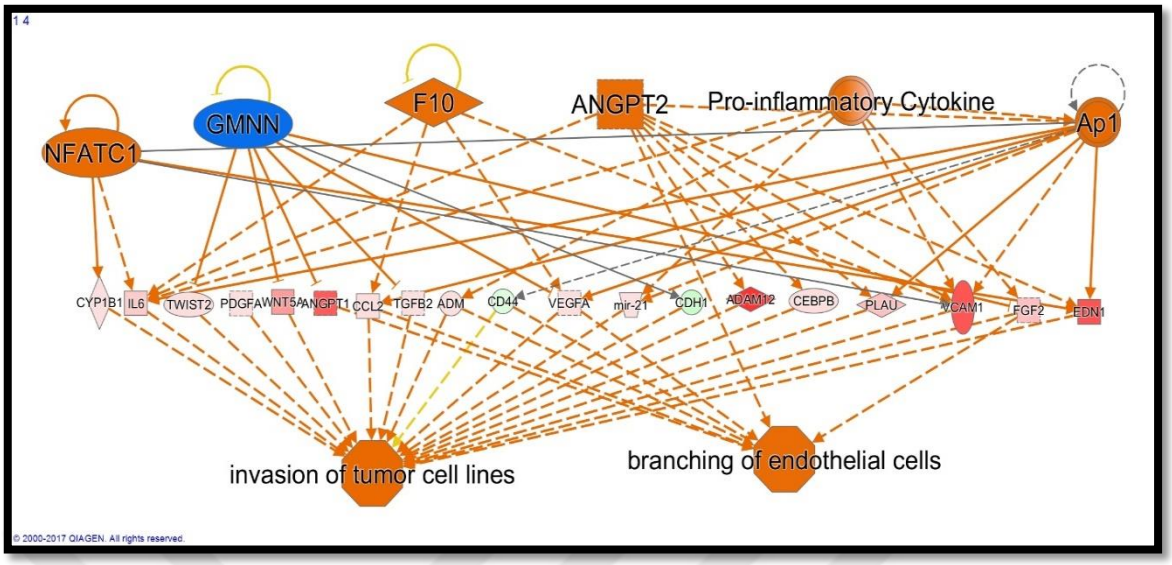

Figure 3.43 Gene expression network related to tumor cell invasion and endothelial branching in LT-TNF samples. Orange color means predicted activation and pink to red color means increased expression in an increasing magnitude.

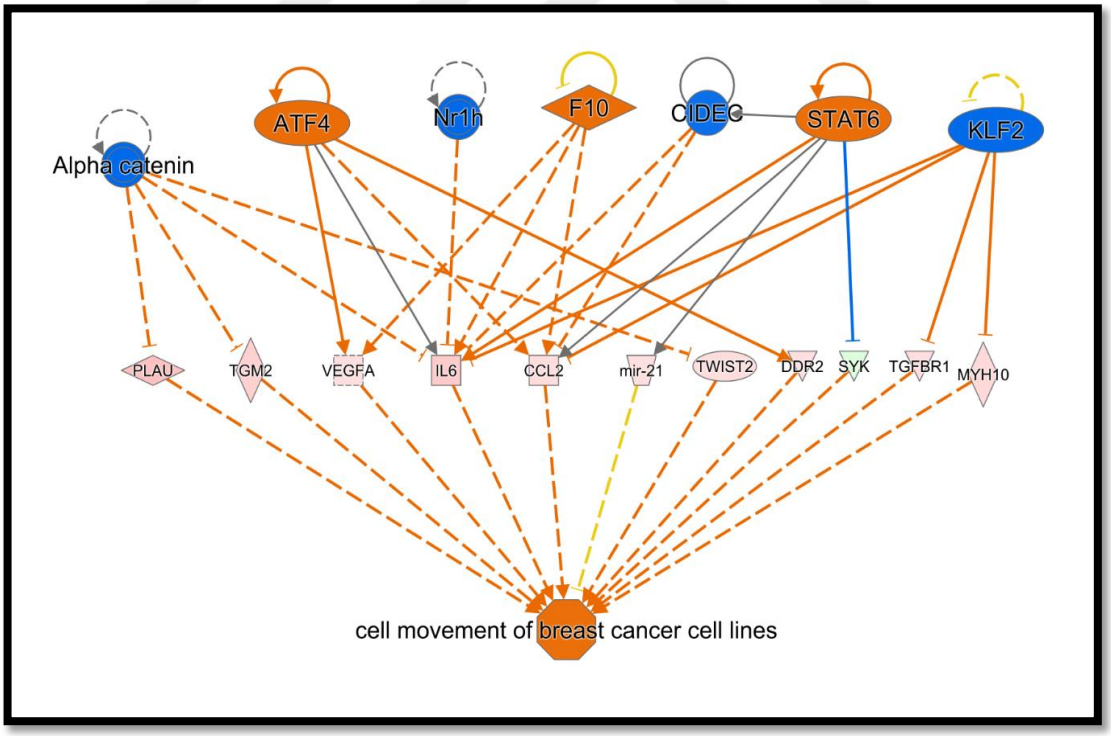

Figure 3.44 Gene expression network related to cell movement in LT-TNF samples. Orange color means predicted activation and pink to red color means increased expression in an increasing magnitude.

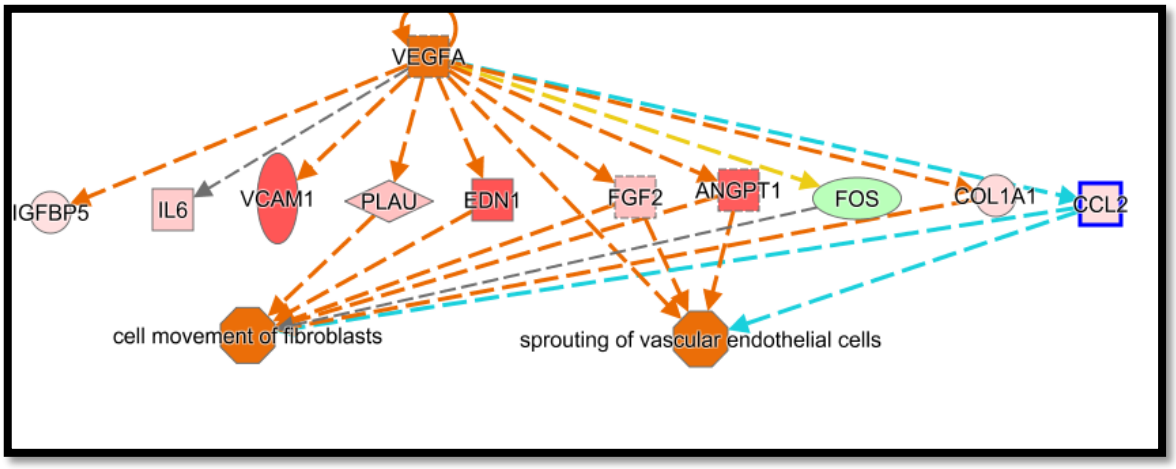

Figure 3.45 Gene expression network related to downstream gene network of VEGFA in LT-TNF treated cells. Orange color means predicted activation and pink to red color means increased expression in an increasing magnitude.

4. DISCUSSION

Cancer can be described as an accumulation of genetic and epigenetic changes leading to uncontrolled division and proliferation of cells as a result of irreversible and irreparable degradation of the biochemical mechanisms and pathways in once healthy and functioning cells. Cancer does not have a standard treatment since each cancer has its own unique molecular-pathological combination. Moreover, many cancer types have accepted subtypes which are distinguished by mutations, surface markers and other traits that alter the ideal treatment strategy and prognosis. In recent years with emerging high-throughput methods such as Next-generation sequencing (NGS), each tumor can be considered as unique which can lead to personalized therapy for each individual in the future. Therefore, acceptance of the differences between cancer types and, accordingly, development of new treatment methods will be appropriate, if better treatment, survival and life quality for patients is in question.

Chordoma is uniquely destructive. Conventionally, aggressive tumors are highly proliferative and motile and also have high grade. Chordoma cells are slow and their proliferation rate is low and they are considered as low-intermediate grade. However chordomas are locally very aggressive and they have a very high rate of local relapse. Tumors are usually located very close to vital neurons and organs. Chordoma is considered as having a low metastatic potential. Chordoma survival time averages to 6 years and distant metastasis occurs at very late stages of the disease. The structure of tumors make it hard for complete resection, which leads to frequent recurrence. Chordoma patients face very low life quality pre and post-operatively. Lack of sufficient knowledge on molecular mechanisms that lead to chordoma tumorigenesis and the steps a tumor takes until terminal disease, makes it hard to treat. Molecular markers that might help physicians decide on a treatment strategy are lacking. Currently there is no consensus on how to treat the disease.

This PhD study has been dedicated to elucidating the regulatory roles of miRNAs on the disease. A reliable miRNA profile has been determined. Additionally potential targets that can play important roles in pathways that are constitutively active in chordoma, have been revealed. Regulatory role of non-coding RNAs has been under the spotlight for the last decade. There is a fast accumulation of data about how these RNAs take part in molecular

mechanisms in various biological activities, proving it is not solely protein-coding gene expression that should be focused on.

hsa-miR-31 inhibits the metastasis of breast cancer [192]. Downregulation of has-miR- 31 affects prognosis in medulloblastoma [193]. A possible mechanism of inhibition for miR-31 through p53 in serous ovarian carcinomas and has been presented [194]. miR-31 expression in chordoma cell lines downregulated c-MET and radixin. As a receptor tyrosine kinase, MET has been correlated with mitogenic and transforming functions through phosphorylation [195]. Elevated c-MET levels result in increased invasion, apoptosis inhibition, angiogenesis [196]. In a study, the bone tumor with most abundant c-MET expression has been found to be chordoma, where 94% of chordoma tumors were positively stained [146]. miR-31 decreased cell viability in U-CH1, U-CH2 and MUG-Chor1. miR-31-3p induced apoptosis in the cell lines and caused S-phase cell cycle arrest. Our findings support these previous findings, and miR-31-3p can be considered as a candidate pro-apoptotic miRNA for chordomas. The current study suggests that there can be connection between low miR-31 levels and high c-MET levels in chordomas by impaired inhibition of its expression by the miRNA. Further studies should be done to understand if this relationship is direct or indirect. Additionally, miR-31 can potentially regulate Radixin (RDX), a gene associated with cell survival and motility, in chordomas, which could help explain the apoptotic effects of miR-31 expression in chordoma cells.

DNMT1 and DNMT3B levels have increased with the inhibition of miR-148a. miRNAs are known to regulate gene families, and it is significant that two genes of the DNMT family were found to be affected by miR-148a in this study. miR-148a could be a regulator of apoptosis by targeting DNMT1 and DNMT3B in chordomas. The two genes are associated with apoptosis in cancer cells and embryonic cells [197,198].

Although miR-148a has been reported to induce apoptosis in colorectal and pancreatic cancer by suppressing Bcl-2, inhibiting the miRNA significantly increased apoptosis in this study [199,200]. This effect may be similar in gastric cancer cells, in which miR-148a increases cell proliferation by targeting p27 [201]. miR-140-3p was previously associated with recurrence and tumor invasion spinal chordoma samples [202]. This result supports the findings of the current study.

The validated targets BIRC5 and TRPS1 and the predicted target KIT level in all three chordoma cell lines were regulated by miR-222. In breast cancer, miR-222 abundance was associated with poorer prognosis and a distinguishable pattern for each breast cancer subtype [203]. BIRC5 and its product survivin inhibit apoptosis and promote cell proliferation [204]. In sacral chordomas, survivin causes poor prognosis and tumor vascularization. [128]. The c-KIT proto-oncogene is a potential therapeutic target in cancers. Abundant c-KIT expression was observed in a number of chordoma samples [36]. In the current study a strong decrease in KIT expression in all three chordoma cell lines as a result of ectopic miR-222-3p overexpression was observed, which may imply that it can play a role in regulating c-KIT expression in chordomas similar to the relation in gastrointestinal stromal tumors [205,206]. This result supports the findings of the current study.

In the current study the level of TRPS1 decreased in miR-222 abundant condition. Tricho-rhino-phalangeal syndrome is a disease caused by non-functional TRPS1 and the lack of Runx2 regulation, which results in defective endochondral ossification [207]. During embryonic development, Runx2 is a key molecule in chondrocyte differentiation, and it is known to control the important chordoma and notochord marker Galectin-3 [208,91]. Chondrocytic differentiation may be related to the chondroid chordoma subtype. In one study, neoplastic chordoid cells were shown to have as having a chondrocytic differentiation potential, a process similar to vertebral development by which the notochord differentiates into nucleus pulposus. Moreover, the adult nucleus pulposus has increased vimentin levels and loses CK19 and EMA. In the same study, the chondroid locus in the tumors exhibited loss of EMA and CK19, which is consistent with the fact that U-CH1 cells, which have a higher level of TRPS1, have less abundance of these markers when compared with MUG-Chor1 cells [209]. These previous findings suggest that TRPS1 could act as a very important regulator of chondrocytic differentiation and pathogenesis in chordomas, and miR-222 may be playing a crucial role in this network. TRPS1 also functions as a regulator of E-cadherin and vimentin by suppressing ZEB2. When TRPS1 is suppressed in breast cancer by miR-222, the E-cadherin expression decreases and vimentin expression increases, which results in EMT [203]. When we checked for the EMT genes in Mug-Chor1, which expresses much higher miR-222 than U-CH1, we observed that the MET markers were less abundant and the EMT markers were more abundant in MUG-Chor1. Therefore, we can speculate that MUG-Chor1 may represent a more aggressive chordoma tumor than U-CH1, and these cell

lines may reflect different steps in the progression of the disease. These results also suggest that miR-222 may play an important role in the pathways leading to EMT of chordoma cells.

The effects of the miRNAs on cell viability were consistent with the cell cycle analysis. miR-31 can be considered as the most potent miRNA in cell cycle S-phase to the G2/M phase transition arrest among the miRNAs that have been analyzed. A similar effect of miR-31 has been reported in liver cancer [210].

LIF is a versatile cytokine with a variety of functions and a complex role in cancer. LIF is an essential actor in embryonic implantation and inhibits the differentiation of mouse embryonic stem cells [211]. In recent studies, LIF has been shown to promote the development and progression of cancer [212,189,213]. Both intrinsic and extrinsic LIF can increase proliferation in vitro, and promote tumor growth in vivo [212-214,183]. LIF overexpression promotes resistance to chemotherapy and radiotherapy [212,213] and has been observed in samples from a variety of tumors, including breast, colorectal, lung, head and neck, and nasopharyngeal carcinoma. It also correlates with a poor clinical outcome in patients. LIF can activate a range of signaling pathways including STAT3, MTOR, MAPK, and p53 [214]. These pathways are also known to play a role in chordoma tumors [215]. Still, little is known about the underlying mechanisms by which LIF can lead to tumor progression, as the studies in this field are limited.

Chordomas are rare tumors of the spine exhibiting excessive chemoresistance and radioresistance, and lacking any confirmed drug therapy. Results from this study suggest that LIF increases the aggressive features of chordoma cells. We have observed that it promotes anchorage-independent growth of chordoma cells in soft agar, and it might also play a role in chordoma metastasis as it increases in vitro trans-well migration and invasion at the first and third weeks of LIF treatment. MET, which is an important gene for local invasion and patient outcome, was shown to be dramatically increased upon LIF treatment in the current study [135,112,216]. Interestingly, when the pro-invasion and pro-migration effects of LIF decline and neutralize after the third week of treatment, the colony and tumorosphere formation abilities of chordoma cells emerge and increase at the fifth and eighth week of exogenous exposure to LIF.

In our further findings, LIF decreased the E-cadherin and CK19 levels while it increased ZEB2 abundance at week 5, which suggests that it may play a role in EMT transition in

chordoma cells. As a late EMT marker, ZEB2 elevation happened at week 5 in both cell lines, whereas the epithelial markers were suppressed throughout the entire 8 weeks, which was a result of the EMT progression. Surface cancer stem-cell marker levels on chordoma cells are consistent with this data, and mRNA levels of NANOG, Oct4, and KLF4 were elevated. Chemoresistance is also increased by LIF treatment, and we observed an increase in the abundance of the ABCG2 drug efflux molecule on the surface of chordoma cells. On both the functional and molecular level, LIF-treated cells show a more motile and invasive character at the first and third week of LIF treatment. As these traits steadily decreased, an increase in tumorosphere formation and anchorage-independent growth alongside, and an increase in CSC and drug-resistance markers at the fifth and eighth weeks was observed. This process can be associated with events during metastasis, in which tumor cells invade the tissue envelope and migrate, eventually settling in other tissues.

The effects of the intrinsic LIF level in chordoma tumor samples were in harmony with the extrinsic effects on chordoma cell lines. In the chordoma cohort, MET and KLF4 levels were significantly correlated with the intrinsic LIF level. Our study presents the first data demonstrating that LIF level is positively correlated with tumor size in patients. Even more importantly the study exhibits that LIF expression is associated with shorter overall relapse-free survival in chordoma patients.

The evaluation of gene networks and pathways that were influenced by LIF presented intriguing results. Although the conventional LIF pathways such as mTOR, AKT, and JAK/STAT3 were not affected, the mRNA profile of LIF-treated chordoma cells showed an outstanding increase in inflammatory pathways. Tumor-promoting inflammation is considered as one of the hallmarks of cancer [153], and LIF is a pro-inflammatory molecule, especially in the spinal cord, as shown by overexpression and knockout studies [217,182]. LIF can pass through the blood-brain barrier during inflammation with the help of the tumor necrosis factor [218]. LIF has recently been shown to activate fibroblasts for a pro-invasive role, promoting cancer cell invasion [190]. In one study, programmed cell death ligand 1 (PD-L1) expression was correlated with tumor-infiltrating lymphocytes (TILs) in chordomas. Furthermore, the data suggests that TILs are associated with metastasis in a chordoma patient cohort [161]. In the current study, TNFAIP2 expression level was checked, which is downstream of the TNF-α and pro-inflammatory NF-kB pathway. Thus, we aimed to find out if extrinsic LIF treatment of chordoma cell lines or intrinsic levels of LIF in our

tissue samples can affect TNFAIP2 expression level. The TNFAIP2 level positively correlated with LIF in chordoma samples and cell lines. Inflammatory pathways such as NF-kB, activated by LIF, might be the driving force of EMT, migration, invasion, and cancer stem-like cell characteristics in chordomas. As the current study and the previous study on TILs and chordomas suggest, chordoma tumors are prone to tumor-promoting inflammation, which can explain their high local invasive character. Chordoma cells respond to extrinsic LIF, to which they are likely to be exposed from the inflammatory tumor microenvironment. As tumor samples exhibit high LIF levels, chordoma cells can also create an inflammatory environment intracellularly, and might secrete LIF into neighboring tumor cells or the tissue microenvironment.

There are few studies of LIF and its relationship to cancer and, to date, the connection between LIF and inflammation in cancer has not been reported. As one of the hallmarks of cancer, tumor-promoting inflammation is a promising field of study for chordoma tumor progression but these studies are very limited. The LIF level can be an important prognostic factor for chordoma patients, and LIF or the LIF receptor (or both) can be a drug target in novel treatment strategies. In summary, this study presents data on the effects of LIF on chordoma migration, invasion, chemoresistance, EMT, and clinicopathological factors. LIF plays a vital role in promoting tumor inflammation and in patients' outcome. Our findings can help determine whether LIF is a biomarker for chordoma progression and a potential target. Our results emphasize tumor-promoting inflammation as a pathway that drives chordoma progression.

Tumor associated macrophages (TAM) account for a big portion of the tumor infiltrating leukocytes in human cancers. The degree of infiltration is associated with poor outcome of disease. Although it is conventionally considered as a mechanism to fight the tumor, this process helps majority of tumors and carries it to a more advanced stage [219,220]. In chordoma, tumor infiltration has been shown to correlate with chordoma metastasis [161]. Tumor infiltrating immune cells play a role in the classical 6 hallmarks of cancers, which are cell growth, blocked growth inhibition, escaping cell death, limitless replication, angiogenesis and invasion of tissue envelope, and also in the 2 emerging hallmarks which are tumor-promoting inflammation and avoiding of immune destruction in the tumor microenvironment [221,153].

TNF-α, alongside IL-1 and IL-6, is one of the most notable of the secreted factors into the extra-cellular matrix after tumor infiltration of leukocytes [222]. In the case of tumor promoting inflammation, LIF, alongside VEGF, CSF1 and interleukins 4, 6 and 10 plays a role in recruiting macrophages towards the tumor and conditioning of the extracellular matrix, resulting in the transformation of the leukocyte into TAM. TAMs and other infiltrated cells secrete a number of factors into the tumor microenvironment including TNF-α to cause angiogenesis, invasiveness, tumor growth, metastasis and immunosuppression. Findings also show that TNF-α is produced by tumor cells and tumor associated cells [223]. TNF-α is involved in tumor cell growth in the inflammatory environment [222]. TNF-α promotes cell survival by acting on TNFR1 and TNFR2, which induce anti-apoptotic pathways [223].

Interestingly, tumor infiltrating cells have the ability to locally suppress immune functions eventually protecting the tumor. Unlike in the presence of pathogens, under sterile inflammatory circumstances in cancer, MHC class II molecule production of leukocytes are suppressed by tumor cell derived TGF-β1, IL-10 and PGE2 [222]. IL-10 and TNF-α in the tumor microenvironment induce expression of PD-L1 in ovarian carcinoma which leads to direct inhibition of immune responses by TAMs [224]. In chordomas PD-L1 level has been found to be correlated with metastasis. Moreover, PD-L1 expression is correlated with elevated tumor infiltration of leukocytes [161]. Noticeably in the current study, Ingenuity Pathway Analysis indicated an elevation of TNF-α and activation of the canonical IL-10 pathway. These findings suggest an important network of TNF-α, IL-10 and PD-L1 might be present in chordomas with immunosuppressing effects in the tumor microenvironment. CSF-1 and TNF-α production of tumor cells recruit TAMs that produce metalloproteinase 2,3,7 and 9. During local invasion of tumors TAMs accompany tumor cells [225].

Angiogenesis is one of the key steps for tumor metastasis by which intravasation is made possible. Under hypoxic conditions, cancer cells need this function as well in order to survive. VEGF is one of the factors that turns on the angiogenic switch in cancer cells. As shown in Figures 3.42 and 3.44 and Table 3.3, long term TNF-α treatment but not short-term treatment dramatically boosts vascularization pathways. HIF-1 signalling is also induced in the LT-TNF group. Along with VEGF, IL-8 and CXCL8, TNF-α is directly angiogenic [222]. Data in this thesis suggest that chordoma cells can also produce such angiogenic molecules and might be able to secrete them to the tumor micromilieu to induce angiogenesis

after being conditioned by leukocytes for a certain amount of time as a result of tumor infiltration. TNFR2 receptor activity has been associated with CD133 positive cells in renal cell carcinoma, which provides the cells with increased proliferative ability and drug resistance [226]. Previously, CD133 positive cells have been associated with chordoma stem-like cells [227]. Therefore, $CD133^{+}$ cells in chordoma may carry out their cancer stem-like cell properties such as chemoresistance specifically through TNF-α and one of its receptors, TNFR2.

In this study, short-term, and long-term TNF-α treatment had similar and distinct effects on chordoma cells. Both increased the ability of chordoma cells to migrate and invade. Early mesenchymal markers appeared at short-term treatment and in long-term treatment the late mesenchymal marker ZEB2 was abundant as expected. As the microarray analysis indicates, short-term TNF treated samples exhibited an increase in expression patterns related directly to TNF-α such as TNFR2 signaling. In long-term TNF-α treated cells similar effects were observed, with the addition of angiogenic pathways and CSC related pathways such as WNT3A downstream genes. These results further support the proposed metastatic model in chordoma that is potentially caused by tumor promoting inflammation in which, pro-inflammatory effectors such as LIF and TNF-α are activated. Such effects depend on the duration of exposure, from invasion and motility at early stages towards CSC-like state and angiogenesis at the later stages.

Targeting of the pro-inflammatory pathways in cancers is already underway. Thalidomide is an inhibitor of VEGF, bFGF and TNF-α which acts by degrading TNF-α in monocytes [228,229]. Thalidomide was shown to be effective in Kaposi's sarcoma, multiple myeloma, metastatic prostate cancer, melanoma, breast cancer and metastatic renal cell carcinoma the drug is tested in phase II trials [230]. Infliximab is another drug against TNF-α that has been tested in cancer [231]. More TNF-α inhibitors are available such as etanercept, adalimumab, golimumab and certolizumab. TNFR blockers and specifically TNFR2 blockers may be of use in chordoma treatment. Serum TNF-α concentration increases and can be monitored in cancer patients [232,233]. Furthermore increased TNF-α levels in benign and malignant tumors has prognostic value [234,235]. Taken together, these findings suggest that TNF-α is a potential prognostic factor for a number of cancers including chordoma and it can be targeted by drug repurposing and combined therapy against disease progression and chemoresistance.

5. CONCLUSION

Overall, this study suggests that miRNAs have a great potential to regulate important genes and pathways in chordomas. miR-31, miR-140-3p, miR-148a, and miR-222-3p are prominent miRNAs that affect key genes, proliferation, the cell cycle, apoptosis, and cell viability. These findings provide a platform to delineate the differential regulation of cancer-related genes in chordoma tumors. To date, this is the most comprehensive study in the field of chordoma miRNA research in terms of functional studies and target genes. These findings may aid in discovering new pathways of tumorigenesis and disease progression as well as markers and therapeutic targets for chordomas. Additional functional studies and patient samples are needed to uncover the role of these miRNAs and their targets in pathways and gene networks for a better understanding of the molecular biology of chordomas for the development of novel strategies for treating the disease.

Additionally, this study presents data on the effects inflammatory cytokines on chordoma migration, invasion, chemoresistance, EMT, and clinicopathological factors. LIF and TNF-α together play a vital role in promoting tumor inflammation and in patients' outcome. Our findings can help determine whether LIF is a biomarker for chordoma progression and a potential target. The effects of the TNF-α molecule on chordomas added to the findings that tumor promoting inflammation and tumor infiltrating cells can be important factors behind chordoma pathogenesis, progression and metastasis. Taken together, these findings present strong evidence that tumor-promoting inflammation might be a strong driver of chordoma tumors from tumorigenesis to advanced and metastatic disease. The study may aspire translational research in which tumor promoting inflammation can be targeted by anti-inflammatory drugs specific to tumor microenvironment associated leukocytes in an effort to find a cure for this orphan disease.

This work was supported by Scientific and Technological Research Council of Turkey [Grant number 112S485].

REFERENCES

1. J. Bjornsson, L. E. Wold, M. J. Ebersold and E. R. Laws. Chordoma of the Mobile Spine. A Clinicopathologic Analysis of 40 Patients. *Cancer*, 71:735-740, 1993.

2. M. L. McMaster, A. M. Goldstein, C. M. Bromley, N. Ishibe and D. M. Parry. Chordoma: Incidence and Survival Patterns in the United States, 1973-1995. *Cancer Causes Control*, 12:1-11, 2001.

3. C. Horbinski, G. J. Oakley, K. Cieply, G. S. Mantha, M. N. Nikiforova, S. Dacic and R. R. Seethala. The Prognostic Value of Ki-67, P53, Epidermal Growth Factor Receptor, 1p36, 9p21, 10q23, and 17p13 in Skull Base Chordomas. *Archives of Pathology and Laboratory Medicine*, 134:1170-1176, 2010.

4. N. Sundaresan, G. Rosen and S. Boriani. Primary Malignant Tumors of the Spine. *The Orthopedic Clinics of North America*, 40:21-36, 2009.

5. J. R. Salisbury, M. H. Deverell, M. J. Cookson and W. F. Whimster. Three-Dimensional Reconstruction of Human Embryonic Notochords: Clue to the Pathogenesis of Chordoma. *Journal of Pathology*, 171:59-62, 1993.

6. C. S. Bailey, C. G. Fisher, M. C. Boyd and M. F. Dvorak. En Bloc Marginal Excision of a Multilevel Cervical Chordoma. Case Report. *Journal of Neurosurgery Spine*, 4:409-414, 2006.

7. T. Ailon, R. Torabi, C. G. Fisher, L. D. Rhines, M. J. Clarke, C. Bettegowda, S. Boriani, Y. J. Yamada, N. Kawahara, P. P. Varga, J. H. Shin, A. Saghal and Z. L. Gokaslan. Management of Locally Recurrent Chordoma of the Mobile Spine and Sacrum: A Systematic Review. *Spine*, 20:193-198, 2016.

8. V. Gellner, P. V. Tomazic, B. Lohberger, K. Meditz, E. Heitzer, M. Mokry, W. Koele, A. Leithner, B. Liegl-Atzwanger and B. Rinner. Establishment of Clival Chordoma Cell Line

Mug-Cc1 and Lymphoblastoid Cells as a Model for Potential New Treatment Strategies. *Scientific Reports*, 6:24195, 2016.

9. A. Saito, T. Hasegawa, T. Shimoda, G. Toda, S. Hirohashi, G. Tajima and Y. Moriya. Dedifferentiated Chordoma: A Case Report. *Japanese Journal of Clinical Oncology*, 28:766-771, 1998.

10. S. A. Hanna, R. Tirabosco, A. Amin, R. C. Pollock, J. A. Skinner, S. R. Cannon, A. Saifuddin and T. W. Briggs. Dedifferentiated Chordoma: A Report of Four Cases Arising 'De Novo'. *The Journal of Bone and Joint Surgery*, 90:652-656, 2008.

11. M. J. Kelley, J. F. Korczak, E. Sheridan, X. Yang, A. M. Goldstein and D. M. Parry. Familial Chordoma, a Tumor of Notochordal Remnants, Is Linked to Chromosome 7q33. *American Journal of Human Genetics*, 69:454-460, 2001.

12. K. E. Wang, Z. Wu, K. Tian, L. Wang, S. Hao, L. Zhang and J. Zhang. Familial Chordoma: A Case Report and Review of the Literature. *Oncology Letters*, 10:2937-2940, 2015.

13. X. R. Yang, D. Ng, D. A. Alcorta, N. J. Liebsch, E. Sheridan, S. Li, A. M. Goldstein, D. M. Parry and M. J. Kelley. T (Brachyury) Gene Duplication Confers Major Susceptibility to Familial Chordoma. *Nature Genetics*, 41:1176-1178, 2009.

14. L. Lee-Jones, I. Aligianis, P. A. Davies, A. Puga, P. A. Farndon, A. Stemmer-Rachamimov, V. Ramesh and J. R. Sampson. Sacrococcygeal Chordomas in Patients with Tuberous Sclerosis Complex Show Somatic Loss of Tsc1 or Tsc2. *Genes Chromosomes and Cancer*, 41:80-85, 2004.

15. M. L. McMaster, A. M. Goldstein and D. M. Parry. Clinical Features Distinguish Childhood Chordoma Associated with Tuberous Sclerosis Complex (Tsc) from Chordoma in the General Paediatric Population. *Journal of Medical Genetics*, 48:444-449, 2011.

16. T. A. Rich, A. Schiller, H. D. Suit and H. J. Mankin. Clinical and Pathologic Review of 48 Cases of Chordoma. *Cancer*, 56:182-187, 1985.

17. T. E. Kaiser, D. J. Pritchard and K. K. Unni. Clinicopathologic Study of Sacrococcygeal Chordoma. *Cancer*, 53:2574-2578, 1984.

18. S. Boriani, S. Bandiera, R. Biagini, P. Bacchini, L. Boriani, M. Cappuccio, F. Chevalley, A. Gasbarrini, P. Picci and J. N. Weinstein. Chordoma of the Mobile Spine: Fifty Years of Experience. *Spine*, 31:493-503, 2006.

19. R. Volpe and A. Mazabraud. A Clinicopathologic Review of 25 Cases of Chordoma (a Pleomorphic and Metastasizing Neoplasm). *American Journal of Surgical Pathology*, 7:161-170, 1983.

20. C. M. McPherson, D. Suki, I. E. McCutcheon, Z. L. Gokaslan, L. D. Rhines and E. Mendel. Metastatic Disease from Spinal Chordoma: A 10-Year Experience. *Journal of Neurosurgery Spine*, 5:277-280, 2006.

21. G. Vergara, B. Belinchon, F. Valcarcel, M. Veiras, I. Zapata and A. de la Torre. Metastatic Disease from Chordoma. *Clinical Translational Oncology*, 10:517-521, 2008.

22. E. Gay, L. N. Sekhar, E. Rubinstein, D. C. Wright, C. Sen, I. P. Janecka and C. H. Snyderman. Chordomas and Chondrosarcomas of the Cranial Base: Results and Follow-up of 60 Patients. *Neurosurgery*, 36:887-896, 1995.

23. P. Bergh, L. G. Kindblom, B. Gunterberg, F. Remotti, W. Ryd and J. M. Meis-Kindblom. Prognostic Factors in Chordoma of the Sacrum and Mobile Spine - a Study of 39 Patients. *Cancer*, 88:2122-2134, 2000.

24. S. Asano, N. Kawahara and T. Kirino. Intradural Spinal Seeding of a Clival Chordoma. *Acta Neurochirurgica (Wien)*, 145:599-603, 2003.

25. S. M. Magrini, M. G. Papi, F. Marletta, S. Tomaselli, E. Cellai, V. Mungai and G. Biti. Chordoma-Natural History, Treatment and Prognosis. The Florence Radiotherapy Department Experience (1956-1990) and a Critical Review of the Literature. *Acta Oncologica*, 31:847-851, 1992.

26. D. Smolders, X. Wang, A. Drevelengas, F. Vanhoenacker and A. M. De Schepper. Value of Mri in the Diagnosis of Non-Clival, Non-Sacral Chordoma. *Skeletal Radiology*, 32:343-350, 2003.

27. M. A. Torres, E. L. Chang, A. Mahajan, D. G. Lege, B. A. Riley, X. Zhang, M. Lii, D. G. Kornguth, C. E. Pelloski and S. Y. Woo. Optimal Treatment Planning for Skull Base Chordoma: Photons, Protons, or a Combination of Both? *International Journal of Radiation Oncology, Biology, Physics.*, 74:1033-1039, 2009.

28. D. C. Dahlin and C. S. Maccarty. Chordoma. *Cancer*, 5:1170-1178, 1952.

29. S. Takahashi, T. Kawase, K. Yoshida, A. Hasegawa and J. E. Mizoe. Skull Base Chordomas: Efficacy of Surgery Followed by Carbon Ion Radiotherapy. *Acta Neurochirurgica (Wien)*, 151:759-769, 2009.

30. M. Amichetti, M. Cianchetti, D. Amelio, R. M. Enrici and G. Minniti. Proton Therapy in Chordoma of the Base of the Skull: A Systematic Review. *Neurosurgical Review*, 32:403-416, 2009.

31. J. E. Mizoe, A. Hasegawa, R. Takagi, H. Bessho, T. Onda and H. Tsujii. Carbon Ion Radiotherapy for Skull Base Chordoma. *Skull Base*, 19:219-224, 2009.

32. G. F. Fleming, P. S. Heimann, J. K. Stephens, M. A. Simon, M. K. Ferguson, R. S. Benjamin and B. L. Samuels. Dedifferentiated Chordoma. Response to Aggressive Chemotherapy in Two Cases. *Cancer*, 72:714-718, 1993.

33. N. Presneau, A. Shalaby, B. Idowu, P. Gikas, S. R. Cannon, I. Gout, T. Diss, R. Tirabosco and A. M. Flanagan. Potential Therapeutic Targets for Chordoma: Pi3k/Akt/Tsc1/Tsc2/Mtor Pathway. *British Journal of Cancer*, 100:1406-1414, 2009.

34. H. Hof, T. Welzel and J. Debus. Effectiveness of Cetuximab/Gefitinib in the Therapy of a Sacral Chordoma. *Onkologie*, 29:572-574, 2006.

35. K. Schonegger, E. Gelpi, D. Prayer, K. Dieckmann, C. Matula, M. Hassler, J. A. Hainfellner and C. Marosi. Recurrent and Metastatic Clivus Chordoma: Systemic Palliative Therapy Retards Disease Progression. *Anticancer Drugs*, 16:1139-1143, 2005.

36. E. Tamborini, F. Miselli, T. Negri, M. S. Lagonigro, S. Staurengo, G. P. Dagrada, S. Stacchiotti, E. Pastore, A. Gronchi, F. Perrone, A. Carbone, M. A. Pierotti, P. G. Casali and S. Pilotti. Molecular and Biochemical Analyses of Platelet-Derived Growth Factor Receptor (Pdgfr) B, Pdgfra, and Kit Receptors in Chordomas. *Clinical Cancer Research*, 12:6920-6928, 2006.

37. P. G. Casali, A. Messina, S. Stacchiotti, E. Tamborini, F. Crippa, A. Gronchi, R. Orlandi, C. Ripamonti, C. Spreafico, R. Bertieri, R. Bertulli, M. Colecchia, E. Fumagalli, A. Greco, F. Grosso, P. Olmi, M. A. Pierotti and S. Pilotti. Imatinib Mesylate in Chordoma. *Cancer*, 101:2086-2097, 2004.

38. F. Orzan, M. R. Terreni, M. Longoni, N. Boari, P. Mortini, C. Doglioni and P. Riva. Expression Study of the Target Receptor Tyrosine Kinase of Imatinib Mesylate in Skull Base Chordomas. *Oncology Reports*, 18:249-252, 2007.

39. S. Stacchiotti, E. Tamborini, S. Lo Vullo, F. Bozzi, A. Messina, C. Morosi, A. Casale, F. Crippa, E. Conca, T. Negri, E. Palassini, A. Marrari, E. Palmerini, L. Mariani, A. Gronchi, S. Pilotti and P. G. Casali. Phase Ii Study on Lapatinib in Advanced Egfr-Positive Chordoma. *Annals of Oncology*, 24:1931-1936, 2013.

40. C. Yang, F. J. Hornicek, K. B. Wood, J. H. Schwab, E. Choy, H. Mankin and Z. F. Duan. Blockage of Stat3 with Cddo-Me Inhibits Tumor Cell Growth in Chordoma. *Spine*, 35:1668-1675, 2010.

41. J. Schwab, C. Antonescu, P. Boland, J. Healey, A. Rosenberg, P. Nielsen, J. Iafrate, T. Delaney, S. Yoon, E. Choy, D. Harmon, K. Raskin, C. Yang, H. Mankin, D. Springfield, F. Hornicek and Z. F. Duan. Combination of Pi3k/Mtor Inhibition Demonstrates Efficacy in Human Chordoma. *Anticancer Research*, 29:1867-1871, 2009.

42. S. Stacchiotti, A. Marrari, E. Tamborini, E. Palassini, E. Virdis, A. Messina, F. Crippa, C. Morosi, A. Gronchi, S. Pilotti and P. G. Casali. Response to Imatinib Plus Sirolimus in Advanced Chordoma. *Annals of Oncology*, 20:1886-1894, 2009.

43. R. Chugh, R. Dunn, M. M. Zalupski, J. S. Biermann, V. K. Sondak, J. R. Mace, K. M. Leu, W. F. Chandler and L. H. Baker. Phase Ii Study of 9-Nitro-Camptothecin in Patients with Advanced Chordoma or Soft Tissue Sarcoma. *Journal of Clinical Oncology*, 23:3597-3604, 2005.

44. B. Loehn, R. R. Walvekar, A. Harton and D. Nuss. Mandibular Metastasis from a Skull Base Chordoma: Report of a Case with Review of Literature. *Skull Base*, 19:363-368, 2009.

45. N. Singhal, D. Kotasek and F. X. Parnis. Response to Erlotinib in a Patient with Treatment Refractory Chordoma. *Anticancer Drugs*, 20:953-955, 2009.

46. I. M. Siu, J. Ruzevick, Q. Zhao, N. Connis, Y. C. Jiao, C. Bettegowda, X. W. Xia, P. C. Burger, C. L. Hann and G. L. Gallia. Erlotinib Inhibits Growth of a Patient-Derived Chordoma Xenograft. *Plos One*, 8, 2013.

47. S. Scheipl, B. Lohberger, B. Rinner, E. V. Froehlich, A. Beham, F. Quehenberger, A. Lazary, P. Pal Varga, J. Haybaeck, A. Leithner and B. Liegl. Histone Deacetylase Inhibitors as Potential Therapeutic Approaches for Chordoma: An Immunohistochemical and Functional Analysis. *Journal of Orthopaedic Research*, 31:1999-2005, 2013.

48. T. Naka, C. Boltze, A. Samii, C. Herold, H. Ostertag, Y. Iwamoto, Y. Oda, M. Tsuneyoshi, D. Kuester and A. Roessner. Skull Base and Nonskull Base Chordomas: Clinicopathologic and Immunohistochemical Study with Special Reference to Nuclear Pleomorphism and Proliferative Ability. *Cancer*, 98:1934-1941, 2003.

49. A. E. Rosenberg, G. P. Nielsen, S. B. Keel, L. G. Renard, M. M. Fitzek, J. E. Munzenrider and N. J. Liebsch. Chondrosarcoma of the Base of the Skull: A Clinicopathologic Study of 200 Cases with Emphasis on Its Distinction from Chordoma. *American Journal of Surgical Pathology*, 23:1370-1378, 1999.

50. J. X. O'Connell, L. G. Renard, N. J. Liebsch, J. T. Efird, J. E. Munzenrider and A. E. Rosenberg. Base of Skull Chordoma. A Correlative Study of Histologic and Clinical Features of 62 Cases. *Cancer*, 74:2261-2267, 1994.

51. C. Thieblemont, P. Biron, F. Rocher, D. Bouhour, J. Y. Bobin, J. P. Gerard and J. Y. Blay. Prognostic Factors in Chordoma: Role of Postoperative Radiotherapy. *European Journal of Cancer*, 31:2255-2259, 1995.

52. K. W. Chen, H. L. Yang, J. Lu, J. Y. Liu and X. Q. Chen. Prognostic Factors of Sacral Chordoma after Surgical Therapy: A Study of 36 Patients. *Spinal Cord*, 48:166-171, 2010.

53. A. A. Sandberg and J. A. Bridge. Updates on the Cytogenetics and Molecular Genetics of Bone and Soft Tissue Tumors. Synovial Sarcoma. *Cancer Genetics Cytogenetics*, 133:1-23, 2002.

54. F. Bayrakli, I. Guney, T. Kilic, M. Ozek and M. N. Pamir. New Candidate Chromosomal Regions for Chordoma Development. *Surgical Neurology*, 68:425-430, 2007.

55. P. Brandal, B. Bjerkehagen, H. Danielsen and S. Heim. Chromosome 7 Abnormalities Are Common in Chordomas. *Cancer Genetics and Cytogenetics*, 160:15-21, 2005.

56. K. H. Hallor, J. Staaf, G. Jonsson, M. Heidenblad, F. Vult von Steyern, H. C. Bauer, M. Ijszenga, P. C. Hogendoorn, N. Mandahl, K. Szuhai and F. Mertens. Frequent Deletion of

the Cdkn2a Locus in Chordoma: Analysis of Chromosomal Imbalances Using Array Comparative Genomic Hybridisation. *British Journal of Cancer*, 98:434-442, 2008.

57. A. Kuzniacka, F. Mertens, B. Strombeck, J. Wiegant and N. Mandahl. Combined Binary Ratio Labeling Fluorescence in Situ Hybridization Analysis of Chordoma. *Cancer Genetics and Cytogenetics*, 151:178-181, 2004.

58. S. Scheil, S. Bruderlein, T. Liehr, H. Starke, J. Herms, M. Schulte and P. Moller. Genome-Wide Analysis of Sixteen Chordomas by Comparative Genomic Hybridization and Cytogenetics of the First Human Chordoma Cell Line, U-Ch1. *Genes Chromosomes Cancer*, 32:203-211, 2001.

59. D. L. Persons, J. A. Bridge and J. R. Neff. Cytogenetic Analysis of Two Sacral Chordomas. *Cancer Genetics and Cytogenetics*, 56:197-201, 1991.

60. M. Miozzo, L. Dalpra, P. Riva, M. Volonta, F. Macciardi, S. Pericotti, M. G. Tibiletti, M. Cerati, K. Rohde, L. Larizza and A. M. Fuhrman Conti. A Tumor Suppressor Locus in Familial and Sporadic Chordoma Maps to 1p36. *International Journal of Cancer*, 87:68-72, 2000.

61. L. P. Le, G. P. Nielsen, A. E. Rosenberg, D. Thomas, J. M. Batten, V. Deshpande, J. Schwab, Z. F. Duan, R. J. Xavier, F. J. Hornicek and A. J. Iafrate. Recurrent Chromosomal Copy Number Alterations in Sporadic Chordomas. *Plos One*, 6, 2011.

62. M. B. Eisenberg, M. Woloschak, C. Sen and D. Wolfe. Loss of Heterozygosity in the Retinoblastoma Tumor Suppressor Gene in Skull Base Chordomas and Chondrosarcomas. *Surgical Neurology*, 47:156-160, 1997.

63. L. Klingler, J. Shooks, P. N. Fiedler, A. Marney, M. G. Butler and H. S. Schwartz. Microsatellite Instability in Sacral Chordoma. *Journal of Surgical Oncology*, 73:100-103, 2000.

64. P. Riva, F. Crosti, F. Orzan, L. Dalpra, P. Mortini, A. Parafioriti, B. Pollo, A. M. F. Conti, M. Miozzo and L. Larizza. Mapping of Candidate Region for Chordoma Development to 1p36.13 by Loh Analysis. *International Journal of Cancer*, 107:493-497, 2003.

65. R. J. Diaz, M. Guduk, R. Romagnuolo, C. A. Smith, P. Northcott, D. Shih, F. Berisha, A. Flanagan, D. G. Munoz, M. D. Cusimano, M. N. Pamir and J. T. Rutka. High-Resolution Whole-Genome Analysis of Skull Base Chordomas Implicates Fhit Loss in Chordoma Pathogenesis. *Neoplasia*, 14:788-798, 2012.

66. V. Barresi, A. Ieni, G. Branca and G. Tuccari. Brachyury: A Diagnostic Marker for the Differential Diagnosis of Chordoma and Hemangioblastoma Versus Neoplastic Histological Mimickers. *Disease Markers*, 2014:514753, 2014.

67. S. R. Henderson, D. Guiliano, N. Presneau, S. McLean, R. Frow, S. Vujovic, J. Anderson, N. Sebire, J. Whelan, N. Athanasou, A. M. Flanagan and C. Boshoff. A Molecular Map of Mesenchymal Tumors. *Genome Bioolgy*, 6:76, 2005.

68. S. Vujovic, S. Henderson, N. Presneau, E. Odell, T. S. Jacques, R. Tirabosco, C. Boshoff and A. M. Flanagan. Brachyury, a Crucial Regulator of Notochordal Development, Is a Novel Biomarker for Chordomas. *Journal of Pathology*, 209:157-165, 2006.

69. B. J. O'Hara, A. Paetau and M. Miettinen. Keratin Subsets and Monoclonal Antibody Hbme-1 in Chordoma: Immunohistochemical Differential Diagnosis between Tumors Simulating Chordoma. *Human Pathology*, 29:119-126, 1998.

70. K. K. Almefty, S. Pravdenkova, J. Sawyer and O. Al-Mefty. Impact of Cytogenetic Abnormalities on the Management of Skull Base Chordomas. *Journal of Neurosurgery*, 110:715-724, 2009.

71. A. K. Bhadra and A. T. Casey. Familial Chordoma. A Report of Two Cases. *Journal of Bone and Joint Surgery*, 88:634-636, 2006.

72. J. Stepanek, S. A. Cataldo, M. J. Ebersold, N. M. Lindor, R. B. Jenkins, K. Unni, B. G. Weinshenker and R. L. Rubenstein. Familial Chordoma with Probable Autosomal Dominant Inheritance. *American Journal of Medical Genetics*, 75:335-336, 1998.

73. N. Pillay, V. Plagnol, P. S. Tarpey, S. B. Lobo, N. Presneau, K. Szuhai, D. Halai, F. Berisha, S. R. Cannon, S. Mead, D. Kasperaviciute, J. Palmen, P. J. Talmud, L. G. Kindblom, M. F. Amary, R. Tirabosco and A. M. Flanagan. A Common Single-Nucleotide Variant in T Is Strongly Associated with Chordoma. *Nature Genetics*, 44:1185-1187, 2012.

74. J. F. Korczak, M. J. Kelley, K. A. Allikian, A. A. Shah, A. M. Goldstein and D. M. Parry. Genomic Screen for Linkage in a Family with Autosomal Dominant Chordoma. *American Journal of Human Genetics*, 61:400-400, 1997.

75. I. Camacho-Arroyo, G. Gonzalez-Aguero, A. Gamboa-Dominguez, M. A. Cerbon and R. Ondarza. Progesterone Receptor Isoforms Expression Pattern in Human Chordomas. *Journal of Neuro-Oncology*, 49:1-7, 2000.

76. M. L. Deniz, T. Kilic, I. Almaata, O. Kurtkaya, A. Sav and M. N. Pamir. Expression of Growth Factors and Structural Proteins in Chordomas: Basic Fibroblast Growth Factor, Transforming Growth Factor Alpha, and Fibronectin Are Correlated with Recurrence. *Neurosurgery*, 51:753-760, 2002.

77. J. H. Schwab, P. J. Boland, N. P. Agaram, N. D. Socci, T. H. Guo, G. O'Toole, X. H. Wang, E. Ostroumov, C. Hunter, J. A. Block, S. Doty, S. Ferrone, J. H. Healey and C. Antonescu. Chordoma and Chondrosarcoma Gene Profile: Implications for Immunotherapy. *Cancer Immunology Immunotherapy*, 58:339-349, 2009.

78. S. Scheil-Bertram, R. Kappler, A. von Baer, E. Hartwig, M. Sarkar, M. Serra, S. Bruderlein, B. Westhoff, I. Melzner, B. Bassaly, J. Herms, H. H. Hugo, M. Schulte and P. Moller. Molecular Profiling of Chordoma. *International Journal of Oncology*, 44:1041-1055, 2014.

79. A. El-Heliebi, T. Kroneis, K. Wagner, K. Meditz, D. Kolb, J. Feichtinger, G. G. Thallinger, F. Quehenberger, B. Liegl-Atzwanger and B. Rinner. Resolving Tumor Heterogeneity: Genes Involved in Chordoma Cell Development Identified by Low-Template Analysis of Morphologically Distinct Cells. *Plos One*, Epub, 2014.

80. H. Zhou, C. B. Chen, J. Lan, C. Liu, X. G. Liu, L. A. Jiang, F. Wei, Q. J. Ma, G. T. Dang and Z. J. Liu. Differential Proteomic Profiling of Chordomas and Analysis of Prognostic Factors. *Journal of Surgical Oncology*, 102:720-727, 2010.

81. S. Kilgore and R. A. Prayson. Apoptotic and Proliferative Markers in Chordomas: A Study of 26 Tumors. *Annals of Diagnostic Pathology*, 6:222-228, 2002.

82. P. M. Weinberger, Z. Yu, D. Kowalski, J. Joe, P. Manger, A. Psyrri and C. T. Sasaki. Differential Expression of Epidermal Growth Factor Receptor, C-Met, and Her2/Neu in Chordoma Compared with 17 Other Malignancies. *Archives of Otolaryngology - Head and Neck Surgery*, 131:707-711, 2005.

83. S. Han, C. Polizzano, G. P. Nielsen, F. J. Hornicek, A. E. Rosenberg and V. Ramesh. Aberrant Hyperactivation of Akt and Mammalian Target of Rapamycin Complex 1 Signaling in Sporadic Chordomas. *Clinical Cancer Research*, 15:1940-1946, 2009.

84. N. Presneau, A. Shalaby, B. Idowu, P. Gikas, S. R. Cannon, I. Gout, T. Diss, R. Tirabosco and A. M. Flanagan. Potential Therapeutic Targets for Chordoma: Pi3k/Akt/Tsc1/Tsc2/Mtor Pathway. *British Journal of Cancer*, 100:1406-1414, 2009.

85. Y. Hu, A. Mintz, S. R. Shah, A. Quinones-Hinojosa and W. Hsu. The Fgfr/Mek/Erk/Brachyury Pathway Is Critical for Chordoma Cell Growth and Survival. *Carcinogenesis*, 35:1491-1499, 2014.

86. M. M. Trucco, O. Awad, B. A. Wilky, S. D. Goldstein, R. L. Huang, R. L. Walker, P. Shah, V. Katuri, N. Gul, Y. L. J. Zhu, E. F. McCarthy, I. Paz-Priel, P. S. Meltzer, C. P. Austin, M. H. Xia and D. M. Loeb. A Novel Chordoma Xenograft Allows in Vivo Drug

Testing and Reveals the Importance of Nf-Kappa B Signaling in Chordoma Biology. *Plos One*, 8, 2013.

87. J. Sommer, D. M. Itani, K. C. Homlar, V. L. Keedy, J. L. Halpern, G. E. Holt, H. S. Schwartz, C. M. Coffin, M. J. Kelley and J. M. Cates. Methylthioadenosine Phosphorylase and Activated Insulin-Like Growth Factor-1 Receptor/Insulin Receptor: Potential Therapeutic Targets in Chordoma. *The Journal of Pathology*, 220:608-617, 2010.

88. S. Scheipl, E. V. Froehlich, A. Leithner, A. Beham, F. Quehenberger, M. Mokry, H. Stammberger, P. P. Varga, A. Lazary, R. Windhager, S. Gattenloehner and B. Liegl. Does Insulin-Like Growth Factor 1 Receptor (Igf-1r) Targeting Provide New Treatment Options for Chordomas? A Retrospective Clinical and Immunohistochemical Study. *Histopathology*, 60:999-1003, 2012.

89. J. M. Meis and A. A. Giraldo. Chordoma. An Immunohistochemical Study of 20 Cases. *Archives of Pathology and Laboratory Medicine*, 112:553-556, 1988.

90. J. R. Salisbury. Demonstration of Cytokeratins and an Epithelial Membrane Antigen in Chondroid Chordoma. *The Journal of Pathology*, 153:37-40, 1987.

91. W. Gotz, M. Kasper, N. Miosge and R. C. Hughes. Detection and Distribution of the Carbohydrate Binding Protein Galectin-3 in Human Notochord, Intervertebral Disc and Chordoma. *Differentiation*, 62:149-157, 1997.

92. T. Naka, Y. Oda, Y. Iwamoto, N. Shinohara, H. Chuman, M. Fukui and M. Tsuneyoshi. Immunohistochemical Analysis of E-Cadherin, Alpha-Catenin, Beta-Catenin, Gamma-Catenin, and Neural Cell Adhesion Molecule (Ncam) in Chordoma. *Journal of Clinical Pathology*, 54:945-950, 2001.

93. H. Horiguchi, T. Sano, Z. R. Qian, M. Hirokawa, N. Kagawa, T. Yamaguchi, T. Hirose and S. Nagahiro. Expression of Cell Adhesion Molecules in Chordomas: An Immunohistochemical Study of 16 Cases. *Acta Neuropathologica*, 107:91-96, 2004.

94. A. Triana, C. Sen, D. Wolfe and R. Hazan. Cadherins and Catenins in Clival Chordomas - Correlation of Expression with Tumor Aggressiveness. *American Journal of Surgical Pathology*, 29:1422-1434, 2005.

95. S. Romeo and P. C. Hogendoorn. Brachyury and Chordoma: The Chondroid-Chordoid Dilemma Resolved? *The Journal of Pathology*, 209:143-146, 2006.

96. A. I. Kavka and J. B. Green. Tales of Tails: Brachyury and the T-Box Genes. *Biochimica et Biophysica Acta*, 1333:73-84, 1997.

97. H. J. Fehling, G. Lacaud, A. Kubo, M. Kennedy, S. Robertson, G. Keller and V. Kouskoff. Tracking Mesoderm Induction and Its Specification to the Hemangioblast During Embryonic Stem Cell Differentiation. *Development*, 130:4217-4227, 2003.

98. R. S. Beddington, P. Rashbass and V. Wilson. Brachyury--a Gene Affecting Mouse Gastrulation and Early Organogenesis. *Development Supplement*:157-165, 1992.

99. B. G. Herrmann. Expression Pattern of the Brachyury Gene in Whole-Mount Twis/Twis Mutant Embryos. *Development*, 113:913-917, 1991.

100. D. Stott, A. Kispert and B. G. Herrmann. Rescue of the Tail Defect of Brachyury Mice. *Genes and Development*, 7:197-203, 1993.

101. N. Christoforou, R. A. Miller, C. M. Hill, C. C. Jie, A. S. McCallion and J. D. Gearhart. Mouse Es Cell-Derived Cardiac Precursor Cells Are Multipotent and Facilitate Identification of Novel Cardiac Genes. *Journal of Clinical Investigation*, 118:894-903, 2008.

102. S. L. Paige, T. Osugi, O. K. Afanasiev, L. Pabon, H. Reinecke and C. E. Murry. Endogenous Wnt/Beta-Catenin Signaling Is Required for Cardiac Differentiation in Human Embryonic Stem Cells. *Plos One*, 5:11134, 2010.

103. F. R. Schubert, A. Fainsod, Y. Gruenbaum and P. Gruss. Expression of the Novel Murine Homeobox Gene Sax-1 in the Developing Nervous System. *Mechanisms of Development*, 51:99-114, 1995.

104. J. C. Park, Y. K. Chae, C. H. Son, M. S. Kim, J. Lee, K. Ostrow, D. Sidransky, M. O. Hoque and C. Moon. Epigenetic Silencing of Human T (Brachyury Homologue) Gene in Non-Small-Cell Lung Cancer. *Biochemical and Biophysical Research Communications*, 365:221-226, 2008.

105. A. R. Sangoi, M. S. Dulai, A. H. Beck, D. J. Brat and H. Vogel. Distinguishing Chordoid Meningiomas from Their Histologic Mimics: An Immunohistochemical Evaluation. *American Journal of Surgical Pathology*, 33:669-681, 2009.

106. H. Takei and S. Z. Powell. Novel Immunohistochemical Markers in the Diagnosis of Nonglial Tumors of Nervous System. *Advances in Anatomic Pathology*, 17:150-153, 2010.

107. W. Hsu, A. Mohyeldin, S. R. Shah, C. M. ap Rhys, L. F. Johnson, N. I. Sedora-Roman, T. A. Kosztowski, O. A. Awad, E. F. McCarthy, D. M. Loeb, J. P. Wolinsky, Z. L. Gokaslan and A. Quinones-Hinojosa. Generation of Chordoma Cell Line Jhc7 and the Identification of Brachyury as a Novel Molecular Target. *Journal of Neurosurgery*, 115:760-769, 2011.

108. A. C. Nelson, N. Pillay, S. Henderson, N. Presneau, R. Tirabosco, D. Halai, F. Berisha, P. Flicek, D. L. Stemple, C. D. Stern, F. C. Wardle and A. M. Flanagan. An Integrated Functional Genomics Approach Identifies the Regulatory Network Directed by Brachyury (T) in Chordoma. *Journal of Pathology*, 228:274-285, 2012.

109. L. Zhang, S. Guo, J. H. Schwab, G. P. Nielsen, E. Choy, S. Ye, Z. Zhang, H. Mankin, F. J. Hornicek and Z. Duan. Tissue Microarray Immunohistochemical Detection of Brachyury Is Not a Prognostic Indicator in Chordoma. *Plos One*, Epub, 2013.

110. M. Shimoda, T. Sugiura, I. Imajyo, K. Ishii, S. Chigita, K. Seki, Y. Kobayashi and K. Shirasuna. The T-Box Transcription Factor Brachyury Regulates Epithelial-Mesenchymal

Transition in Association with Cancer Stem-Like Cells in Adenoid Cystic Carcinoma Cells. *Bmc Cancer*, 12:377, 2012.

111. C. Palena, D. E. Polev, K. Y. Tsang, R. I. Fernando, M. Litzinger, L. L. Krukovskaya, A. V. Baranova, A. P. Kozlov and J. Schlom. The Human T-Box Mesodermal Transcription Factor Brachyury Is a Candidate Target for T-Cell-Mediated Cancer Immunotherapy. *Clinical Cancer Research*, 13:2471-2478, 2007.

112. Z. Duan, E. Choy, G. P. Nielsen, A. Rosenberg, J. Iafrate, C. Yang, J. Schwab, H. Mankin, R. Xavier and F. J. Hornicek. Differential Expression of Microrna (Mirna) in Chordoma Reveals a Role for Mirna-1 in Met Expression. *Journal of Orthopaedic Research*, 28:746-752, 2010.

113. Z. Duan, J. Shen, X. Yang, P. Yang, E. Osaka, E. Choy, G. Cote, D. Harmon, Y. Zhang, G. P. Nielsen, D. Spentzos, H. Mankin and F. Hornicek. Prognostic Significance of Mirna-1 (Mir-1) Expression in Patients with Chordoma. *Journal of Orthopaedic Research*, 32:695-701, 2014.

114. O. F. Bayrak, S. Gulluoglu, E. Aydemir, U. Ture, H. Acar, B. Atalay, Z. Demir, S. Sevli, C. J. Creighton, M. Ittmann, F. Sahin and M. Ozen. Microrna Expression Profiling Reveals the Potential Function of Microrna-31 in Chordomas. *Journal of Neuro-Oncology*, 115:143-151, 2013.

115. C. Long, L. Jiang, F. Wei, C. Ma, H. Zhou, S. M. Yang, X. G. Liu and Z. J. Liu. Integrated Mirna-Mrna Analysis Revealing the Potential Roles of Mirnas in Chordomas. *Plos One*, Epub, 2013.

116. B. Rinner, A. Weinhaeusel, B. Lohberger, E. V. Froehlich, W. Pulverer, C. Fischer, K. Meditz, S. Scheipl, S. Trajanoski, C. Guelly, A. Leithner and B. Liegl. Chordoma Characterization of Significant Changes of the DNA Methylation Pattern. *Plos One*, Epub, 2013.

117. R. S. Herbst. Review of Epidermal Growth Factor Receptor Biology. *International Journal of Radiation Oncology Biology Physics*, 59:21-26, 2004.

118. A. Shalaby, N. Presneau, H. T. Ye, D. Halai, F. Berisha, B. Idowu, A. Leithner, B. Liegl, T. R. W. Briggs, K. Bacsi, L. G. Kindblom, N. Athanasou, M. F. Amary, P. C. W. Hogendoorn, R. Tirabosco and A. M. Flanagan. The Role of Epidermal Growth Factor Receptor in Chordoma Pathogenesis: A Potential Therapeutic Target. *Journal of Pathology*, 223:336-346, 2011.

119. K. Ptaszynski, A. Szumera-Cieckiewicz, J. Owczarek, A. Mrozkowiak, M. Pekul, J. Baranska and P. Rutkowski. Epidermal Growth Factor Receptor (Egfr) Status in Chordoma. *Polish Journal of Pathology*, 60:81-87, 2009.

120. R. Akhavan-Sigari, M. R. Gaab, V. Rohde, M. Abili and H. Ostertag. Expression of Pdgfr-Alpha, Egfr and C-Met in Spinal Chordoma: A Series of 52 Patients. *Anticancer Research*, 34:623-630, 2014.

121. N. C. Reich, M. Oren and A. J. Levine. Two Distinct Mechanisms Regulate the Levels of a Cellular Tumor Antigen, P53. *Molecular and Cellular Biology*, 3:2143-2150, 1983.

122. R. Pallini, G. Maira, F. Pierconti, M. L. Falchetti, E. Alvino, G. Cimino-Reale, E. Fernandez, E. D'Ambrosio and L. M. Larocca. Chordoma of the Skull Base: Predictors of Tumor Recurrence. *Journal of Neurosurgery*, 98:812-822, 2003.

123. K. Sakai, K. Hongo, Y. Tanaka and J. Nakayama. Analysis of Immunohistochemical Expression of P53 and the Proliferation Marker Ki-67 Antigen in Skull Base Chordomas: Relationships between Their Expression and Prognosis. *Brain Tumor Pathology*, 24:57-62, 2007.

124. A. Matsuno, T. Sasaki, T. Nagashima, R. Matsuura, H. Tanaka, M. Hirakawa, M. Murakami and T. Kirino. Immunohistochemical Examination of Proliferative Potentials and the Expression of Cell Cycle-Related Proteins of Intracranial Chordomas. *Human Pathology*, 28:714-719, 1997.

125. Y. Yakkioui, Y. Temel, D. Creytens, A. Jahanshahi, R. Fleischeuer, R. G. Santegoeds and J. J. Van Overbeeke. A Comparison of Cell-Cycle Markers in Skull Base and Sacral Chordomas. *World Neurosurgery*, Epub 2013.

126. J. B. Park, C. K. Lee, J. S. Koh, J. K. Lee, E. Y. Park and K. D. Riew. Overexpressions of Nerve Growth Factor and Its Tropomyosin-Related Kinase a Receptor on Chordoma Cells. *Spine* 32:1969-1973, 2007.

127. S. Fukuda and L. M. Pelus. Survivin, a Cancer Target with an Emerging Role in Normal Adult Tissues. *Molecular Cancer Therapeutics*, 5:1087-1098, 2006.

128. C. Chen, H. L. Yang, K. W. Chen, G. L. Wang, J. Lu, Q. Yuan, Y. P. Gu and Z. P. Luo. High Expression of Survivin in Sacral Chordoma. *Medical Oncology*, 30:529, 2013.

129. M. Auger, B. Raney, D. Callender, P. Eifel and N. G. Ordonez. Metastatic Intracranial Chordoma in a Child with Massive Pulmonary Tumor Emboli. *Pediatric Pathology*, 14:763-770, 1994.

130. A. Guedes, B. G. Barreto, L. G. Barreto, I. B. de Oliveira Araujo, A. C. Queiroz, D. A. Athanazio and P. R. Athanazio. Metastatic Parachordoma. *Journal of Cutaneous Pathology*, 36:270-273, 2009.

131. A. Perasole, D. Infantolino and F. Spigariol. Aspiration Cytology and Immunocytochemistry of Sacral Chordoma with Liver Metastases: A Case Report. *Diagnostic Cytopathology*, 7:277-281, 1991.

132. G. Maira, R. Pallini, C. Anile, E. Fernandez, F. Salvinelli, M. L. LaRocca and G. F. Rossi. Surgical Treatment of Clival Chordomas: The Transsphenoidal Approach Revisited. *Journal of Neurosurgery*, 85:784-792, 1996.

133. T. Naka, D. Kuester, C. Boltze, T. O. Schulz, A. Samii, C. Herold, H. Ostertag and A. Roessner. Expression of Matrix Metalloproteinases-1, -2, and -9; Tissue Inhibitors of Matrix Metalloproteinases-1 and -2; Cathepsin B; Urokinase Plasminogen Activator; and

Plasminogen Activator Inhibitor, Type I in Skull Base Chordoma. *Human Pathology*, 39:217-223, 2008.

134. T. Naka, C. Boltze, D. Kuester, T. O. Schulz, A. Samii, M. Herold, H. Ostertag and A. Roessner. Expression of Matrix Metalloproteinase (Mmp)-1, Mmp-2, Mmp-9, Cathepsin B, and Urokinase Plasminogen Actovator in Non-Skull Base Chordoma. *American Journal of Clinical Pathology*, 122:926-930, 2004.

135. T. Naka, C. Boltze, A. Samii, M. Samii, C. Herold, H. Ostertag, Y. Iwamoto, Y. Oda, M. Tsuneyoshi, D. Kuester and A. Roessner. Expression of C-Met, Low-Molecular-Weight Cytokeratin, Matrix Metalloproteinases-1 and -2 in Spinal Chordoma. *Histopathology*, 54:607-613, 2009.

136. Z. L. Gokaslan, S. K. Chintala, J. E. York, V. Boyapati, S. Jasti, R. Sawaya, G. Fuller, D. M. Wildrick, G. L. Nicolson and J. S. Rao. Expression and Localization of Urokinase-Type Plasminogen Activator in Human Spinal Column Tumors. *Clinical and Experimental Metastasis*, 16:713-719, 1998.

137. Z. L. Gokaslan, S. K. Chintala, J. E. York, V. Boyapati, S. Jasti, R. Sawaya, G. Fuller, D. M. Wildrick, G. L. Nicolson and J. S. Rao. Expression and Role of Matrix Metalloproteinases Mmp-2 and Mmp-9 in Human Spinal Column Tumors. *Clinical and Experimental Metastasis*, 16:721-728, 1998.

138. K. Mori, T. Chano, R. Kushima, S. Hukuda and H. Okabe. Expression of E-Cadherin in Chordomas: Diagnostic Marker and Possible Role of Tumor Cell Affinity. *Virchows Archiv*, 440:123-127, 2002.

139. T. Negri, P. Casieri, F. Miselli, M. Orsenigo, C. Piacenza, S. Stacchiotti, P. Bidoli, P. G. Casali, M. A. Pierotti, E. Tamborini and S. Pilotti. Evidence for Pdgfra, Pdgfrb and Kit Deregulation in an Nsclc Patient. *British Journal of Cancer*, 96:180-181, 2007.

140. C. Haeckel, S. Krueger, D. Kuester, H. Ostertag, M. Samii, F. Buehling, D. Broemme, B. Czerniak and A. Roessner. Expression of Cathepsin K in Chordoma. *Human Pathology*, 31:834-840, 2000.

141. M. Zhou, K. W. Chen, H. L. Yang, G. L. Wang, J. Lu, Y. M. Ji, C. S. Wu and C. Chen. Expression of Insulin-Like Growth Factor Ii Mrna-Binding Protein 3 (Imp3) in Sacral Chordoma. *Journal of Neuro-Oncology*, 116:77-82, 2014.

142. C. Birchmeier, W. Birchmeier, E. Gherardi and G. F. Vande Woude. Met, Metastasis, Motility and More. *Nature Reviews Molecular Cell Biology*, 4:915-925, 2003.

143. L. J. Appleman. Met Signaling Pathway: A Rational Target for Cancer Therapy. *Journal of Clinical Oncology*, 29:4837-4838, 2011.

144. L. L. Pisters, P. Troncoso, H. E. Zhau, W. Li, A. C. von Eschenbach and L. W. Chung. C-Met Proto-Oncogene Expression in Benign and Malignant Human Prostate Tissues. *The Journal Urology*, 154:293-298, 1995.

145. W. F. Grigioni, M. Fiorentino, A. D'Errico, A. Ponzetto, T. Crepaldi, M. Prat and P. M. Comoglio. Overexpression of C-Met Protooncogene Product and Raised Ki67 Index in Hepatocellular Carcinomas with Respect to Benign Liver Conditions. *Hepatology*, 21:1543-1546, 1995.

146. T. Naka, Y. Iwamoto, N. Shinohara, M. Ushijima, H. Chuman and M. Tsuneyoshi. Expression of C-Met Proto-Oncogene Product (C-Met) in Benign and Malignant Bone Tumors. *Modern Pathology*, 10:832-838, 1997.

147. T. Naka, D. Kuester, C. Boltze, S. Scheil-Bertram, A. Samii, C. Herold, H. Ostertag, S. Krueger and A. Roessner. Expression of Hepatocyte Growth Factor and C-Met in Skull Base Chordoma. *Cancer*, 112:104-110, 2008.

148. E. Aydemir, O. F. Bayrak, F. Sahin, B. Atalay, G. T. Kose, M. Ozen, S. Sevli, A. B. Dalan, M. E. Yalvac, T. Dogruluk and U. Ture. Characterization of Cancer Stem-Like Cells in Chordoma Laboratory Investigation. *Journal of Neurosurgery*, 116:810-820, 2012.

149. B. Lohberger, B. Rinner, N. Stuendl, M. Absenger, B. Liegl-Atzwanger, S. M. Walzer, R. Windhager and A. Leithner. Aldehyde Dehydrogenase 1, a Potential Marker for Cancer Stem Cells in Human Sarcoma. *Plos One*, Epub, 2012.

150. W. Hsu, A. Mohyeldin, S. R. Shah, Z. L. Gokaslan and A. Quinones-Hinojosa. Role of Cancer Stem Cells in Spine Tumors: Review of Current Literature. *Neurosurgery*, 71:117-125, 2012.

151. M. Karin. Nuclear Factor-Kappab in Cancer Development and Progression. *Nature*, 441:431-436, 2006.

152. B. B. Aggarwal, R. V. Vijayalekshmi and B. Sung. Targeting Inflammatory Pathways for Prevention and Therapy of Cancer: Short-Term Friend, Long-Term Foe. *Clinical Cancer Research*, 15:425-430, 2009.

153. D. Hanahan and R. A. Weinberg. Hallmarks of Cancer: The Next Generation. *Cell*, 144:646-674, 2011.

154. M. Schafer and S. Werner. Cancer as an Overhealing Wound: An Old Hypothesis Revisited. *Nature Reviews Molecular Cell Biology*, 9:628-638, 2008.

155. S. B. Coffelt, C. E. Lewis, L. Naldini, J. M. Brown, N. Ferrara and M. De Palma. Elusive Identities and Overlapping Phenotypes of Proangiogenic Myeloid Cells in Tumors. *American Journal of Pathology*, 176:1564-1576, 2010.

156. D. G. DeNardo, P. Andreu and L. M. Coussens. Interactions between Lymphocytes and Myeloid Cells Regulate Pro- Versus Anti-Tumor Immunity. *Cancer Metastasis Reviews*, 29:309-316, 2010.

157. M. Egeblad, E. S. Nakasone and Z. Werb. Tumors as Organs: Complex Tissues That Interface with the Entire Organism. *Developmental Cell*, 18:884-901, 2010.

158. C. Murdoch, M. Muthana, S. B. Coffelt and C. E. Lewis. The Role of Myeloid Cells in the Promotion of Tumour Angiogenesis. *Nature Reviews Cancer*, 8:618-631, 2008.

159. B. Z. Qian and J. W. Pollard. Macrophage Diversity Enhances Tumor Progression and Metastasis. *Cell*, 141:39-51, 2010.

160. Meningioma of the Cervical Spinal Dura with Post-Operative Uremia and Renal Insufficiency. *Clinical Bulletin of Univ Hospital Cleveland (Ohio)*, 10:12-14, 1946.

161. Y. Feng, J. Shen, Y. Gao, Y. Liao, G. Cote, E. Choy, I. Chebib, H. Mankin, F. Hornicek and Z. Duan. Expression of Programmed Cell Death Ligand 1 (Pd-L1) and Prevalence of Tumor-Infiltrating Lymphocytes (Tils) in Chordoma. *Oncotarget*, 6:11139-11149, 2015.

162. A. H. Beck, I. Espinosa, B. Edris, R. Li, K. Montgomery, S. Zhu, S. Varma, R. J. Marinelli, M. van de Rijn and R. B. West. The Macrophage Colony-Stimulating Factor 1 Response Signature in Breast Carcinoma. *Clinical Cancer Research*, 15:778-787, 2009.

163. C. Steidl, T. Lee, S. P. Shah, P. Farinha, G. Han, T. Nayar, A. Delaney, S. J. Jones, J. Iqbal, D. D. Weisenburger, M. A. Bast, A. Rosenwald, H. K. Muller-Hermelink, L. M. Rimsza, E. Campo, J. Delabie, R. M. Braziel, J. R. Cook, R. R. Tubbs, E. S. Jaffe, G. Lenz, J. M. Connors, L. M. Staudt, W. C. Chan and R. D. Gascoyne. Tumor-Associated Macrophages and Survival in Classic Hodgkin's Lymphoma. *New England Journal of Medicine*, 362:875-885, 2010.

164. L. S. Hammes, R. R. Tekmal, P. Naud, M. I. Edelweiss, N. Kirma, P. T. Valente, K. J. Syrjanen and J. S. Cunha-Filho. Macrophages, Inflammation and Risk of Cervical Intraepithelial Neoplasia (Cin) Progression--Clinicopathological Correlation. *Gynecologic Oncology*, 105:157-165, 2007.

165. I. H. Bronkhorst, L. V. Ly, E. S. Jordanova, J. Vrolijk, M. Versluis, G. P. Luyten and M. J. Jager. Detection of M2-Macrophages in Uveal Melanoma and Relation with Survival. *Investigative Ophthalmology and Visual Science*, 52:643-650, 2011.

166. M. Karin and Y. Ben-Neriah. Phosphorylation Meets Ubiquitination: The Control of Nf-[Kappa]B Activity. *Annual Review of Immunology*, 18:621-663, 2000.

167. H. Wajant. The Role of Tnf in Cancer. *Results and Problems in Cell Differentiation*, 49:1-15, 2009.

168. F. Balkwill. Tumour Necrosis Factor and Cancer. *Nature Reviews Cancer*, 9:361-371, 2009.

169. S. Wu, C. M. Boyer, R. S. Whitaker, A. Berchuck, J. R. Wiener, J. B. Weinberg and R. C. Bast, Jr. Tumor Necrosis Factor Alpha as an Autocrine and Paracrine Growth Factor for Ovarian Cancer: Monokine Induction of Tumor Cell Proliferation and Tumor Necrosis Factor Alpha Expression. *Cancer Research*, 53:1939-1944, 1993.

170. M. J. Chuang, K. H. Sun, S. J. Tang, M. W. Deng, Y. H. Wu, J. S. Sung, T. L. Cha and G. H. Sun. Tumor-Derived Tumor Necrosis Factor-Alpha Promotes Progression and Epithelial-Mesenchymal Transition in Renal Cell Carcinoma Cells. *Cancer Science*, 99:905-913, 2008.

171. P. Bhat-Nakshatri, H. Appaiah, C. Ballas, P. Pick-Franke, R. Goulet, Jr., S. Badve, E. F. Srour and H. Nakshatri. Slug/Snai2 and Tumor Necrosis Factor Generate Breast Cells with Cd44+/Cd24- Phenotype. *Bmc Cancer*, 10:411, 2010.

172. N. Muthukumaran, K. E. Miletti-Gonzalez, A. K. Ravindranath and L. Rodriguez-Rodriguez. Tumor Necrosis Factor-Alpha Differentially Modulates Cd44 Expression in Ovarian Cancer Cells. *Molecular Cancer Research*, 4:511-520, 2006.

173. J. W. Antoon, R. Lai, A. P. Struckhoff, A. M. Nitschke, S. Elliott, E. C. Martin, L. V. Rhodes, N. S. Yoon, V. A. Salvo, B. Shan, B. S. Beckman, K. P. Nephew and M. E. Burow.

Altered Death Receptor Signaling Promotes Epithelial-to-Mesenchymal Transition and Acquired Chemoresistance. *Scientific Reports*, 2:539, 2012.

174. S. T. Wu, G. H. Sun, C. Y. Hsu, C. S. Huang, Y. H. Wu, H. H. Wang and K. H. Sun. Tumor Necrosis Factor-Alpha Induces Epithelial-Mesenchymal Transition of Renal Cell Carcinoma Cells Via a Nuclear Factor Kappa B-Independent Mechanism. *Experimental Biology and Medicine (Maywood)*, 236:1022-1029, 2011.

175. L. Zhang, M. Jiao, K. Wu, L. Li, G. Zhu, X. Wang, D. He and D. Wu. Tnf-Alpha Induced Epithelial Mesenchymal Transition Increases Stemness Properties in Renal Cell Carcinoma Cells. *International Journal of Clinical and Experimental Medicine*, 7:4951-4958, 2014.

176. D. P. Gearing, T. Druck, K. Huebner, J. Overhauser, D. J. Gilbert, N. G. Copeland and N. A. Jenkins. The Leukemia Inhibitory Factor Receptor (Lifr) Gene Is Located within a Cluster of Cytokine Receptor Loci on Mouse Chromosome 15 and Human Chromosome 5p12-P13. *Genomics*, 18:148-150, 1993.

177. P. C. Heinrich, I. Behrmann, G. Muller-Newen, F. Schaper and L. Graeve. Interleukin-6-Type Cytokine Signalling through the Gp130/Jak/Stat Pathway. *The Biochememistry Journal*, 334:297-314, 1998.

178. D. Arthan, S. K. Hong and J. I. Park. Leukemia Inhibitory Factor Can Mediate Ras/Raf/Mek/Erk-Induced Growth Inhibitory Signaling in Medullary Thyroid Cancer Cells. *Cancer Lett*ers 297:31-41, 2010.

179. H. Slaets, D. Dumont, J. Vanderlocht, J. P. Noben, P. Leprince, J. Robben, J. Hendriks, P. Stinissen and N. Hellings. Leukemia Inhibitory Factor Induces an Antiapoptotic Response in Oligodendrocytes through Akt-Phosphorylation and up-Regulation of 14-3-3. *Proteomics*, 8:1237-1247, 2008.

180. M. Lotz, T. Moats and P. M. Villiger. Leukemia Inhibitory Factor Is Expressed in Cartilage and Synovium and Can Contribute to the Pathogenesis of Arthritis. *Journal of Clinical Investigation*, 90:888-896, 1992.

181. P. M. Waring, G. J. Carroll, D. A. Kandiah, G. Buirski and D. Metcalf. Increased Levels of Leukemia Inhibitory Factor in Synovial Fluid from Patients with Rheumatoid Arthritis and Other Inflammatory Arthritides. *Arthritis and Rheumatism*, 36:911-915, 1993.

182. B. J. Kerr and P. H. Patterson. Leukemia Inhibitory Factor Promotes Oligodendrocyte Survival after Spinal Cord Injury. *Glia*, 51:73-79, 2005.

183. S. Kuphal, S. Wallner and A. K. Bosserhoff. Impact of Lif (Leukemia Inhibitory Factor) Expression in Malignant Melanoma. *Experimental and Molecular Pathology*, 95:156-165, 2013.

184. H. Kamohara, M. Ogawa, T. Ishiko, K. Sakamoto and H. Baba. Leukemia Inhibitory Factor Functions as a Growth Factor in Pancreas Carcinoma Cells: Involvement of Regulation of Lif and Its Receptor Expression. *International Journal of Oncology*, 30:977-983, 2007.

185. I. Garcia-Tunon, M. Ricote, A. Ruiz, B. Fraile, R. Paniagua and M. Royuela. Osm, Lif, Its Receptors, and Its Relationship with the Malignance in Human Breast Carcinoma (in Situ and in Infiltrative). *Cancer Investigation*, 26:222-229, 2008.

186. M. Wysoczynski, K. Miekus, K. Jankowski, J. Wanzeck, S. Bertolone, A. Janowska-Wieczorek, J. Ratajczak and M. Z. Ratajczak. Leukemia Inhibitory Factor: A Newly Identified Metastatic Factor in Rhabdomyosarcomas. *Cancer Research*, 67:2131-2140, 2007.

187. J. S. Fitzgerald, S. A. Tsareva, T. G. Poehlmann, L. Berod, A. Meissner, F. M. Corvinus, B. Wiederanders, E. Pfitzner, U. R. Markert and K. Friedrich. Leukemia Inhibitory Factor Triggers Activation of Signal Transducer and Activator of Transcription 3, Proliferation,

Invasiveness, and Altered Protease Expression in Choriocarcinoma Cells. *International Journal of Biochemistry and Cellular Biology*, 37:2284-2296, 2005.

188. S. Maruta, S. Takiguchi, M. Ueyama, Y. Kataoka, Y. Oda, M. Tsuneyoshi and H. Iguchi. A Role for Leukemia Inhibitory Factor in Melanoma-Induced Bone Metastasis. *Clinical and Experimental Metastasis*, 26:133-141, 2009.

189. X. Yue, Y. Zhao, C. Zhang, J. Li, Z. Liu, J. Liu and W. Hu. Leukemia Inhibitory Factor Promotes Emt through Stat3-Dependent Mir-21 Induction. *Oncotarget*, 2015.

190. J. Albrengues, I. Bourget, C. Pons, V. Butet, P. Hofman, S. Tartare-Deckert, C. C. Feral, G. Meneguzzi and C. Gaggioli. Lif Mediates Proinvasive Activation of Stromal Fibroblasts in Cancer. *Cell Reports*, 7:1664-1678, 2014.

191. B. Rinner, E. V. Froehlich, K. Buerger, H. Knausz, B. Lohberger, S. Scheipl, C. Fischer, A. Leithner, C. Guelly, S. Trajanoski, K. Szuhai and B. Liegl. Establishment and Detailed Functional and Molecular Genetic Characterisation of a Novel Sacral Chordoma Cell Line, Mug-Chor1. *International Journal of Oncology*, 40:443-451, 2012.

192. S. Valastyan, A. Chang, N. Benaich, F. Reinhardt and R. A. Weinberg. Activation of Mir-31 Function in Already-Established Metastases Elicits Metastatic Regression. *Genes and Development*, 25:646-659, 2011.

193. E. Ferretti, E. De Smaele, A. Po, L. Di Marcotullio, E. Tosi, M. S. B. Espinola, C. Di Rocco, R. Riccardi, F. Giangaspero, A. Farcomeni, I. Nofroni, P. Laneve, U. Gioia, E. Caffarelli, I. Bozzoni, I. Screpanti and A. Gulino. Microrna Profiling in Human Medulloblastoma. *International Journal of Cancer*, 124:568-577, 2009.

194. C. J. Creighton, M. D. Fountain, Z. Yu, A. K. Nagaraja, H. Zhu, M. Khan, E. Olokpa, A. Zariff, P. H. Gunaratne, M. M. Matzuk and M. L. Anderson. Molecular Profiling Uncovers a P53-Associated Role for Microrna-31 in Inhibiting the Proliferation of Serous Ovarian Carcinomas and Other Cancers. *Cancer Research*, 70:1906-1915, 2010.

195. A. de Luca, N. Arena, L. M. Sena and E. Medico. Met Overexpression Confers Hgf-Dependent Invasive Phenotype to Human Thyroid Carcinoma Cells in Vitro. *Journal of Cellular Physiology*, 180:365-371, 1999.

196. P. M. Comoglio, S. Giordano and L. Trusolino. Drug Development of Met Inhibitors: Targeting Oncogene Addiction and Expedience. *Nature Revews Drug Discovery*, 7:504-516, 2008.

197. H. Kimura, I. Suetake and S. Tajima. Exogenous Expression of Mouse Dnmt3 Induces Apoptosis in Xenopus Early Embryos. *Journal of Biochemistry*, 131:933-941, 2002.

198. T. Abe, M. Toyota, H. Suzuki, M. Murai, K. Akino, M. Ueno, M. Nojima, A. Yawata, H. Miyakawa, T. Suga, H. Ito, T. Endo, T. Tokino, Y. Hinoda and K. Imai. Upregulation of Bnip3 by 5-Aza-2'-Deoxycytidine Sensitizes Pancreatic Cancer Cells to Hypoxia-Mediated Cell Death. *Journal of Gastroenterology*, 40:504-510, 2005.

199. R. Zhang, M. Li, W. Zang, X. Chen, Y. Wang, P. Li, Y. Du, G. Zhao and L. Li. Mir-148a Regulates the Growth and Apoptosis in Pancreatic Cancer by Targeting Cckbr and Bcl-2. *Tumour Biology*, 35:837-844, 2014.

200. H. Zhang, Y. Li, Q. Huang, X. Ren, H. Hu, H. Sheng and M. Lai. Mir-148a Promotes Apoptosis by Targeting Bcl-2 in Colorectal Cancer. *Cell Death and Differentiation*, 18:1702-1710, 2011.

201. S. L. Guo, Z. Peng, X. Yang, K. J. Fan, H. Ye, Z. H. Li, Y. Wang, X. L. Xu, J. Li, Y. L. Wang, Y. Teng and X. Yang. Mir-148a Promoted Cell Proliferation by Targeting P27 in Gastric Cancer Cells. *International Journal of Biological Science*, 7:567-574, 2011.

202. M. X. Zou, W. Huang, X. B. Wang, G. H. Lv, J. Li and Y. W. Deng. Identification of Mir-140-3p as a Marker Associated with Poor Prognosis in Spinal Chordoma. *International Journal of Clinical and Experimental Pathology*, 7:4877-4885, 2014.

203. S. Stinson, M. R. Lackner, A. T. Adai, N. Yu, H. J. Kim, C. O'Brien, J. Spoerke, S. Jhunjhunwala, Z. Boyd, T. Januario, R. J. Newman, P. Yue, R. Bourgon, Z. Modrusan, H. M. Stern, S. Warming, F. J. de Sauvage, L. Amler, R. F. Yeh and D. Dornan. Trps1 Targeting by Mir-221/222 Promotes the Epithelial-to-Mesenchymal Transition in Breast Cancer. *Science Signaling*, 4:38-41, 2011.

204. S. K. Chiou, M. K. Jones and A. S. Tarnawski. Survivin - an Anti-Apoptosis Protein: Its Biological Roles and Implications for Cancer and Beyond. *Medical Science Monitor*, 9:25-29, 2003.

205. C. M. Gits, P. F. van Kuijk, M. B. Jonkers, A. W. Boersma, W. F. van Ijcken, A. Wozniak, R. Sciot, P. Rutkowski, P. Schoffski, T. Taguchi, R. H. Mathijssen, J. Verweij, S. Sleijfer, M. Debiec-Rychter and E. A. Wiemer. Mir-17-92 and Mir-221/222 Cluster Members Target Kit and Etv1 in Human Gastrointestinal Stromal Tumours. *British Journal of Cancer*, 109:1625-1635, 2013.

206. M. Koelz, J. Lense, F. Wrba, M. Scheffler, H. P. Dienes and M. Odenthal. Down-Regulation of Mir-221 and Mir-222 Correlates with Pronounced Kit Expression in Gastrointestinal Stromal Tumors. *International Journal of Oncology*, 38:503-511, 2011.

207. D. Napierala, K. Sam, R. Morello, Q. Zheng, E. Munivez, R. A. Shivdasani and B. Lee. Uncoupling of Chondrocyte Differentiation and Perichondrial Mineralization Underlies the Skeletal Dysplasia in Tricho-Rhino-Phalangeal Syndrome. *Human Molecular Genetics*, 17:2244-2254, 2008.

208. M. Stock, H. Schafer, S. Stricker, G. Gross, S. Mundlos and F. Otto. Expression of Galectin-3 in Skeletal Tissues Is Controlled by Runx2. *Journal of Biological Chemistry*, 278:17360-17367, 2003.

209. D. Gottschalk, M. Fehn, S. Patt, W. Saeger, T. Kirchner and T. Aigner. Matrix Gene Expression Analysis and Cellular Phenotyping in Chordoma Reveals Focal Differentiation Pattern of Neoplastic Cells Mimicking Nucleus Pulposus Development. *American Journal of Pathology*, 158:1571-1578, 2001.

210. H. S. Kim, K. S. Lee, H. J. Bae, J. W. Eun, Q. Shen, S. J. Park, W. C. Shin, H. D. Yang, M. Park, W. S. Park, Y. K. Kang and S. W. Nam. Microrna-31 Functions as a Tumor Suppressor by Regulating Cell Cycle and Epithelial-Mesenchymal Transition Regulatory Proteins in Liver Cancer. *Oncotarget*, 6:8089-8102, 2015.

211. W. Hu, Z. Feng, A. K. Teresky and A. J. Levine. P53 Regulates Maternal Reproduction through Lif. *Nature*, 450:721-724, 2007.

212. X. Li, Q. Yang, H. Yu, L. Wu, Y. Zhao, C. Zhang, X. Yue, Z. Liu, H. Wu, B. G. Haffty, Z. Feng and W. Hu. Lif Promotes Tumorigenesis and Metastasis of Breast Cancer through the Akt-Mtor Pathway. *Oncotarget*, 5:788-801, 2014.

213. C. Long, L. Jiang, F. Wei, C. Ma, H. Zhou, S. Yang, X. Liu and Z. Liu. Integrated Mirna-Mrna Analysis Revealing the Potential Roles of Mirnas in Chordomas. *Plos One*, Epub, 2013.

214. H. Yu, X. Yue, Y. Zhao, X. Li, L. Wu, C. Zhang, Z. Liu, K. Lin, Z. Y. Xu-Monette, K. H. Young, J. Liu, Z. Shen, Z. Feng and W. Hu. Lif Negatively Regulates Tumour-Suppressor P53 through Stat3/Id1/Mdm2 in Colorectal Cancers. *Nature Communications*, 5:5218, 2014.

215. S. Gulluoglu, O. Turksoy, A. Kuskucu, U. Ture and O. F. Bayrak. The Molecular Aspects of Chordoma. *Neurosurgical Review*, 39:185-196 2016.

216. O. F. Bayrak, S. Gulluoglu, E. Aydemir, U. Ture, H. Acar, B. Atalay, Z. Demir, S. Sevli, C. J. Creighton, M. Ittmann, F. Sahin and M. Ozen. Microrna Expression Profiling Reveals the Potential Function of Microrna-31 in Chordomas. *Journal of Neurooncology*, 115:143-151, 2013.

217. B. J. Kerr and P. H. Patterson. Potent Pro-Inflammatory Actions of Leukemia Inhibitory Factor in the Spinal Cord of the Adult Mouse. *Experimental Neurologyl*, 188:391-407, 2004.

218. W. Pan, C. Yu, H. Hsuchou, Y. Zhang and A. J. Kastin. Neuroinflammation Facilitates Lif Entry into Brain: Role of Tnf. *American Journal of Physiology and Cell Physiology*, 294:1436-1442, 2008.

219. J. W. Pollard. Trophic Macrophages in Development and Disease. *Nature Reviews Immunology*, 9:259-270, 2009.

220. A. Mantovani, P. Allavena, A. Sica and F. Balkwill. Cancer-Related Inflammation. *Nature*, 454:436-444, 2008.

221. D. Hanahan and R. A. Weinberg. The Hallmarks of Cancer. *Cell*, 100:57-70, 2000.

222. C. E. Lewis and J. W. Pollard. Distinct Role of Macrophages in Different Tumor Microenvironments. *Cancer Research*, 66:605-612, 2006.

223. W. W. Lin and M. Karin. A Cytokine-Mediated Link between Innate Immunity, Inflammation, and Cancer. *Journal of Clinical Investigation*, 117:1175-1183, 2007.

224. I. Kryczek, L. Zou, P. Rodriguez, G. Zhu, S. Wei, P. Mottram, M. Brumlik, P. Cheng, T. Curiel, L. Myers, A. Lackner, X. Alvarez, A. Ochoa, L. Chen and W. Zou. B7-H4 Expression Identifies a Novel Suppressive Macrophage Population in Human Ovarian Carcinoma. *Journal of Experimental Medicine*, 203:871-881, 2006.

225. S. Goswami, E. Sahai, J. B. Wyckoff, M. Cammer, D. Cox, F. J. Pixley, E. R. Stanley, J. E. Segall and J. S. Condeelis. Macrophages Promote the Invasion of Breast Carcinoma Cells Via a Colony-Stimulating Factor-1/Epidermal Growth Factor Paracrine Loop. *Cancer Research*, 65:5278-5283, 2005.

226. R. S. Al-Lamki, J. Wang, J. Yang, N. Burrows, P. H. Maxwell, T. Eisen, A. Y. Warren, S. Vanharanta, S. Pacey, P. Vandenabeele, J. S. Pober and J. R. Bradley. Tumor Necrosis Factor Receptor 2-Signaling in Cd133-Expressing Cells in Renal Clear Cell Carcinoma. *Oncotarget*, 7:24111-24124, 2016.

227. E. Aydemir, O. F. Bayrak, F. Sahin, B. Atalay, G. T. Kose, M. Ozen, S. Sevli, A. B. Dalan, M. E. Yalvac, T. Dogruluk and U. Ture. Characterization of Cancer Stem-Like Cells in Chordoma. *Journal of Neurosurgery*, 116:810-820, 2012.

228. B. M. Kenyon, F. Browne and R. J. D'Amato. Effects of Thalidomide and Related Metabolites in a Mouse Corneal Model of Neovascularization. *Experimental Eye Research*, 64:971-978, 1997.

229. E. P. Sampaio, E. N. Sarno, R. Galilly, Z. A. Cohn and G. Kaplan. Thalidomide Selectively Inhibits Tumor Necrosis Factor Alpha Production by Stimulated Human Monocytes. *Journal of Experimental Medicine*, 173:699-703, 1991.

230. T. Eisen, C. Boshoff, I. Mak, F. Sapunar, M. M. Vaughan, L. Pyle, S. R. Johnston, R. Ahern, I. E. Smith and M. E. Gore. Continuous Low Dose Thalidomide: A Phase Ii Study in Advanced Melanoma, Renal Cell, Ovarian and Breast Cancer. *British Journal of Cancer*, 82:812-817, 2000.

231. M. L. Harrison, E. Obermueller, N. R. Maisey, S. Hoare, K. Edmonds, N. F. Li, D. Chao, K. Hall, C. Lee, E. Timotheadou, K. Charles, R. Ahern, D. M. King, T. Eisen, R. Corringham, M. DeWitte, F. Balkwill and M. Gore. Tumor Necrosis Factor Alpha as a New Target for Renal Cell Carcinoma: Two Sequential Phase Ii Trials of Infliximab at Standard and High Dose. *Journal of Clinical Oncology*, 25:4542-4549, 2007.

232. A. Ferrajoli, M. J. Keating, T. Manshouri, F. J. Giles, A. Dey, Z. Estrov, C. A. Koller, R. Kurzrock, D. A. Thomas, S. Faderl, S. Lerner, S. O'Brien and M. Albitar. The Clinical Significance of Tumor Necrosis Factor-Alpha Plasma Level in Patients Having Chronic Lymphocytic Leukemia. *Blood*, 100:1215-1219, 2002.

233. M. I. Ahmed, E. E. Salahy, S. T. Fayed, N. G. El-Hefnawy and A. Khalifa. Human Papillomavirus Infection among Egyptian Females with Cervical Carcinoma: Relationship to Spontaneous Apoptosis and Tnf-Alpha. *Clinical Biochemistry*, 34:491-498, 2001.

234. I. Garcia-Tunon, M. Ricote, A. Ruiz, B. Fraile, R. Paniagua and M. Royuela. Role of Tumor Necrosis Factor-Alpha and Its Receptors in Human Benign Breast Lesions and Tumors (in Situ and Infiltrative). *Cancer Science*, 97:1044-1049, 2006.

235. V. Michalaki, K. Syrigos, P. Charles and J. Waxman. Serum Levels of Il-6 and Tnf-Alpha Correlate with Clinicopathological Features and Patient Survival in Patients with Prostate Cancer. *British Journal of Cancer*, 90:2312-2316, 2004.